ELSEVIER

Biochimica et Biophysica Acta 1188 (1994) 167–204

BBA Biochimica et Biophysica Acta

Nickel hydrogenases: in search of the active site

Simon P.J. Albracht *

E.C. Slater Institute, BioCentrum Amsterdam, University of Amsterdam, Plantage Muidergracht 12, NL-1018 TV Amsterdam, The Netherlands

Received 17 June 1994

Keywords: Hydrogenase; Hydrogen activation; Nickel; Iron-sulfur; Energy; Catalysis

Contents

Abbreviations: DCIP, 2,6-dichlorophenolindophenol; ENDOR, electron nuclear double resonance; EPR, electron paramagnetic resonance; ESEEM, electron spin echo envelope modulation; EXAFS, extended X-ray absorption fine structure; F_{420}, 8-hydroxy-5-deazaflavin; F_{430}, factor F_{430} (prosthetic group of methyl-coenzyme M reductase); FTIR, Fourier transform infrared; LEFE, linear electric field effect; MCD, magnetic circular dichroism; PMS, phenazinemethosulphate; XANES, X-ray absorption near edge structure; XAS, X-ray absorption spectroscopy.

* Corresponding author. Fax: + 31 20 5255124.

SSDI 0005-2728(94)00122-7

1. Introduction

Since nickel was first discovered in hydrogenase in 1981 [83] many reviews on various aspects of nickel hydrogenases have appeared [34,64,78,94,125,150,154, 213,218,219,227]. It is therefore of little additional value to repeat this information here to great extent. Rather, after an introduction into the field of hydrogenases, I will focus on various aspects of nickel hydrogenases which I consider of importance to understand the mechanism of action of the enzyme and the architecture of the hydrogen-activating site.

1.1. History and occurrence

More than 100 years ago Hoppe-Seyler [99] noticed that bacteria in river mud might be responsible for quantitative decomposition of formate into H_2 and CO_2. After the isolation of pure cultures of H_2-producing and H_2-oxidizing bacteria [91,109,151], one realized that H_2 might play an important role in the metabolism of bacteria. The enzyme responsible for hydrogen activation was termed 'hydrogenase' by Stephenson and Stickland in 1931 [185,186] in a study on the reduction of methylene blue by H_2 catalyzed by bacteria from river mud. At present hydrogenases have been detected in a great number of micro-organisms.

In order to acquire energy-rich reducing equivalents, many bacteria have the capacity to oxidize H_2 to two protons and two electrons. By definition, the standard oxidation-reduction potential of the equilibrium $2H^+ + 2e \leftrightarrow H_2$ is -413 mV at pH 7.0, 25°C and 1 bar of H_2. The reducing equivalents thus obtained enable bacteria to reduce a variety of substrates, notably CO_2, and to generate sufficient energy for ATP synthesis.

Bacteria living in an anaerobic environment, using the fermentation of organic substrates for the supply of energy-rich reducing equivalents, often dispose of their excess of electrons by way of the reduction of protons. The major source of reducing equivalents for H_2 production is the metabolite pyruvate. It can be converted to acetyl-CoA plus formate, whereupon the latter is decomposed into H_2 and CO_2 by the formate-hydrogen-lyase reaction in which hydrogenase is involved. Pyruvate can also be oxidized by the enzyme pyruvate : ferredoxin oxidoreductase to acetyl-CoA and CO_2. Reduced ferredoxin subsequently transfers its electrons to a hydrogenase.

In nature, H_2 is also produced in N_2-fixing organisms. A sizeable amount of reducing equivalents used by the enzyme nitrogenase for the ATP-dependent reduction of N_2 to NH_3 is 'spoiled' by the enzyme in a reaction with protons: at least one molecule of H_2 is formed for every molecule of N_2 reduced. As this would mean a loss of energy for the organism, hydrogenase in such organisms recaptures the energy-rich reducing equivalents.

Ideas about the function of hydrogenases in nature have already been reviewed in the late seventies [2,171]. In 1966 Ackrell et al. [1] first described the likely existence of multiple hydrogenase systems in bacteria. In 1986 Lissolo et al. [131] found three genetically different hydrogenases in *Desulfovibrio vulgaris*. This reinforced the idea [149] that molecular hydrogen plays a central role in the bioenergetics of sulphate-reducing bacteria [64]. By now multiple, genetically different, hydrogenases have been detected in many bacteria.

It has been known for more than two decades that hydrogenases contain non-heme Fe as an essential component. In 1971 it was first shown, that like in most other non-heme iron proteins, the Fe atoms were arranged in Fe-S clusters [92,127,147,148]. In the 1970s,

many more examples of hydrogenases with Fe-S clusters were found [172]. Consequently it was generally assumed that the active site in all hydrogenases was an Fe-S cluster [2].

1.2. Classes of hydrogenases

The field was stirred quite a bit by the rediscovery of an observation of Bartha and Ordal [20] that 'Knallgas' bacteria thriving on H_2, O_2 and CO_2 required Ni for growth [193]. For *Alcaligenes eutrophus* it was shown that Ni was indispensable for the biosynthesis of active hydrogenase [77]. Around the same time it was recognized [202] that Ni was also involved in two other metabolic processes in bacteria: acetate synthesis from CO_2, as well as CH_4 production from CO_2. The enzymes involved are now known as acetyl-CoA synthase [121,226] and methyl-coenzyme M reductase [58,86, 162].

Purified hydrogenases from many bacteria contain stoichiometric amounts of Ni, as first established by Graf and Thauer in 1981 [83] for the enzyme from *Methanobacterium thermoautotrophicum*, strain Marburg. Since Ni is a transition metal of the 3d group, one might expect to detect EPR signals if the Ni ion would be either trivalent ($3d^7$) or monovalent ($3d^9$). Indeed the purified enzyme from *M. thermoautotrophicum* displayed a simple rhombic EPR signal which could be ascribed to nickel by the use of ^{61}Ni [7], a stable isotope with a nuclear magnetic moment of 3/2 (Fig. 1). Moreover, the signal disappeared upon contact of the enzyme with H_2. This was the first demonstration of redox-active nickel in the enzyme.

A virtually identical EPR signal had earlier been described by Lancaster [123] in membranes from *Methanobacterium bryantii*. At the time, Lancaster [123,124] held the opinion that the signal was due to factor F_{430}. It is now beyond doubt, however, that it originated from membrane-bound hydrogenase. Nickel in F_{430} of methyl-coenzyme M reductase displays quite different EPR spectra [13,162]. In retrospect, the first clear EPR signal of Ni(III) in a purified hydrogenase was spotted by the author in 1981 on a poster display by Daniels et al. [51] on the 7th International Symposium on Flavins and Flavoproteins, Ann Arbor; for unknown reasons, though, no nickel could be detected in the preparation at that time. Also Doddema [54] had earlier reported the presence of nickel in purified hydrogenase from *M. thermoautotrophicum*, but considered it to be an artefact.

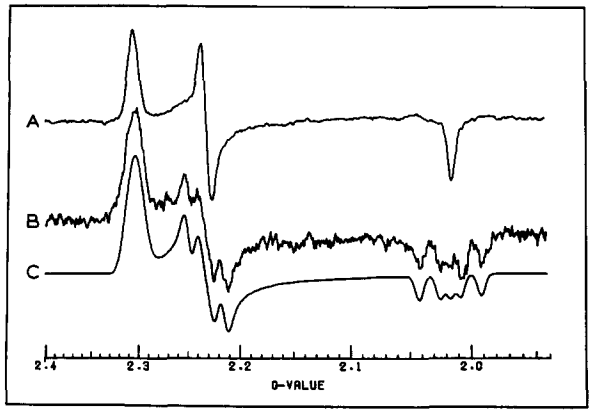

Fig. 1. EPR spectra at 73 K of purified F_{420}-non-reducing hydrogenase from *M. thermoautotrophicum* strain Marburg. (A) Oxidized enzyme. (B) Enzyme 80% enriched in ^{61}Ni. (C) Computer simulation. (Adapted from Albracht et al. [7].)

Although the majority of the hydrogenases known today contains nickel, this certainly does not hold for all. From several bacteria hydrogenases have been purified in which no other metal than Fe could be detected (*Acetobacter woodii* [156], *Acetomicrobium flavidum* [169], *Clostridium pasteurianum* [3,41], *Desulfovibrio desulfuricans* ATCC 7757 [93], possibly *Desulfovibrio salexigens* [64], *D. vulgaris* [103,205], *Megasphaera elsdenii* [74], *Thermatoga maritima* [108] and *Trichomonas vaginalis* [152]). Hence these enzymes clearly belong to a separate class. Recently genes presumably encoding Fe-hydrogenases in *Desulfovibrio fructosovorans* (Malki, S., Saimmaime, I., Rousset, M., Dermoun, Z. and Belaich, J.P., personal communication) and *Clostridium acetobutylicum* (Gorwa, M.F., Croux, C. and Soucaille, P., personal communication) have been cloned and sequenced.

In *M. thermoautotrophicum* a hydrogenase has been found that does not contain transition metals at all [231]. It is supposed to function in the reduction of methylenetetrahydromethanopterin by hydrogen.

Using the available evidence in literature that metal ions (Ni and/or Fe) are involved in all hydrogenases but one, two main classes can be recognized at present:

A. Enzymes in which no other metal than Fe could be detected. These enzymes are here called Fe-hydrogenases (in literature also often referred to as 'Fe-only' hydrogenases). They contain several Fe-S clusters and a novel cluster proposed to host 6 Fe atoms [87,88] (for review see [6]). The nucleotide sequences of the genes encoding the Fe-hydrogenases from *D. vulgaris* [215] and *C. pasteurianum* (hydrogenase-I) [142], as well as from a gene called *HydC* in *D. vulgaris* supposed to encode a possible second Fe-hydrogenase [187], are now known. The Cys residues in these three sequences have been lined up by Meyer and Gagnon [142]. Fig. 2 shows a modified and extended version of this comparison. There are two blocks of 4 Cys (classical CxxCxxCxxxC motifs) present in all. Meyer and Gagnon [142] therefore suggested the presence of two classical cubane clusters. This is in line with earlier conclusions by Wang et al. [220] and Hagen and coworkers [88,216] based on physico-chemical measurements. The clusters were called the F-clusters or Ferredoxin clusters to distinguish them from the hydrogen-activating cluster

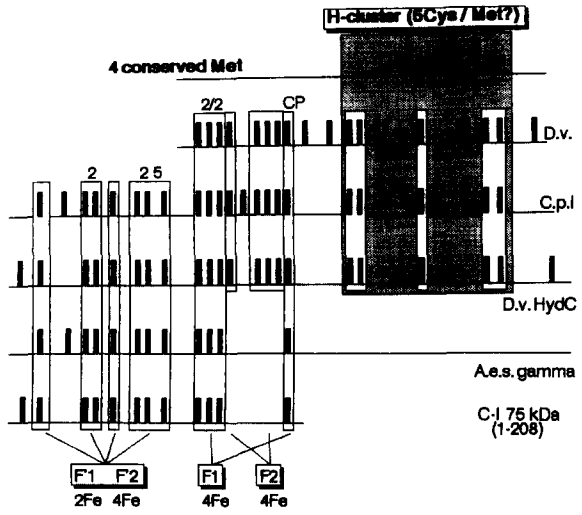

Fig. 2. Sequence homology between Fe-hydrogenases, the soluble Ni-hydrogenase from *A. eutrophus* and mitochondrial NADH:Q oxidoreductase. The upper line shows the position of 4 conservative Met residues in Fe-hydrogenases. In the other lines, only Cys residues are indicated. Abbreviations: A.e.s. hydrogenase, soluble hydrogenase from *A. eutrophus*; Complex I, mitochondrial NADH:Q oxidoreductase; D.v., Fe-hydrogenase from *D. vulgaris*; C.p.I., Fe-hydrogenase I from *C. pasteurianum*; D.v.HydC, *HydC* gene from *D. vulgaris*; A.e.s.gamma, γ-subunit of the NAD^+-reducing hydrogenase from *A. eutrophus*; C-I 75 kDa (1–208), sequence of the first 208 amino-acid residues of the 75 kDa subunit of mitochondrial Complex I. See text for further details.

or H-cluster, which has quite different physico-chemical properties. The five conserved Cys residues in the C-terminal part of the sequences are supposed to host the H-cluster. Possibly also one or more of the four conserved Met residues in this region are involved [142].

The remaining two [4Fe-4S] clusters in the *C. pasteurianum* hydrogenase-I [5] were assumed to be located in the N-terminal region of this enzyme [142], although the Cys-residue pattern is not like that for typical cubane clusters. Adams and coworkers [80] have recently re-examined the Fe-S clusters in the Fe-hydrogenases from *C. pasteurianum* (hydrogenase-I), *T. maritima* and *D. vulgaris* with Resonance-Raman spectroscopy. It was concluded that the *C. pasteurianum* and *T. maritima* enzymes, but not the *D. vulgaris* enzyme, contained quite likely a [2Fe-2S] cluster. In the *C. pasteurianum* enzyme this cluster possibly has rather unusual properties (e.g. its EPR spectrum cannot be observed at 60 K). Hence, one of the clusters located in the N-terminal region of the *C. pasteurianum* hydrogenase-I is now supposed to be a [2Fe-2S] cluster.

Van Dongen, as referred to in [142] (see also [188]), noted already that the N-terminal region of the *HydC* gene of *D. vulgaris* was homologous to the N-terminal region of the γ subunit (diaphorase part) of the soluble Ni-hydrogenase of *A. eutrophus* [203], and to the N-terminus of the 75 kDa subunit of mitochondrial NADH:Q oxidoreductase [163]. Homology between the latter two was also reported by Walker and coworkers [153]. When one combines all this information, then an interesting picture emerges (Fig. 2). It so appears that the N-terminal part of *C. pasteurianum* hydrogenase-I, containing the Cys patterns supposed to accommodate an atypical [2Fe-2S] cluster, an atypical [4Fe-4S] cluster and a classical cubane cluster, presumably has been used by nature during the evolution to form the diaphorase part of the *A. eutrophus* H_2:NAD^+ oxidoreductase and the 75 kDa subunit of mitochondrial NADH:Q oxidoreductase.

B. Enzymes containing Fe-S clusters and a Ni ion, here termed Ni-hydrogenases. Iron-sulphur clusters of the $[4Fe\text{-}4S]^{2+(2+:1+)}$ type and the $[3Fe\text{-}4S]^{1+(1+:0)}$ type can be found here. Nickel hydrogenases are considerably less active (0.1–0.8 mmol H_2/min/mg in hydrogen-uptake or production assays with artificial electron acceptors or donors) than iron hydrogenases (5–10 mmol H_2/min/mg evolution; 10–50 mmol H_2/min/mg uptake), but have a K_m for H_2 (usually a few μM) two orders of magnitude lower than that of Fe-hydrogenases. Some Ni-hydrogenases contain Se and can be as active as Fe-hydrogenases [183].

1.3. Potential importance of hydrogenase for the storage of solar energy

Photoproduction of H_2 has already been reported in 1942 with algae [81]. After the oil crisis of 1973, hydrogenases enjoyed a much increased attention due to potentially applicable aspects of the enzyme. The first international conference on hydrogenases and hydrogen metabolism was held shortly afterwards [172]. One of the underlying ideas was that hydrogenase, in combination with the capacity of Photosystem II of chloroplasts or cyanobacteria to oxidize water to O_2 and low-potential reducing equivalents, might be employed to construct a reactor for the biophotolysis of water to H_2 and O_2, driven by solar energy (Fig. 3). The products thus formed can be used to regain the stored energy by just burning the H_2 to H_2O again, thereby closing the cyclic nature of this attractive sequence of reactions to store and use the abundant solar energy available on the earth's surface (world average: 350 W/m^2).

Experiments demonstrating the feasibility of such an approach were published in the mid- and late 1970s and have been extensively reviewed by Weaver et al. in 1980 [222]. Limited stability of the biological components involved, as well as the intrinsic low-energy yield of chloroplasts made such protein-based systems of no practical use. Yet these experiments have stimulated the interest of many research groups in unraveling the structure and the mechanism of action of the active

sites involved in the water-oxidizing complex in Photosystem II, as well as the H_2-activating site in hydrogenases. Mimicking the active sites of these systems in cheap and stable catalysts would certainly boost the commercial and political interest in the use of solar energy, also in view of the growing concern about the global CO_2 production through the use of fossil fuels.

2. Nickel hydrogenases

2.1. Hydrogenase is an oxidoreductase

Hydrogenase is a redox enzyme. As pointed out by Krasna [117], the H_2 molecule is split heterolytically ($H_2 \rightarrow H^+ + H^-$). At the H_2-site, therefore, the enzyme is most likely involved in the transfer of two reducing equivalents at a time. Further transfer of electrons in nickel hydrogenases presumably proceeds in packages of one electron only. Consequently, a functional analogy with iron-sulphur-containing flavoproteins, like the mitochondrial NADH : Q oxidoreductase, comes to the mind of this author. In the latter enzyme an $n = 2$ redox group (FMN) is present together with several $n = 1$ redox groups (the Fe-S clusters) [22]. The substrate NADH is in redox equilibrium with the enzyme whereby two electrons are involved. In fact, like hydrogenases, NADH : Q oxidoreductase splits its substrate NADH 'heterolytically' ($NADH \rightarrow NAD^+ + H^-$), whereafter it oxidizes the hydride. One therefore might depict hydrogenases as composed of three parts (Fig. 4). Part 1 contains the H_2-activating site. Here the H_2/H^+ chemistry is taking place. It is reasonable to assume that this part must be able to accommodate two electrons at a time. Part 2 is the electron-transfer part which guides electrons to part 3. In view of the iron and sulphide content of nickel hydrogenases, this part is expected to contain Fe-S clusters. Part 3 takes care of reduction of the electron acceptor of the enzyme. In many hydrogenases parts 1 and 2 are directly linked to enzymes or polypeptide complexes (part 3) containing additional prosthetic groups like Fe-S clusters, flavin, molybdenum or cytochromes. This can lead to a direct electro-chemical connection of H_2 with NAD^+, F_{420}, quinones or a heterodisulphide. Part 3 thus is the electro-chemical interface of hydrogenase with the metabolism of the micro-organism and determines the specificity and role of the hydrogenase involved. The interface between part 2 and part 3 can be considered as a purely electronic interface. During purification of hydrogenases, part 3 is sometimes easily lost.

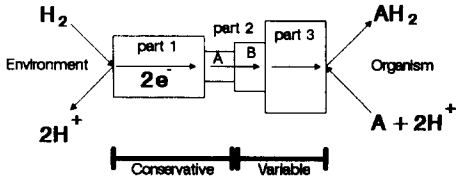

Fig. 4. Schematic representation of nickel hydrogenases as an oxidoreductase. Part 1 contains the hydrogen-activating site. Part 2 serves as an electronic interface between part 1 and part 3. Part 3 is an electro-chemical interface which accepts electrons from part 2 and reduces a substrate in the organism.

From a biochemical point of view hydrogenases are called hydrogen : acceptor oxidoreductases. The aim of this review is a better understanding of the H_2-activating site; therefore all proteins capable of activating hydrogen in a nickel-dependent way will be considered as Ni-hydrogenases, irrespective of their intactness. Given the great variability of part 3 in nickel hydrogenases, one can imagine that the Fe-S clusters involved in the electronic interface in part 2B might vary among the several enzymes. On the other hand, a conservative architecture is expected for the H_2-activating site in part 1 and the contact of part 2 (2A) with part 1.

2.2. The subunits and their amino-acid sequences

The large progress on the genetic level in the last few years makes it possible to formulate certain boundaries for the minimal functional unit involved in the hydrogen-activating site. All presently-known nickel hydrogenases contain at least two subunits with approximate molecular masses of 46–72 kDa (large subunit) and 23–38 kDa (small subunit). The amino-acid sequences derived from the structural genes encoding the two subunits are now known for some 24 different enzymes. Sequence comparisons of most of them have been reviewed recently [154,218,227]. As I will make use of the conservative amino acids in trying to localize the basic parts required for the active site, this information, including the latest sequences, is briefly discussed below.

2.2.1. The 'large' or nickel-binding subunit

The large subunit contains five short stretches of sequence with conservative amino acids. Starting from the N-terminus, the first conservative motif (here called

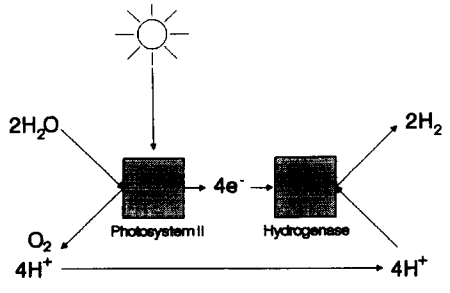

Fig. 3. Biophotolysis of water using the catalytic properties of Photosystem II of green plants, and hydrogenase.

motif 1L) is an R-G-x-E sequence present within the first 62 amino acids of all sequences, but one: in the hydrogenase functional in the formate-hydrogen-lyase system of *Escherichia coli*, further called *E. coli* hydrogenase-3, this motif is shifted by some 140 residues. The second motif (2L) is R-x-C-G-x-C-x-x-x-H. It is remarkable that the spacing between both motifs is exactly the same in all known sequences but one. There are 16 amino acids between the E residue in motif 1L and the R residue in motif 2L, except for the sequence of the *E. coli* hydrogenase-3, where this spacing is 17 residues. This is why Voordouw [218] considered both motifs as one conservative 'element'. The presence of six residues with potential metal-binding capacity (2 Arg, 1 Glu, 2 Cys and 1 His) at fixed positions in the N-terminus is highly intriguing. These conservative residues might constitute (part of) a metal-coordination site.

A little further on in the sequence there is a histidine-rich region in many enzymes. In 10 out of 22 known sequences of this part, a stretch H-x-H-x-x-H-x-x-H-L-H-x-L is present. This region was already noticed in the earliest determined sequences [157,158] and was initially considered as a possible candidate for nickel binding. The underlined H and L residues are present in all known sequences, except in *E. coli* hydrogenase-3, where the Leu is an Ala residue. The Hx_6L motif is called here motif 3L. The conservative H in motif 3L is between 12 and 42 residues apart from the last H in motif 2L. The His-rich region found in a number of hydrogenases is a potential candidate for metal binding. As will be discussed later, copper, which is present in some hydrogenases, is considered as a potential candidate for binding at this site.

More to the C-terminal site there is a fourth motif (4L): G-x-x-x-x-P-R-G-x-x-x-H. The distance between the first G in this motif and the conservative L in motif 3L is greatly variable and ranges from 188 to 406 amino-acid residues.

At the very end a fifth motif (5L) with two cysteines is present: D-P-C-x-x-C-x-x-H. The codon for cysteine is usually a TGC triplet, but in the Se-containing nickel hydrogenases from *Desulfovibrio baculatus* [217] and *Methanococcus voltae* [90] the codon for the first cysteine in this motif is replaced by a TGA triplet, usually a stop-codon, but here coding for selenocysteine as in formate dehydrogenase from *E. coli* [26,230] and glutathione peroxidase from mouse cells [38]. There is now conclusive evidence from EPR measurements on ^{77}Se-enriched ($I = 1/2$) hydrogenases from *D. baculatus* [96] and *M. voltae* [184], as well as from EXAFS measurements on the *D. baculatus* enzyme [57] that Se is a ligand to nickel in these hydrogenases. Consequently it can be concluded that the first cysteine in motif 5L is a ligand to nickel. This then also suggests a role for the aspartic acid residue, the second cysteine residue and the histidine residue in this motif in the coordination of nickel. In the methyl-viologen reducing Se-enzyme from *M. voltae*, the carboxy-terminal region is encoded by a separate gene [90]. The corresponding mature peptide is only 25 amino acids long and contains motif 5L [183].

In all predicted sequences but one (*E. coli* hydrogenase-3) motif 5L ends with a H residue and in more than half of the predicted sequences a V residue is next. It has been demonstrated that in the mature enzyme from *Azotobacter vinelandii* the nickel-binding subunit is 1663 Da smaller than indicated by the amino-acid sequence deduced from the encoding DNA [82]. As the N-terminus of the mature protein was identical to the DNA-predicted sequence, it was proposed that C-terminal processing, whereby the His-Val bond in the large subunit of this hydrogenases is hydrolysed by a specific protease, may be an essential step in the formation of active enzyme. Indications for possible processing of the large subunit had earlier been noticed for the enzyme from *D. baculatus* [139] and for hydrogenases 1 and 2 from *E. coli* [134]. Evidence for C-terminal processing has now also been obtained for several other Ni-hydrogenases [79,113,141,183]. For the hydrogenase-3 from *E. coli* the processing has been demonstrated in vitro [167]. Experiments with the isolated precursor form of the large subunit of this enzyme and the product of the *hycH* gene indicate that only the latter protein is required for C-terminal processing [166].

Interestingly, a part of the motifs 1L and 2L, namely the $RGxEx_{16}R$ pattern, as well as motif 3L and parts of the motifs 4L and 5L can also be recognized [14] in the 49 kDa subunit [65] of mitochondrial NADH:Q oxidoreductase, suggesting an evolutionary relationship.

All nickel hydrogenases studied so far seem to contain at least one Fe-S cluster. As nature usually anchors Fe-S clusters in proteins via coordination to four cysteines (for a recent overview see [138]), this suggests that the large subunit can probably be discounted to bind such a cluster on its own. The two terminal cysteines in motif 5L are quite likely already occupied by binding to nickel. To ascribe the remaining two cysteines as ligands for an Fe-S cluster is rather unlikely. It is not impossible, though, as some [2Fe-2S] clusters are proposed to have up to two non-sulphur ligands [67,85,201].

Hornhardt et al. [100] have described the purification of the nickel-binding subunit of the soluble NAD^+-reducing hydrogenase from a mutant (HF14) of *A. eutrophus*. The preparations contained 0.2–1.4 gram atoms of Ni and 2–3 gram atoms of Fe per 57 kDa molecular mass and showed a maximal hydrogen uptake activity with $K_3Fe(CN)_6$ of 78 nmol/min/mg. Although it was concluded from EPR spectra that one

[4Fe-4S] cluster would be present, the quality of the spectra rather suggest the concentration of the paramagnetic species to be two orders of magnitude lower than the concentration of the peptide. Ni was not detected in these spectra. More recently [101] the same nickel-binding subunit was also purified from another *A. eutrophus* mutant (HF89); again a low H_2-$K_3Fe(CN)_6$ reductase activity could be measured (174 nmol/min/mg). A better physico-chemical characterization of this purified nickel-binding subunit might produce some interesting new results. Sauter [167] has also reported the presence of 0.8–1.8 mol Ni per large subunit of hydrogenase-3 of *E. coli*, when overexpressing the *hycE* gene. Regretably, no further details (Fe content, activity) were reported.

2.2.2. The 'small' or Fe-S subunit

In the small subunits of all Ni-hydrogenases three motifs (motifs 1S–3S) are conserved which make up a pattern $CxxCx_nGxCxxxGx_mGCPP$, where n is 61 to 106 and m is 24 to 61 (Fig. 5). Surprisingly this pattern is also found [14] in the PSST subunit of mitochondrial NADH:Q oxidoreductase [15,66], except for the first Cys which is a Leu there. In 17 Ni-hydrogenases 6 additional conservative Cys residues are found in three more motifs (motifs 4S–6S; see Fig. 5). Together these motifs make a pattern $Cx'x''x_nCx_5CxGPx_5Cx_mCxxC$, where n is very often 25 and m is 10 to 18. In eight sequences x' is a Tyr residue, in seven sequences this is a Pro and in two sequences there is a Glu at this position. In 16 sequences x'' is an Arg residue. These 17 enzymes are termed here 'standard' nickel hydrogenases (Fig. 6).

In three enzymes, namely the F_{420}-reducing enzymes from *M. voltae* (both the normal and the Se-containing one) and from *M. thermoautotrophicum*, these six conservative Cys residues are not present; instead two CxxCxxCxxxC patterns typical for two classical cubane clusters are found. In two enzymes, namely the soluble NAD^+-reducing hydrogenase of *A. eutrophus* and hydrogenase-3 of *E. coli*, none of these additional Cys are present, simply due to the fact that the polypeptide stops shortly after the motifs 1S–3S (Figs. 5 and 6). Also the small subunit is synthesized as a precursor form. The N-terminal region (32–50 residues) of this precursor is removed upon maturation [113,126,133, 140].

It seems reasonable to conclude from this information that the minimal unit required for the activation and oxidation of hydrogen involves at most only the large subunit and the motifs 1S–3S from the small subunit.

2.3. The Fe-S clusters

Presently the *Desulfovibrio gigas* hydrogenase is one of the best characterized enzymes in terms of its contents of Fe-S clusters. Extensive Mössbauer measurements [104,199] on oxidized ^{57}Fe-enriched ($I = 1/2$) enzyme showed that 27% of the Fe was present in a $[3Fe\text{-}4S]^+$ cluster with an $S = 1/2$ ground state, whereas the remaining Fe showed up as two diamagnetic $[4Fe\text{-}4S]^{2+}$ clusters. The $[3Fe\text{-}4S]^+$ cluster has a rather sharp EPR signal slightly above $g = 2$. The 3Fe cluster could be reduced to an $S = 2$ system, before reduction of the cubanes took place (Fig. 7). Upon complete reduction of the enzyme, the 3Fe cluster remained an $S = 2$ $[3Fe\text{-}4S]^0$ cluster and the cubane clusters were reduced to the $S = 1/2$ $[4Fe\text{-}4S]^+$ state.

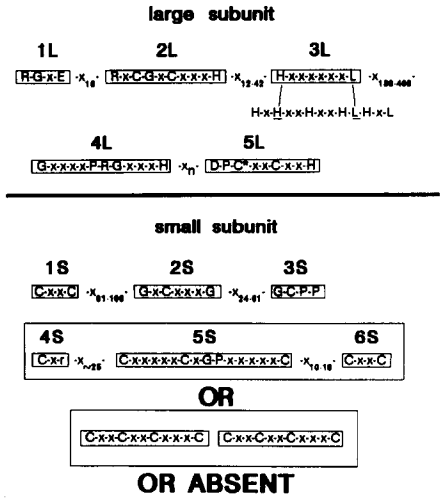

Fig. 5. Schematic representation of the conservative motifs in the amino-acid sequences of the two subunits of nickel hydrogenases. The C* residue in motif 5L is a selenocysteine in some enzymes. The 'r' residue in motif 4S is an Arg residue in nearly all motifs. In some hydrogenases, the motifs 4S, 5S and 6S are replaced by two Cys-motifs for regular cubane Fe-S clusters. In a few enzymes only the motifs 1S, 2S and 3S are present.

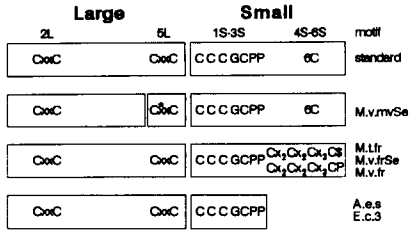

Fig. 6. Schematic representation of (mainly conservative) Cys residues in the subunits of nickel hydrogenases. In the large subunit the Cys residues reside in motifs 2L and 5L and are strictly conservative. In the small subunit the first 4 Cys residues come from the motifs 1S-3S (strictly conservative), while the rest comes from motifs conservative in many, but not all hydrogenases. Abbreviations: M.v.mvSe, selenium-containing methyl-viologen reducing hydrogenase from *M. voltae*; M.t.fr, F_{420}-reducing enzyme from *M. thermoautotrophicum* strain ΔH; M.v.frSe and M.v.fr, F_{420}-reducing enzymes from *M. voltae* with and without Se, respectively; A.e.s., soluble NAD^+-reducing enzyme from *A. eutrophus*; E.c.3, hydrogenase-3 from *E. coli*. The $ sign stands for a Q in the F_{420}-reducing enzymes from *M. voltae* (no Se) and *M. thermoautotrophicum*, and for a P in the corresponding Se-containing enzyme from *M. voltae*.

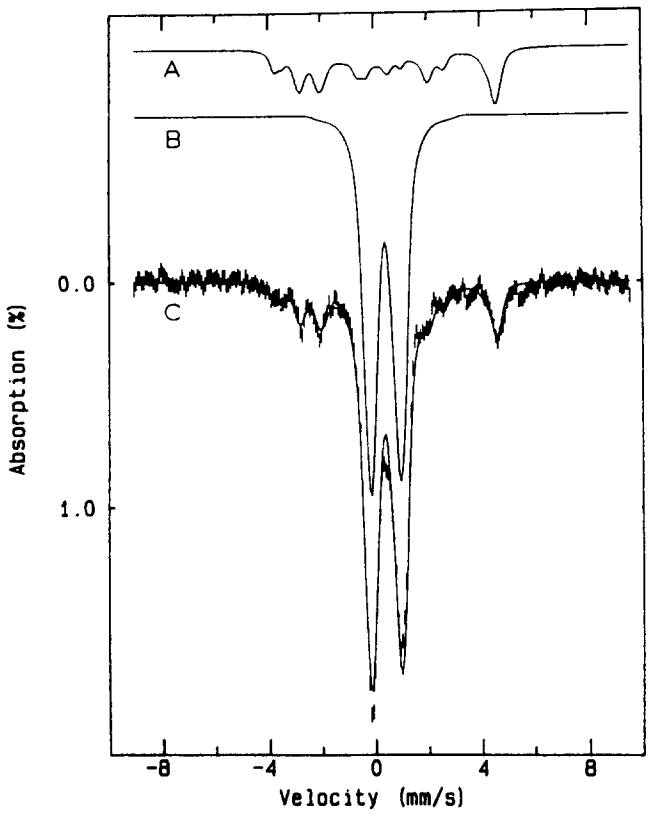

Fig. 7. Mössbauer spectrum of *D. gigas* hydrogenase at 4.2 K in a parallel magnetic field of 1 T. The sample was reduced to a state (−270 mV) where the 3Fe cluster was reduced, but the 4Fe clusters were still oxidized. (A) Theoretical spectrum of the $[3Fe\text{-}4S]^0$ cluster. (B) Theoretical spectrum of the $[4Fe\text{-}4S]^{2+}$ clusters. (C) Experimental spectrum with superimposed theoretical spectrum. (From Teixeira et al. [199] with permission.)

The magnetic hyperfine coupling constants for the reduced 4Fe clusters are noticeably smaller than those of 'normal' cubane clusters, which exhibit a $g = 1.94$ type of EPR spectrum and a $CxxCxxCx_nC$ amino-acid-sequence pattern. Also the EPR spectra of the reduced *D. gigas* enzyme [33,199] do not show the typical $g = 1.94$ type of signals, but are unusually broad. The amino-acid sequence [217] shows that this enzyme belongs to the standard hydrogenases (Fig. 6).

At this point I tentatively assign the 3Fe cluster to be coordinated by Cys residues in motifs 1S-3S in the small subunit, and the atypical 4Fe cluster by Cys residues in the motifs 4S-6S. Hence I assume that in all standard Ni-hydrogenases only six invariant Cys are available for these two cubane clusters. It cannot be ruled out, though, that other Cys residues in the individual polypeptides, when present, might be involved, but these then are at variable positions among the different hydrogenases.

Also the *Chromatium vinosum* has been characterized with Mössbauer spectroscopy [192]. Its Fe-S cluster composition in the reduced state appears to be identical to that of the *D. gigas* enzyme. The EPR spectra were already known to be very similar. The *C. vinosum* enzyme has, however, an extra oxidation state which shows most unusual spectra (see below). The amino-acid sequence of this enzyme has not been determined.

The soluble enzymes from *D. baculatus* and *D. desulfuricans* (Norway) (both bacteria are now considered to be nearly identical [64,200]; the Norway strain has been renamed as *Desulfomicrobium baculatum*), have also been characterized in great detail. The amino-acid sequence shows all characteristics of a standard hydrogenase, except for a selenocysteine which substitutes the first cysteine in motif 5L of the large subunit. Hence one might expect the presence of a 3Fe cluster and two atypical 4Fe clusters. In the oxidized state, however, no EPR signals were present, nor could the Mössbauer spectrum of a $[3Fe\text{-}4S]^+$ cluster be detected [23,96,200]. No Mössbauer spectrum of an $S = 2$ $[3Fe\text{-}4S]^0$ cluster could be observed either; likewise there was also no evidence for an $S = 2$ system in this enzyme from multifield saturation magnetization measurements [221]. In the H_2-reduced state only Mössbauer spectra from cubane clusters were recognized. In view of the standard conservative patterns in the amino-acid sequence, this finding is highly surprising. All 'standard' nickel hydrogenases with two subunits may be expected to contain at least 11–12 gram atoms of iron per gram atom of nickel, like the enzymes from *D. gigas* and *C. vinosum*. It should be noted that 8 gram atoms of Fe per mol of enzyme and substoichiometric amounts of nickel were found in the *D. desulfuricans* enzyme [23], whereas 0.69 gram atoms of Ni and 9.25 gram atoms of Fe per mol of enzyme (i.e. 13.4 Fe/Ni) were found in the *D. baculatus* hydrogenase [96]. Up to 3 spins per Ni have been detected as EPR signals from Fe-S clusters [200].

Also no 3Fe clusters could be detected in the F_{420}-non-reducing hydrogenases from *M. thermoautotrophicum* strain Marburg (EPR) ([7]; Albracht, S.P.J. and Hedderich, R., unpublished observations) and strain ΔH (EPR, MCD) [107], and in the F_{420}-reducing enzyme from the latter bacterium (EPR) [106]. The sequence of the F_{420}-non-reducing enzyme belongs to the standard type of nickel hydrogenases. One possibility is that the 3Fe cluster in these enzymes is modified such that it behaves like a $[4Fe\text{-}4S]^{2+(2+:1+)}$ cluster under all conditions.

Sayavedra-Soto and Arp [168] have reported that replacement of the first Cys residue in motif 1S of the small subunit of *A. vinelandii* hydrogenase by a Ser residue resulted in a decreased hydrogenase activity in cell colonies of the mutants. Replacement of the second Cys residue resulted in much less activity loss. When at the same time the neighbouring (non-conservative) Cys residue was also transformed into a Ser residue, then no activity could be detected. Likewise,

no activity could be detected when the individual Cys residues in motif 6L were replaced by Ser. The authors suggested that these residues are essential for the formation of active enzyme. These studies contradict an earlier observation by the same group [191], that degradation of the small subunit did not affect activity of the hydrogenase of *A. vinelandii*. The conclusions are also at variance with the fact the hydrogenases from *E. coli* (hydrogenase-3) and *A. eutrophus* (the soluble enzyme) do not have any cubane clusters in the small subunit. A physico-chemical characterization of the purified mutant enzyme is obviously required.

2.4. Hydrogenases linked to other enzymes

As briefly mentioned above, it becomes more and more evident that nickel hydrogenases, i.e. the basic structural unit required for the activation and oxidation of hydrogen, are often tightly attached to redox proteins having widely different functions. One example is the F_{420}-reducing hydrogenase from *M. thermoautotrophicum* [76,106,132], where hydrogenase is associated with a flavo-iron-sulphur enzyme able to reduced 8-hydroxy-5-deazaflavin (factor F_{420}). A second example is the soluble NAD^+-reducing hydrogenase from *A. eutrophus* and *Nocardia opaca* [174,177, 229]. These enzymes are in fact $H_2:NAD^+$ oxidoreductases composed of two enzyme units: a nickel hydrogenase and an NADH dehydrogenase. A third example is the formate-hydrogen-lyase system in *E. coli*, which has a built-in nickel hydrogenase (*E. coli* hydrogenase-3), a formate dehydrogenase, hydrophobic subunits for membrane anchoring, as well as subunits analogous to those of the mitochondrial NADH:Q oxidoreductase [27,167]. A fourth example includes Ni-hydrogenases that are linked to a cytochrome *b*, as discovered by Dross et al. [55] in *Wolinella succinogenes*. These enzymes are proposed to react with quinones [55]. A fifth example is the F_{420}-non-reducing hydrogenase from *Methanosarcina barkeri*, which is tightly attached to polypeptides forming a heterodisulphide reductase in this bacterium [97]. All this information illustrates that the Fe-S clusters involved in the electronic interface between part 2 and part 3 (Fig. 4), as well as the electro-chemical interface (part 3 of Fig. 4), can indeed be of variable composition.

2.5. Location of the hydrogen-activating site

The information provided above leads to a picture of nickel hydrogenases where the H_2-activating site involves nickel and is probably highly conserved and located in the large subunit. This picture is also intuitively based on the fact that EPR spectra and other properties of the nickel site in active hydrogenases are amazingly similar. It is reasonable, however, to assume that details around the H_2-activating site might determine properties like the K_m for hydrogen, apparent oxidation-reduction potential, accessibility for hydrogen, oxygen, CO, artificial electron acceptors, etc.

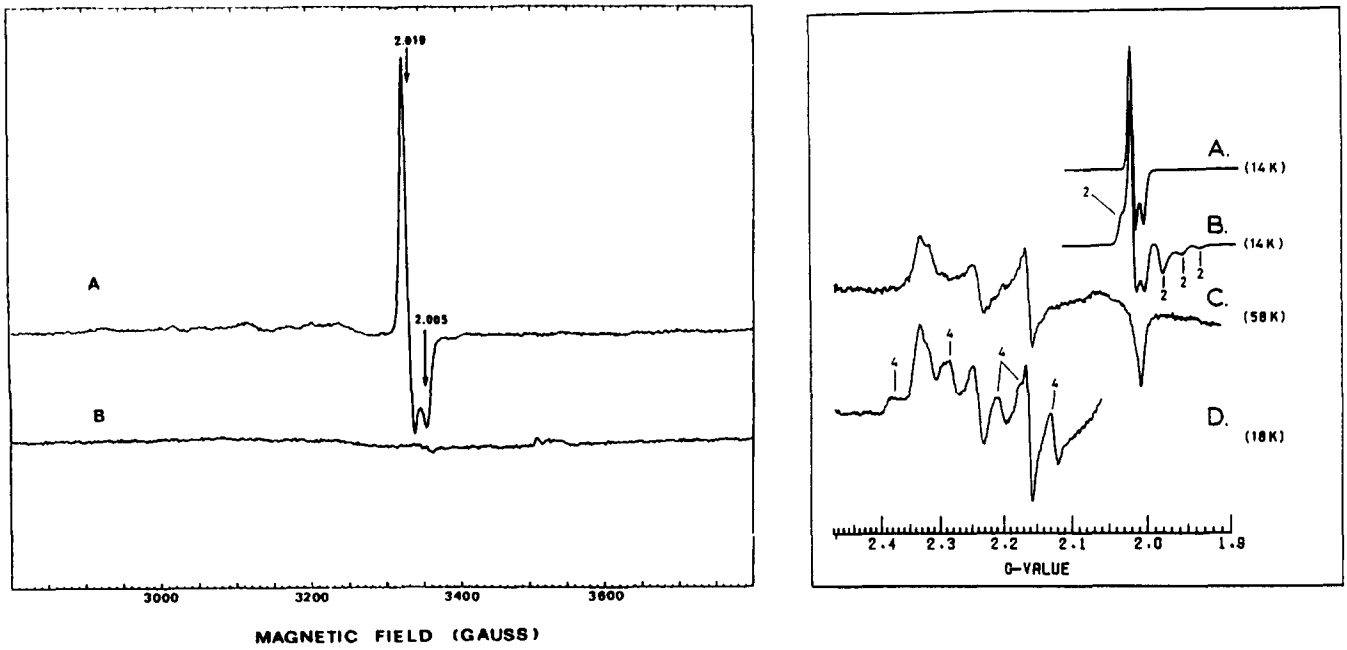

Fig. 8. EPR signals from *C. vinosum* hydrogenase. Left: enzyme from strain D prepared in the presence of 2-mercaptoethanol; (A) oxidized enzyme (11 K); (B) Enzyme reduced with H_2 (11 K); (From Strekas et al. [189] with permission). Right: enzyme from strain DSM 185; (A) oxidized, uncoupled (14 K); (B) oxidized, coupled (14 K); (C) as B, but at 58 K; (D) as B, but at 18 K; The lines marked with 2 and 4 are due to spin coupling. (From Albracht et al. [10].)

All nickel hydrogenases also have motifs 1S–3S in the small subunit in common, so this part might be essential as well. The remaining Cys-residues motifs in the small subunit are less uniform of architecture (accommodating either two atypical 4Fe clusters in motifs 4S–6S or two classical cubane clusters), or are not present at all. Hence, they cannot be essential for hydrogen activation.

3. Inspection of nickel hydrogenases in several states

3.1. Oxidized aerobic enzyme

Purified nickel hydrogenases all seem to contain about 1 Ni atom per molecule. Hydrogenase from *N. opaca* contains more nickel. In fact this enzyme is a complex of two activities, where the extra nickel ions are involved in the association of hydrogenase to an NADH dehydrogenase activity [177,229]. Many oxidized nickel hydrogenases, though not all, show a simple $S = 1/2$ EPR signal of Ni(III) (Fig. 1). One of the reasons that this EPR signal has been overlooked for quite some time is due to its rhombicity and the fact that it often goes hand in hand with an equally intense (same double integral) rather isotropic signal of a $[3Fe\text{-}4S]^{+}$ cluster with a very large amplitude. This sharp signal dominates the spectrum at $T < 20$ K and at the same scale the nickel signal is hardly detectable. The fact that two forms of Ni(III) with different EPR spectra are often present in many preparations further delayed recognition. A typical example is the spectrum of hydrogenase from *C. vinosum* published in 1980 by Strekas et al. [189] (Fig. 8, left-hand panel), where the nickel signals can be recognized if one looks along the base line. Yet another reason for escaping the attention of workers in the field has been that in a number of enzymes a spin coupling between the two forms of Ni(III) and a modified form of the 3Fe cluster leads to most complicated spectra [9,10] which can no longer be detected at $T > 40$ K (Fig. 8, right-hand panel). In some hydrogenases the Ni ions appear to be only partially (e.g. the *D. gigas* enzyme), or not at all (e.g. the NAD^{+}-reducing enzymes from *A. eutrophus* and *N. opaca*, and the enzyme from *D. baculatum*, formerly *D. desulfuricans*, strain Norway) EPR detectable in oxidized enzyme.

In aerobic solutions of most nickel hydrogenases the EPR signature, when present, of the nickel ion is very similar: a rhombic signal with g values between $g = 2$ and $g = 2.3$. There is agreement in the field (see, however, Bagyinka et al. [18]) that this is due to low-spin Ni(III), a $3d^7$ system, in an apparently rhombically-distorted octahedral ligand field, as first proposed by Lancaster in 1980 [124] (see [165] for a theoretical treatment). Similar spectra are observed in several well characterized Ni(III) model compounds [49,89,135, 146,190], some of which (e.g. [84]) are stable in air.

The majority of nickel hydrogenases are stable towards oxygen, although the presence of this gas completely prevents the activity of nearly all enzymes. Carbon monoxide is an inhibitor competitive towards hydrogen. In 'Knallgas' bacteria, which can thrive on a mixture of H_2, O_2 and CO_2, hydrogenase is apparently not hindered in its functioning by the presence of O_2. The soluble enzyme from the Knallgas bacterium *A. eutrophus* H-16, which contains FMN in addition to Fe and nickel, catalyzes the reduction of NAD^{+} by H_2. This reaction is not affected by CO or O_2 [174]. The oxidized enzyme cannot react with H_2, however, unless a catalytic amount of NADH is added. It was found [175] that in the presence of NADH and O_2 the enzyme rapidly denatured in an irreversible way due to the production of superoxide radicals. Even in intact cells inactivation of the soluble enzyme was observed under autotrophic growth conditions [173]. It is likely that in this enzyme the flavin can directly react with oxygen. The membrane-bound enzyme from *A. eutrophus*, which contains no flavin, can be 50% inhibited by 0.8 bar CO [170].

3.1.1. EPR signals of Ni(III) related to ready and unready enzyme

In a number of oxidized enzymes two distinct EPR signals of Ni(III) are observed, often within the same preparation (*D. gigas* [29], *C. vinosum* [9]; *Thiocapsa roseopersicina* [232] and the membrane-bound enzyme from *D. baculatus* [71,198]). The major difference in the EPR signals is the position of the g_y line of the rhombic signal: it can be either at $g = 2.24$ or at $g = 2.16$ (Fig. 8, right-hand panel, trace C). The reason and implications of this finding were not understood until 1985. In that year Fernandez et al. [70] elegantly demonstrated that enzyme preparations of *D. gigas* showing a Ni(III) signal with a g_y value of 2.16 were activated by hydrogen within a few minutes. Enzyme molecules with Ni(III) in a state, where the EPR signal showed a g_y line at 2.24, could be fully activated only after incubation under hydrogen for several hours. Therefore Fernandez et al. [70,71] termed enzyme in this state as 'unready' to react with H_2, whereas enzyme with Ni(III) in a coordination resulting in a $g_y = 2.16$ in the EPR spectrum was called 'ready'. The EPR signal of Ni(III) in unready enzyme has also been observed at room temperature [30], demonstrating that there is no change in coordination of the nickel upon freezing.

When dissolved in anaerobic buffer containing high-potential electron acceptors and subsequently incubated under H_2, the ready enzyme from *D. gigas* could not be converted to an active enzyme [70]. With low-potential electron acceptors activity was observed

within a minute. Such properties have now been found in many nickel hydrogenases: incubation of the ready enzyme in an H_2-containing anaerobic buffer with benzyl viologen leads to H_2-uptake activity within a short time (seconds to minutes), depending on the temperature. Unready enzyme needs incubation under H_2 for a long time (hours), often at elevated temperatures (30–50°C), before activity can be demonstrated in this way. Reduction with excess dithionite in the presence of methyl viologen usually leads to full activity of both forms within seconds, provided that the temperature is sufficiently high. As oxidized nickel hydrogenases are often a mixture of ready and unready enzyme, it is essential to completely activate preparations by reduction, before activity is determined.

In this review, nickel in 'ready' and 'unready' enzyme will be termed Ni_r and Ni_u, respectively. Nickel in active enzyme is called Ni_a.

3.1.2. An unknown redox component X: a special Fe ion?

Some oxidized hydrogenases show complicated EPR signals around $g = 2$, overlapping the simple $S = 1/2$ signal of the $[3Fe\text{-}4S]^+$ cluster (lines marked with '2' in Fig. 8, right-hand panel, trace B). These additional signals are not due to simple non-interacting $S = 1/2$ signals. This was first observed in 1978 [211] for the *C. vinosum* enzyme. Similar interactions have also been detected in enzymes from *Paracoccus denitrificans*, *Pseudomonas pseudoflava* [34] and the membrane-bound hydrogenase from *A. eutrophus* [28,114,176]. Van Heerikhuizen et al. [211,212] demonstrated that reduction of the *C. vinosum* enzyme in this state by ascorbate, in the presence of the redox mediator phenazine methosulphate, resulted in the disappearance of the interaction signal in the $g = 2$ region and a simultaneous increase of the signal of the 3Fe cluster (at that time regarded as a $[4Fe\text{-}4S]^{3+}$ cluster). The reverse was observed upon contact with excess of oxidized cytochrome *c* [212]. To explain these observations an oxidation/reduction of an -S-S- bridge, mediating an exchange interaction between the Fe-S cluster and an unknown paramagnet, was originally suggested. This would require the coupling/uncoupling to be an $n = 2$ redox process.

Some time later, inspired by the discovery of 3Fe clusters [59,111], Albracht et al. [8] considered the possibility that the redox-induced changes might involve a 3Fe/4Fe cluster conversion. Subsequently it was recognized [9,10] that the coupled nickel signal (lines marked with '4' in Fig. 8, right-hand panel, trace D) responded in a similar fashion. In the presence of a mediator cocktail the process titrated as a reversible $n = 1$ process in enzymes from *A. eutrophus* {membrane-bound enzyme; E'_0(pH 7.0) = +160 mV [176]}, *T. roseopersicina* {E'_0(pH 8.1) = +105 mV [36]}, *C. vinosum* strain D {E'_0(pH 7.0) = +160 mV [32]} and *C. vinosum* strain DSM 185 {E'_0(pH 8.0) = +150 mV [48]. Studies on *T. roseopersicina* hydrogenase with pulsed EPR (ESEEM) and LEFE (Linear Electric Field Effect) [37] did not provide any evidence for a conversion of the 3Fe cluster in the uncoupled state into a 4Fe cluster in the coupled state. To explain the coupling between Ni(III) and the 3Fe cluster, a special protein-bound Fe(III) ion, not incorporated in an Fe-S cluster, but situated between nickel and the $[3Fe\text{-}4S]^+$ cluster was proposed to mediate the magnetic interaction between the centres in this enzyme [36]. I will depict this redox equilibrium at this stage as:

$$Ni(III) = X^{ox} = [3Fe\text{-}4S]^+ \longleftarrow e$$

$$\longrightarrow Ni(III)\ X^{red}\ [3Fe\text{-}4S]^+$$

There are two additional observations connected to this equilibrium in the *C. vinosum* enzyme that are not understood: (i) The apparent *g* values of the Fe-S cluster drastically changed. The signal of the non-interacting $[3Fe\text{-}4S]^+$ cluster has true *g* values which are all greater than g_e (g_e being the free-electron value of 2.00232). The signal of the spin-coupled $[3Fe\text{-}4S]^+$ cluster (the lines marked with '2' in Fig. 8, right-hand panel, trace B) apparently has two *g* values greater that g_e and the other smaller than g_e. The position of all lines was dependent on the EPR microwave frequency [10,212]. (ii) The double-integrated intensity of the signals in the $g = 2$ region (Fe-S) increased upon coupling (27%; partial coupling) [11]. If the equilibrium is indeed an $n = 1$ redox reaction, then one might expect a two-fold increase in the intensity upon complete coupling. There was no change in the *g* values of the nickel. Spin coupling was observed for both ready and unready Ni(III) [10,48].

Recently, evidence has been provided indicating that nickel in the ready *C. vinosum* enzyme, but not in the unready enzyme, can rather tightly bind CO upon reduction to the divalent state [17,42]. Once reduced under 1 bar of CO, the apparent potential of nickel is shifted upwards to such an extent that excess of DCIP (E'_0 = +230 mV) was not able to oxidize the nickel to the trivalent state. This enabled the preparation of an enzyme where all redox groups were maximally oxidized, except for nickel, which was restrained in the divalent Ni(II).CO state. So when H_2-reduced, active enzyme was extensively treated with CO (whereby the H_2 was completely removed) and subsequently oxidized with excess DCIP, an EPR signal displayed in Fig. 9 (traces A and B) was obtained [42,192]. This result is strongly reminiscent of that obtained with enzyme treated in the same way in the absence of CO (Fig. 9, trace C). Apparently the the presence of $S = 1/2$ Ni(III) in trace C induces an extra two-fold splitting of all lines in Fig. 9 trace B. Disregarding the low-field line at 2.02, which is due to uncoupled [3Fe-

4S]$^+$ cluster, traces A and B, thus represents a simplified form of trace C: the interaction with $S = 1/2$ nickel has been removed by keeping the nickel in the diamagnetic Ni(II).CO state. Accurate comparison of X- and Q-band EPR spectra (Fig. 9, panel II) revealed that the high-field lines in traces A and B are slightly frequency dependent and hence do not represent true g values. A clear representation of the large electronic differences between the coupled and the uncoupled 3Fe cluster is given in Fig. 10 [192]. These experiments show that the unusual EPR signal (Fig. 10, trace C) does not involve nickel, but is due to a {X^{ox} = [3Fe-4S]$^+$} centre. The slight frequency dependence of the lines of the {X^{ox} = [3Fe-4S]$^+$} signal (Fig. 9, traces A and B), as well as its line shape (Fig. 10, trace C) argue against a simple $S = 1/2$ system. At 9 GHz the EPR lines do follow Curie behaviour, however, between 8 K and 20 K [10], like that of a non-interacting $S = 1/2$ system. Its Mössbauer features do not follow Curie behaviour between 1.5 K and 4.2 K [192]. This points to low-lying excited states and argues against a simple $S = 1/2$ system. Clearly, the {X^{ox} = [3Fe-4S]$^+$} centre is quite a mysterious system.

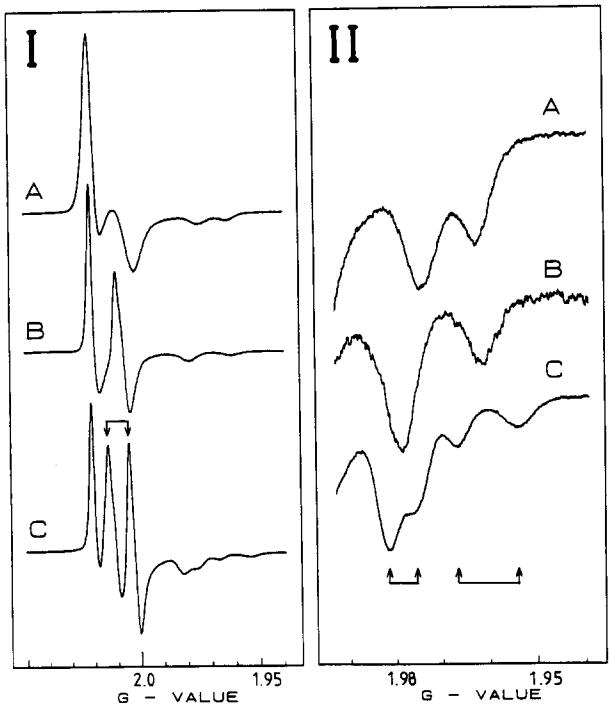

Fig. 9. Influence of the S = 1/2 system of Ni(III) on the EPR spectrum of the {X^{ox} = [3Fe-4S]$^+$} centre in *C. vinosum* hydrogenase. (A) Enzyme in the oxidized state with nickel clamped in the divalent Ni_a(II).CO state (9 GHz, 14 K). (B) As A, but spectra at 35 GHz (21 K). (C) 35 GHz spectra at 16 K of a sample containing nickel as Ni(III). The arrows indicate the splittings caused by the S = 1/2 system of Ni(III). Panel II shows enlargements of the high-field lines of the spectra in panel I. The sharp line around $g = 2.02$ is from a [3Fe-4S]$^+$ cluster in enzyme molecules which did not show coupling. (From Surerus et al. [192].)

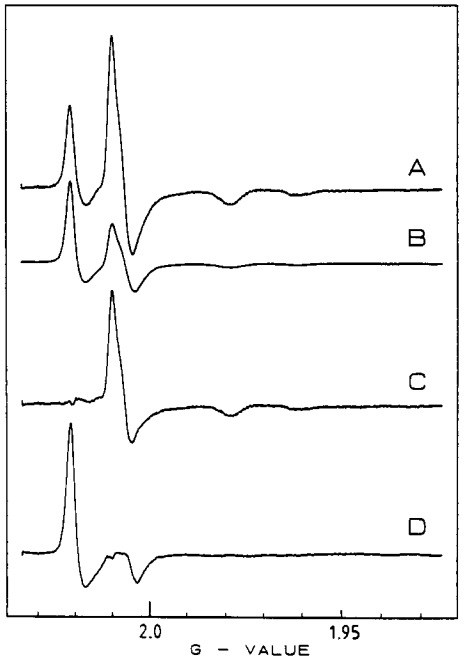

Fig. 10. Comparison of the 35 GHz EPR spectra at 19 K of the [3Fe-4S]$^+$ cluster (D) and the {X^{ox} = [3Fe-4S]$^+$} centre (C) in oxidized *C. vinosum* hydrogenase, in which nickel is in the Ni_a(II).CO state. Spectra were obtained by comparison of spectra from two preparations (A and B) with greatly different ratios of the coupled and the uncoupled state. (From Surerus et al. [192].)

When the 3Fe cluster is part of the {X^{ox} = [3Fe-4S]$^+$} centre, then the Ni(III) centre can weakly couple, indicating that the effective distance between the two centres is within 'coupling range' (not more than about 1 nm). In the uncoupled state, however, the Ni(III) does not notice the spin of the [3Fe-4S] cluster, or the change of its spin state upon reduction: the power saturation curve of Ni(III) remains the same [29]. A recent and more detailed study confirmed this point [16]. The spin-lattice relaxation rate of Ni(III) in hydrogenase of *D. vulgaris* Miyazaki and *D. gigas* did not change upon reduction of the 3Fe cluster from the $S = 1/2$ state to the $S = 2$ state. The authors concluded that the nickel and the 3Fe cluster would be at least 1 nm apart in these enzymes.

Extensive Mössbauer studies [192] of the *C. vinosum* enzyme in the Ni(III) = {X^{ox} = [3Fe-4S]$^+$} and the Ni(II).CO {X^{ox} = [3Fe-4S]$^+$} states showed identical, highly unusual Mössbauer features not observed in any Fe-S protein before. Thus, both in EPR and Mössbauer spectra the familiar features of the 3Fe cluster were considerably changed in enzyme with the {X^{ox} = [3Fe-4S]$^+$} centre. In the uncoupled state, however, 27% of the iron was present in a Mössbauer spectrum typical for such a cluster. This means that oxidation of the group X has a drastic effect on the electronic state of the 3Fe cluster. In the *C. vinosum* enzyme no other metals than Ni, Fe and Cu could be detected by

Neutron-Activation analysis in quantities of importance. Removal of the Cu had no effect on the specific activity, EPR or Mössbauer spectra (Albracht, S.P.J., unpublished observations). Since X seems to be a one-electron redox component, one possibility would be [36] that it is an extra Fe site shuttling between low-spin paramagnetic Fe(III) and low-spin diamagnetic Fe(II) at an E'_0 value of + 150 mV. The Mössbauer data on the *C. vinosum* enzyme [192] provide some evidence for such a putative Fe site, but are certainly not conclusive. The large absorption of the cubane clusters and the fact that no complete coupling could be accomplished with the *C. vinosum* hydrogenase thus far hindered proper characterization of the $\{X^{ox} = [3Fe\text{-}4S]^+\}$ centre in this enzyme. As the properties of the 3Fe cluster are so drastically changed when the putative Fe ion is oxidized, there is probably quite a close connection between the two.

From detailed EXAFS studies on the *T. roseopersicina* enzyme Maroney et al. [137] suggested the presence of Fe atoms at distances of 4.3 Å and 6.2 Å from nickel. In this case the Fe atoms were supposed to be due to a novel Ni,Fe,S cluster.

The studies discussed thus far point to a putative model depicted in Fig. 11 which might serve as a source of inspiration for further experiments. It must be stressed at this point, that at present the evidence that X would be a special Fe ion is just emerging and is not convincing yet, hence I will refer to it as the putative iron.

A most puzzling observation with the *C. vinosum* enzyme might be mentioned at this point. The spin intensity of both the spin-coupled $Ni_{r,u}(III)$ and the $\{X^{ox} = [3Fe\text{-}4S]^+\}$ centre simultaneously decrease when 1 mM 2-mercaptoethanol is added [10,212]. There was hardly any effect on the signals of the uncoupled Ni(III) and the $[3Fe\text{-}4S]^+$ cluster. The effect of 2-mercaptoethanol has also been observed with the membrane-bound enzyme from *A. eutrophus* enzyme and enzymes from several other aerobic hydrogen bacteria [28,176]. This phenomenon is as yet not understood.

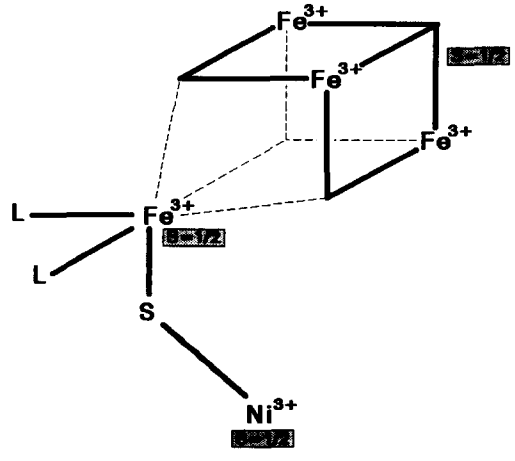

Fig. 11. Possible configuration of Ni, the putative Fe and the [3Fe-4S] cluster in oxidized *C. vinosum* hydrogenase.

3.2. Overview of redox and activity states of nickel hydrogenases

As described in detail in the subsequent sections, the results of activity measurements and redox titrations reported thus far for nickel hydrogenases can be accommodated into a general scheme (Fig. 12). In inactive enzyme, showing EPR signals of $Ni_r(III)$ and/or $Ni_u(III)$, only a Ni(III)/Ni(II) transition can be observed in the presence of mediating redox dyes. There is no further reduction, provided that 'reductive activation' is prevented by keeping the temperature low. In many enzymes also reversible redox changes of X and the 3Fe cluster are observed. In active enzyme a transient EPR signal from a state called Ni-C or $Ni_a(I).H_2$ is observed in the presence of dyes. Also, reversible oxidation of the cubane clusters occurs. No oxidation to Ni(III) can be observed if 'oxidative inactivation' is prevented by working at low temperatures. In the absence of dyes the only reversible reaction of H_2 with the enzyme is the one with active enzyme: the EPR signal of $Ni_a(I).H_2$ disappears with increasing H_2 concentration in an $n = 2$ Nernst reaction; the Fe-S clusters remain reduced. The inactive and active states of the enzyme are not in equilibrium at low temperature (4°C), not even in the presence of a mixture of mediating dyes. At higher temperatures (20–50°C), however, this transition occurs much faster and this has hindered a proper interpretation of earlier redox titrations, which were usually carried out at room temperature.

3.3. Reduced states of the enzyme

3.3.1. Reduction of Ni(III) and the $[3Fe\text{-}4S]^+$ cluster (inactive enzyme)

In redox titrations in the presence of mediating dyes, it has been established [4,28,29,32,34,36,48,64,195,199] that the $[3Fe\text{-}4S]^+$ cluster titrates as an $n = 1$ species with E'_0 values between −75 mV and + 40 mV at pH 7.0. For the Ni(III)/Ni(II) equilibrium E'_0 values between −410 mV and −110 mV were reported. The midpoint potential of Ni(III), but not that of the 3Fe cluster, was found to be dependent on the pH by −60 mV per pH unit, hence the equilibrium can be written as:

$$Ni(III).E + H^+ + e \longleftrightarrow Ni(II).EH^+$$

Curiously enough, only the values for the unready nickel have been reported for enzymes other than the *C. vinosum* hydrogenase. The ready form of nickel did not titrate in a reversible way in the *D. gigas* enzyme

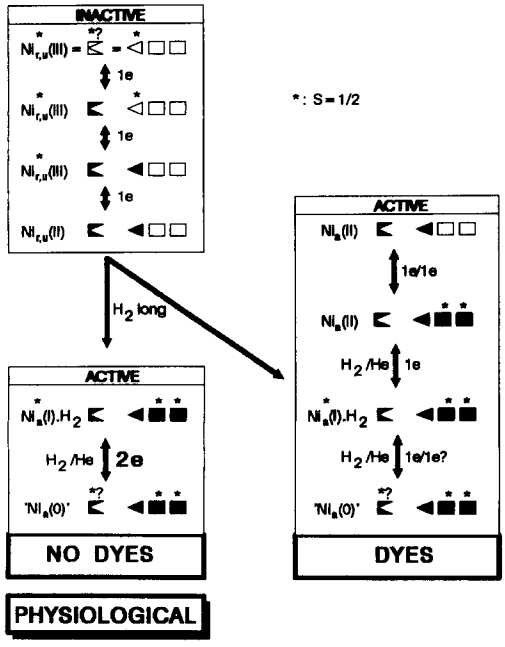

Fig. 12. Redox states of standard nickel hydrogenases. Squares represent [4Fe-4S] clusters; triangles stand for a [3Fe-4S] cluster; the unknown redox group is indicated by the square with a missing triangle portion. Blank symbols stand for oxidized species, black symbols for reduced species. An asteriks indicates a $S = 1/2$ system; the '=' sign stands for spin coupling. 'H_2 long' means a long incubation under hydrogen.

[34,195]. Coremans and coworkers [48] have shown for the *C. vinosum* enzyme that both the $Ni_u(III)$ and the $Ni_r(III)$ titrate as reversible $n = 1$ species when the titration was carried out at 30°C. When corrected for a slow unready to ready conversion during the titration, the apparent midpoint potentials of both forms of nickel was indistinguishable (Fig. 13). When the titration was performed at 2°C, however, the reduction of $Ni_r(III)$ was no longer reversible, whereas the $Ni_u(III)$ form and the $[3Fe\text{-}4S]^+$ cluster could still be oxidized smoothly. So at 2°C the *C. vinosum* enzyme behaved similarly to the *D. gigas* enzyme. Apparently, after reduction of $Ni_r(III)$ there are additional events in the protein prohibiting subsequent re-oxidation of nickel by dyes at 2°C.

3.3.2. Redox properties of nickel in active versus inactive enzyme

For the F_{420}-non-reducing hydrogenase from *M. thermoautotrophicum* it was found [45] that the EPR-silent state of nickel can occur in two completely different activity states of the enzyme (Fig. 14), one being active and the other being not active. These states were not in equilibrium. Starting with unready enzyme in the inactive oxidized state (Fig. 14, upper panel), the $Ni_u(III)/Ni_u(II)$ couple titrated as a reversible $n = 1$ redox component with $E'_0 = -140$ mV at pH 6. Provided that the temperature was kept at 15°C or lower, no other signals from nickel were observed down to −350 mV even after prolonged times (hours). Likewise, 1 bar of H_2 for 1 h did not induce any other Ni signals. Upon rising the potential the $Ni_u(III)$ EPR signal re-appeared. Under no condition the low H_2-uptake activity (3.5% of the maximal attainable activity) changed.

When the *M. thermoautotrophicum* enzyme was first fully activated by incubation under H_2 for some hours, then redox titrations (Fig. 14, lower panel) showed the bell-shaped curve of the EPR signal of Ni-C (optimium at −250 mV, pH 6.0, 45°C, representing about half of the total Ni), an observation very similar to that reported earlier for the *D. gigas* enzyme [29,33,195,199]. The potential was set either by the H_2-partial pressure (−380 mV to −200 mV) or by $K_3Fe(CN)_6$/dithionite (−200 mV to −50 mV). In this case no EPR signals from Ni(III) could be detected within this potential span and the enzyme activity was always high (100% between −200 mV and 0 mV, but decreasing to 70% on going to lower potentials). So with this enzyme there is the interesting situation that in the presence of mediating dyes at −250 mV the enzyme can be either EPR silent and inactive or it can show a maximal Ni-C signal and is active. Likewise at −50 mV it can be either inactive and show a maximal $Ni_u(III)$ EPR signal or it can be EPR silent and maximally active.

With this enzyme it has also been shown [45,46] that when unready enzyme was titrated from high to low redox potentials at a higher temperature (45°C at pH

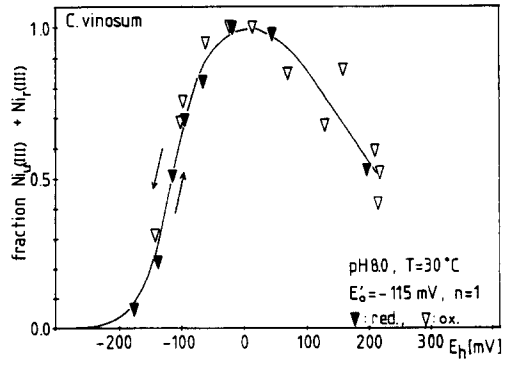

Fig. 13. Redox titration of $Ni_{r,u}(III)$ in hydrogenase from *C. vinosum* at pH 8.0 and 30°C in the presence of dyes. The total Ni(III)-signal intensity $\{Ni_r(III) + Ni_u(III)\}$ observed at 42 K is plotted against the potential. The decrease at potentials greater than 0 mV is due to spin coupling to the $\{X^{ox} = [3Fe\text{-}4S]\}$ centre, which causes the disappearance (relaxation broadening) of the nickel signal at 42 K. Black symbols: reductive titration; blank symbols: oxidative titration. (Modified from Coremans et al. [48].)

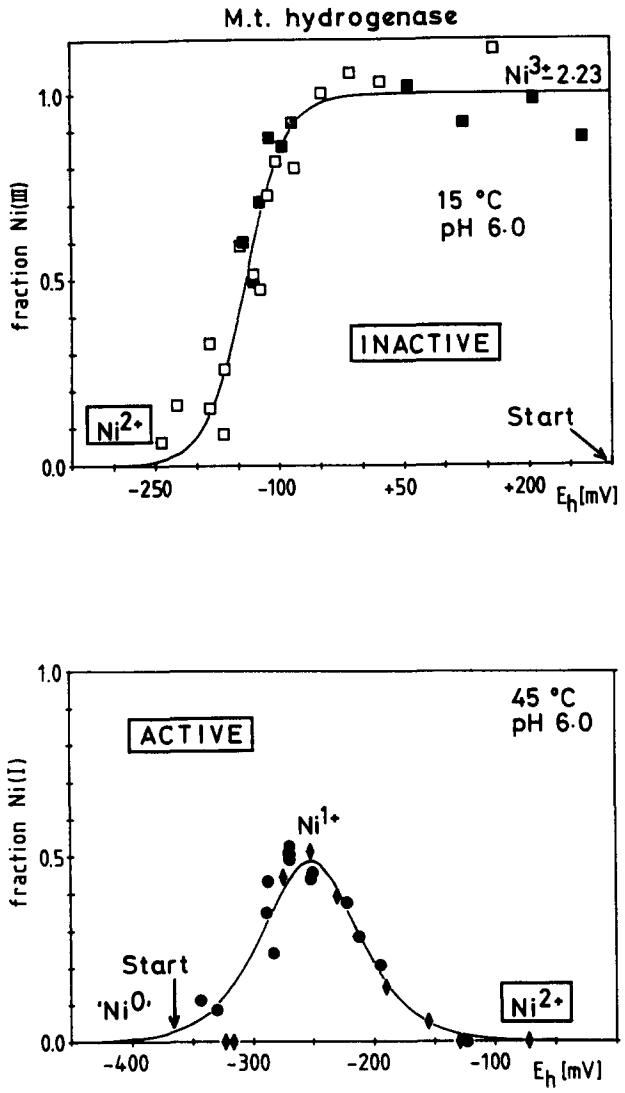

Fig. 14. Redox titrations (dyes present) of active and inactive F_{420}-non-reducing hydrogenase from *M. thermoautotrophicum*, strain Marburg. The upper panel shows a titration of Ni_u(III) at pH 6.0 and 15°C. In the lower panel the behaviour of the Ni_a(I).H_2 species at pH 6.0 and 45°C is shown. The different symbols represent either reductive or oxidative titrations. (Modified from Coremans et al. [45].)

6), then a Ni-C signal developed before the Ni_u(III) signal had completely disappeared (due to reductive activation of part of the enzyme molecules). When starting from reduced active enzyme, the Ni_u(III) signal slowly re-appeared (45°C, pH 6) in a time-dependent non-equilibrium manner upon rising the potential (due to oxidative inactivation).

Clearly the switch between the active and inactive form of the enzyme is what is generally known as the 'reductive activation'. Apparently, the enzyme from *M. thermoautotrophicum*, a microorganism optimally growing at 65°C, cannot quickly switch from active to inactive and back at temperatures at or below 15°C. Hence it was possible to determine the properties of both states independently. These experiments demonstrate that the apparent redox properties of nickel in both states are greatly different.

C. vinosum grows optimally around 30°C. The redox titrations of Ni(III) at 30°C and pH 8 showed that the conversion of Ni_u(III) to Ni_r(III) is a slow process under these conditions [48]. At 2°C this conversion did not take place but then the reduction of Ni_r(III) was irreversible. Both at pH 6 and pH 8 a drop in H_2-uptake activity (assayed at 30°C) was noticed when Ni_r(III) was reduced at 2°C. Activity increased again under conditions where the Ni-C signal appeared (H_2, 45°C at pH 6; at pH 8 some Ni-C signal slowly developed at 2°C already, at potentials lower than −100 mV).

These findings suggest that even reduction of Ni_r(III) to Ni_r(II) in the presence of dyes at 2°C is not giving rise to rapid formation of active enzyme. On the contrary, an *inactive* state of the enzyme was encountered under these conditions. So, an enzyme with {Ni_r(III); X^{red}; $3Fe^{red}$; $2x4Fe^{ox}$} readily gave rise to H_2-uptake activity under the usual assay conditions (H_2, benzyl viologen, anaerobic, 30°C), whereas one with {Ni_r(II); X^{red}; $3Fe^{red}$; $2x4Fe^{ox}$} prepared at 2°C behaved inactive in such an assay. The reason for this is not understood.

It is worthwhile mentioning in this respect that it has been observed for the *D. gigas* enzyme [72] that upon contact of the oxidized anaerobic enzyme with H_2 the EPR signals of Ni_u(III) and the $[3Fe\text{-}4S]^+$ cluster disappeared and a broad signal ascribed to the reduced cubane clusters appeared within 5 min. The preparation was still inactive. Activity could only be measured after 2–4 h and this was accompanied by the appearance of the Ni-C signal. Redox titrations (in the presence of dyes) showed that the cubane clusters have E'_0 values in the range on −290 to −350 mV (−350 mV [33]; −290 mV for one cluster and −340 mV for the other one [199]). Maximal Ni-C signal was obtained in the range of −270 mV to −390 V. This indicates that in the presence of H_2 (no dyes present) the enzyme experienced the reductive power of H_2, enabling extensive reduction of the cubane clusters, before the actual ready to active transition had taken place. Apparently this redox-linked process is not in rapid redox equilibrium with the cubane clusters under these conditions. It demonstrates again that this transition is a slow process.

3.3.3. Redox behaviour of Ni_a(I).H_2 ('Ni-C')

Once over the barrier ('reductive activation') all nickel hydrogenases examined so far show the Ni-C EPR signal [12,29,62,112,144,176,196–198,206]. The Ni-C signal in the enzyme from *C. vinosum* has also been observed at room temperature (Chen, M. and

Albracht, S.P.J., unpublished observations), excluding any freezing artifact. The unpaired spin causing this signal showed considerable nickel-hyperfine interaction in ^{61}Ni-enriched preparations [33,112,144]. Therefore the signal was ascribed to nickel. It was first reported by Moura et al. [144] in the *D. gigas* enzyme and interpreted by these investigators as another form of Ni(III). Being the third signal detected for nickel in hydrogenases, it is often called Ni-C (g_{xyz} = 2.19, 2.16, 2.02). In redox titrations (mediating dyes, room temperature) the signal follows a bell-shaped curve and disappeares virtually completely both at low and high redox potentials (Fig. 14). The signal has also been observed in the absence of mediators. Kojima et al. [112] reported that when the F_{420}-reducing hydrogenase from *M. thermoautotrophicum*, strain ΔH was fully reduced with H_2, then the Ni(III) signal (Ni_u(III) as we now know) of the oxidized enzyme disappeared completely. When the H_2 gas was subsequently replaced by Ar a new rhombic signal (g_{xyz} = 2.196, 2.14, 2.01) appeared. As removal of H_2 means a rise in redox potential, the authors suggested the new signal to be due to a different form of Ni(III), although they did not exclude Ni(I), a $3d^9$ system, as the possible cause for the new signal.

Similar phenomena were observed with the *C. vinosum* enzyme [206]. In addition it was found with this enzyme that rigorous removal of H_2 resulted in the slow disappearance of the new signal, with no other Ni-signals showing up. The transient signal was ascribed here to Ni(I). In retrospect, it was probably Krasna [116] who first observed these EPR signals in dithionite-reduced *C. vinosum* hydrogenase. The reported signals at g = 2.2, 2.125 and 2.06 probably reflected a mixture of the 'dark' and 'light' signals of Ni-C (see later). Although this third nickel signal is usually called the Ni-C signal, I will also refer to nickel in this state as Ni_a(I).H_2 to indicated that: (i) the nickel centre is one electron more reduced than Ni(II); (ii) the enzyme is in its active state; (iii) hydrogen is bound to the nickel centre in this state.

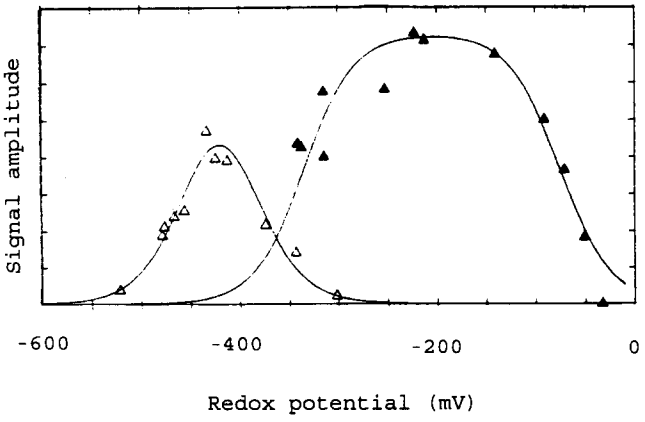

Fig. 15. Effect of the pH on the redox behaviour of the Ni_a(I).H_2 species of *D. gigas* hydrogenase. Open points: redox titration at pH 8.1. Filled points: redox titration at pH 5.7. The lines are composed of two overlapping theoretical n = 1 Nernst plots. (Modified from Cammack et al. [33] with permission.)

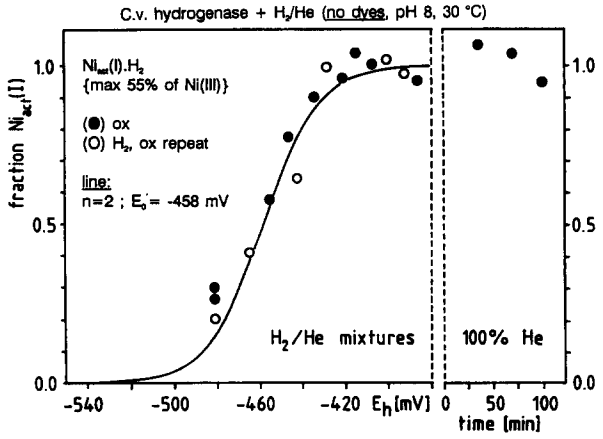

Fig. 16. Effect of the redox potential, set by the hydrogen-partial pressure, on the Ni_a(I).H_2 species in *C. vinosum* hydrogenase at pH 8.0 and 30°C. The solid line is a theoretical n = 2 Nernst curve with a midpoint potential of −458 mV. The titration was performed from high to low partial pressures of hydrogen (black symbols: first time; blank symbols: second time). Even 1.5 h after complete removal of hydrogen, the signal persisted (right-hand panel). (Modified from Coremans et al. [47].)

Cammack et al. [33] have studied the pH dependence of the redox properties of the Ni-C species and showed that the positions of the two slopes of the bell-shaped curve (see Fig. 15) had a different dependence. The low-potential slope moved with −60 mV per pH unit, whereas the high-potential slope moved with −120 mV per pH unit. Consequently a plateau was reached at lower pH values. The low spin concentration at pH 8.1 of nickel in this state (50–60%) was explained by the overlap of the two n = 1 reactions; in agreement with this explanation, more intensity (90–100%) was observed at pH 6.

Although the Ni-C signal has a transient nature in redox titrations in the presence of dyes in all enzymes studied thus far, this is not a true representation of the equilibrium of the enzyme with hydrogen: it is an artifact induced by the dyes. Coremans et al. [47] have shown that active nickel hydrogenases from *C. vinosum* and *M. thermoautotrophicum* strain Marburg are, as expected, in redox equilibrium with the substrate H_2 also in the absence of mediating dyes. In this case, however, the Ni-C EPR signal titrated as an n = 2 redox component (Fig. 16). Even in intact cells of *M. thermoautotrophicum* strain Marburg the Ni-C signal responded in this way [47]. Hence, this reflects the true way in which the enzyme reacts with H_2. Recently, it was reported that the *D. gigas* enzyme presumably behaves similarly [161].

The findings of Coremans et al. [47] have important implications for our thinking about the enzyme. First it is the enzyme displaying the signal characterized to be due to a reduced nickel centre with bound hydrogen [206] (see later), $Ni_a(I).H_2$ or Ni-C, which reacts with H_2, whereby two reducing equivalents are taken up by the enzyme, resulting in the disappearance of the signal of Ni-C. This means that the Ni-C centre, being an $S = 1/2$ system, takes up one electron and that the second electron has to go somewhere else. Coremans et al. [47], taking into account extensive redox-titration studies (dyes present) of Teixeira et al. [199] on the *D. gigas* enzyme, considered one of the low-potential [4Fe-4S] clusters to be a possible candidate for the second electron. In the same report [47] it was also mentioned, however, that the broad EPR signals observed in active enzyme at 4.2 K and ascribed to the cubane clusters, did not noticeably depend on the applied redox potential. This confirmed earlier observations of Van der Zwaan et al. [208,209] who also found that the broad EPR signals did not change when H_2-reduced enzyme was incubated with Ar for a short time (to obtain a large Ni-C signal) or a very long time (when virtually no Ni-C signal was left). Likewise, when H_2-reduced enzyme (no dyes) was extensively treated with CO in the absence of H_2, whereby the initially formed $Ni_a(I).CO$ signal disappeared completely [207], presumably by oxidation to Ni(II) (see later), the broad signals did not noticeably change [209]. This argues against a role of the cubane clusters in the reversible reaction of the active enzyme with H_2 (no dyes). The 3Fe cluster is also discounted, since it remains reduced all the time. It is questionable, therefore, whether Fe-S clusters are involved at all in the $n = 2$ redox equilibrium of H_2 with the enzyme. This is another reason for involving an unkown redox component in the enzyme (Fig. 12) which can take up the second electron.

Mössbauer spectra at 50 K of the H_2-reduced *C. vinosum* enzyme [192] could not be satisfactorily simulated as a summation of one $[3Fe\text{-}4S]^0$ cluster and two $[4Fe\text{-}4S]^+$ clusters (Fig. 17). The difference between the experimental spectrum and the simulation (Fig. 17, traces b) amounted to about 8% of the total absorption of the sample. This would be equivalent to roughly 1 Fe atom with a surprisingly small isomer shift of $\delta =$ 0.05–0.15 mm/s. This species was not observed after oxidation with benzyl viologen. This is an indication that the unknown redox component might be iron, possibly the putative extra Fe atom discussed before. In view of the absence of 4Fe clusters in the small subunits of soluble hydrogenase of *A. eutrophus* (and hydrogenase-3 of *E. coli*), a study of the equilibrium reaction of H_2 with the readily available *Alcaligenes* enzyme might shed further light on this problem.

A second important implications of the equilibrium of the $Ni_a(I).H_2$ state with H_2 is that there must be a second site for H_2 binding. It is assumed [47] that this site represents the real catalytic site where hydrogen is activated under turnover conditions.

3.3.4. Binding of hydrogen and carbon monoxide to $Ni_a(I)$

Van der Zwaan et al. [206] discovered the binding of hydrogen to nickel via the light sensitivity of the enzyme in this state at temperatures below 77 K. This has been found to be a general property of nickel hydrogenases. Also CO can bind to the nickel centre in this state [33,207,210]. Fig. 18 summarizes the relevant evidence from EPR. The Ni-C signal (dark signal) in the *C. vinosum* enzyme is converted into two slightly different EPR signals (light signals) after illumination of the sample with white light (Fig. 18, lower traces). The F_{420}-reducing and the F_{420}-non-reducing hydrogenases from *M. thermoautotrophicum* [13,208,209] and the enzyme from *D. gigas* [107] show only one light-induced signal. The reaction, carried out in the temperature range of 4.2–60 K, was nearly 6-fold slower, when the Ni-C state of the *C. vinosum* enzyme was prepared in a D_2O/D_2 environment, whereas the only isotope effect on the EPR spectra was a small sharpening of the lines of Ni-C (maximally 0.5 mT in the g_y) [206]. Carbon monoxide, an inhibitor competitive towards H_2, gave a

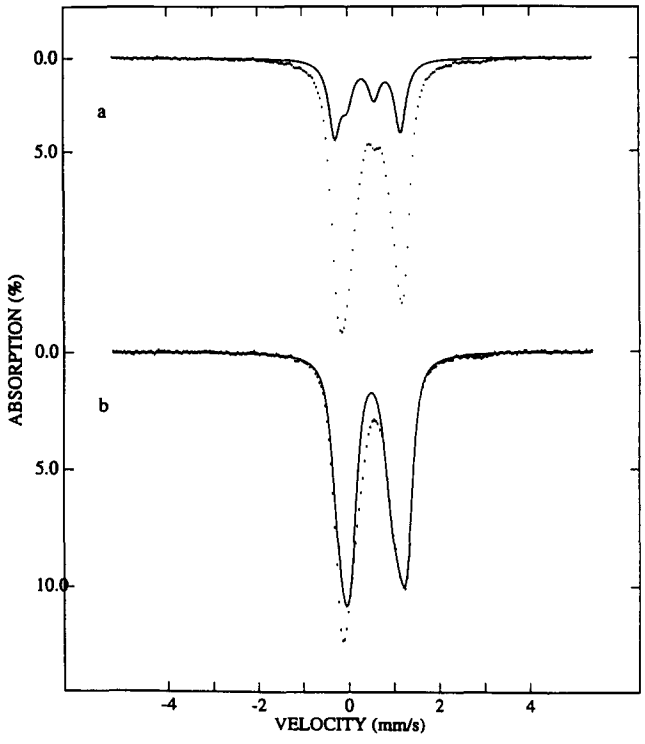

Fig. 17. Zero-field Mössbauer spectrum at 50 K of *C. vinosum* hydrogenase reduced with 1 bar of H_2 (dotted spectrum in (a)). The solid line in (a) is a theoretical spectrum of the $[3Fe\text{-}4S]^0$ cluster. The dotted spectrum in (b) was obtained by subtracting the theoretical spectrum of (a) from the data of (a). The solid line in (b) is a superposition of two quadrupole doublets, representing the two reduced 4Fe clusters. (From Surerus et al. [192].)

different EPR signal. The CO compound was likewise light sensitive (Fig. 18, middle traces). Illumination resulted in an EPR spectrum virtually identical to that obtained after illumination of the Ni-C state. With CO, no effect on the rate of the light-induced reaction or the line widths could be found when prepared from a D_2O/D_2 incubated enzyme. The nearly isotropic superhyperfine splitting of 3 mT from ^{13}CO ($I = 1/2$) provided direct evidence for spin density of the unpaired electron on the C-nucleus (Fig. 18, upper traces). After photodissociation no such splitting was observed anymore, in agreement with the proposed breakage of a Ni-CO bond. Based on these experiments it was proposed [210] that $Ni_a(I)$ can bind H_2 or CO at the same axial position. Although it was initially thought that a simple hydride might be the ligand [206], such a possibility was dismissed when it was brought to our attention that model complexes of $Ni(I).H^-$, with a hydride in axial position showed a strong nearly isotropic superhyperfine splitting of 10 mT [143].

Since 1984 it has become clear that, as discovered by Kubas et al. [118], in a number of model compounds of transition metals molecular hydrogen can act as a ligand [50,98,119] in a side-on configuration [164]. This led Crabtree [50] to propose that dihydrogen might well be a ligand to Ni(III) in hydrogenases. Van der Zwaan et al. [210] favoured binding of dihydrogen to $Ni_a(I)$.

As the g_z of the $Ni_a(I).H_2$ signal is very close to g_e and $g_{xy} > g_z$, it has been assumed [210] that the unpaired spin is in an orbital with a large d_z2 character [223]. Model complexes show that the unpaired spin can then sense the presence of magnetic nuclei in axial position, as evident from EPR spectra with anisotropic superhyperfine splitting in the g_z line in case of dipolar coupling (e.g. [84]), or isotropic hyperfine splitting in the case of exchange interaction (e.g. [143]). The nearly isotropic superhyperfine splitting of the bound ^{13}CO was explained in this way [210]: mixing of the sp-hybrid of the C atom with the d_z2 orbital of the nickel can give the unpaired electron a finite spin density on the ^{13}C nucleus. After photodissociation of the CO, spectra were obtained where the lowest g value is 2.05. This indicates that the unpaired spin is no longer in an orbital with a d_z2 character. It was explained by assuming that the relative energy of the d_z2 orbital in a d^9 system dropped below that of the $d_{x^2-y^2}$ (or even the d_{xy}) orbital. This could result in the observed changes in the EPR spectrum giving spectra with $g_{xy} < g_z$, whereas none of the g values is close to g_e [165,223]. Oxidation of this state to Ni(III) would then result in the electronic configuration $xy(2)$, $z^2(1)$, $x^2 - y^2(0)$ and would explain the EPR spectrum of the trivalent nickel with one of the g values close to 2.

Although the bond between nickel and hydrogen or CO is broken by illumination, the latter molecules stay close to the nickel centre. The reaction is easily carried out at 4.2 K. Warming of the sample to about 200 K in the dark results in a rebinding within 10 min [206,207,210]. Cammack and coworkers [39] have noticed for the *D. gigas* enzyme that the re-appearance of the Ni-C signal at high temperatures, after illumination at low temperatures, was also five-fold slower when the Ni-C signal was produced in D_2O/D_2.

The binding of hydrogen has also been probed with ESEEM [39] and ENDOR [60]. For the *D. gigas* enzyme [60] magnetic interaction of the unpaired spin in the Ni-C state with at least two types of proton has been demonstrated. One type of proton showed a 16.8 MHz splitting, whereas the other type of interaction was much weaker (4.4 MHz). Both types of proton

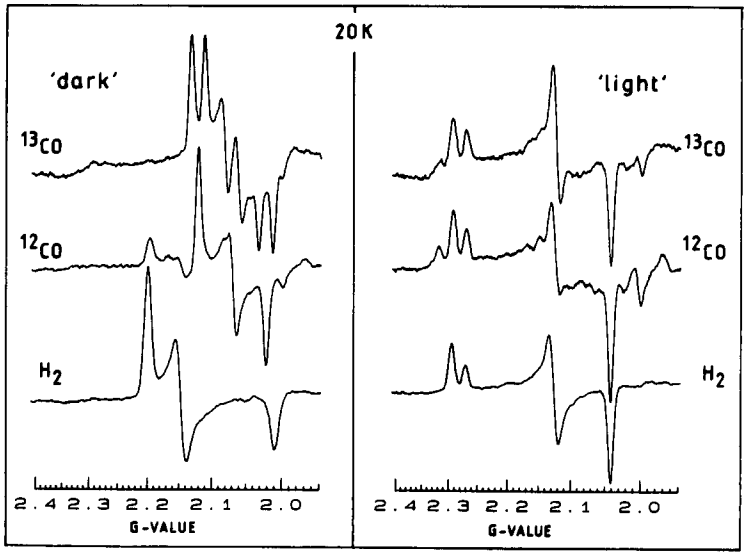

Fig. 18. Binding of hydrogen and ^{13}CO to $Ni_a(I)$ in hydrogenase from *C. vinosum* and the effect of illumination at 20 K. (From Van der Zwaan et al. [210].)

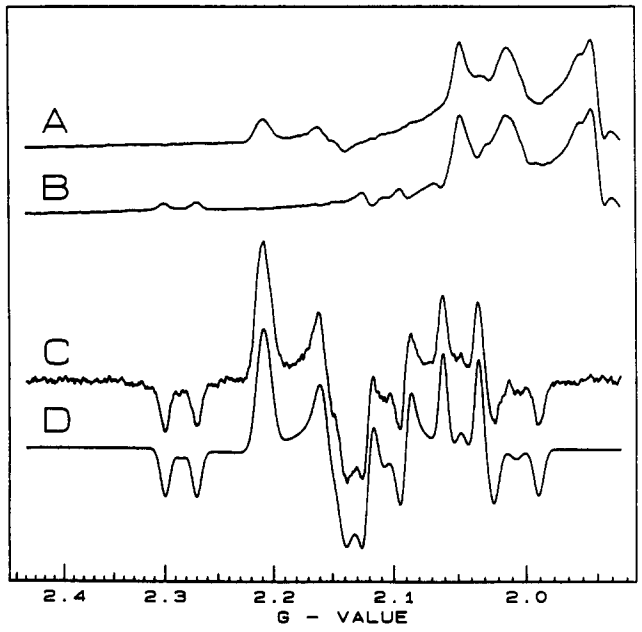

Fig. 19. EPR spectra at 35 K of F_{420}-non-reducing hydrogenase from *M. voltae*, 92% enriched in ^{77}Se, under 5% H_2. (A) Spectrum of dark-adapted sample; (B) Spectrum after illumination with white light; (C) Difference spectrum A minus B; (D) Computer simulation. (From Sorgenfrei et al. [184].)

could be exchanged in D_2O only in the active state of the enzyme. Upon oxidation by air only the weak coupling persisted [39,60]. No apparent changes were observed in the ESEEM studies upon illumination of the Ni-C state [39].

Maroney and coworkers [225] have repeated and extended the ENDOR measurements with the *T. roseopersicina* hydrogenase. As in the *D. gigas* enzyme, at least two types of interacting protons could be observed in the Ni-C state, one with 20 MHz, the other with 12 MHz. The former protons, but not the latter ones, were solvent exchangeable. After illumination at temperatures below 77 K, the 20 MHz coupling disappeared. Upon warming to 200 K in the dark, this coupling appeared again. One can conclude that the 16–20 MHz protons are the same as those responsible for the 0.2–0.5 mT broadening of the EPR signals of $Ni_a(I).H_2$ in the *C. vinosum* enzyme [206] and the *D. gigas* enzyme [52]. These protons originate from hydrogen binding to nickel. The 12 MHz protons in the *T. roseopersicina* enzyme displayed an isotropic coupling and were ascribed to β-CH_2 protons from a cysteine residue [225].

The model [210] in which dihydrogen is in axial position of a monovalent nickel with its unpaired spin in a d_z2 orbital, does still not provide a comfortable explanation for the minute light-sensitive hyperfine interactions observed by EPR and ENDOR. A possible answer to this dilemma came from studies on ^{77}Se-containing F_{420}-non-reducing hydrogenase from *M. voltae* [183,184] (Fig. 19). It was found that the unpaired electron in the both the dark and the light-induced Ni-C state had considerable hyperfine interaction with ^{77}Se (Figs. 19 and 20).

This cannot be explained in the model of van der Zwaan et al. [210]. The superhyperfine interaction was quite anisotropic in the dark signal (g_{xyz} = 2.21, 2.15, 2.01; A_{xyz} = 0.96, 1.55, 5.32 mT; Fig. 20, panel I), but rather isotropic in the light-induced signal (g_{xyz} = 2.05, 2.11, 2.28; A_{xyz} = 4.33, 4.67, 3.81 mT; Fig. 20, panel II). It was concluded that in both cases the unpaired spin pointed to the Se nucleus, being in a d_z2 type of orbital in the dark species, but in a $d_x2_{-y}2$ type of orbital in the light-induced species. To explain these seemingly contradicting observations, it was proposed that the electronic z-direction flipped by 90° upon

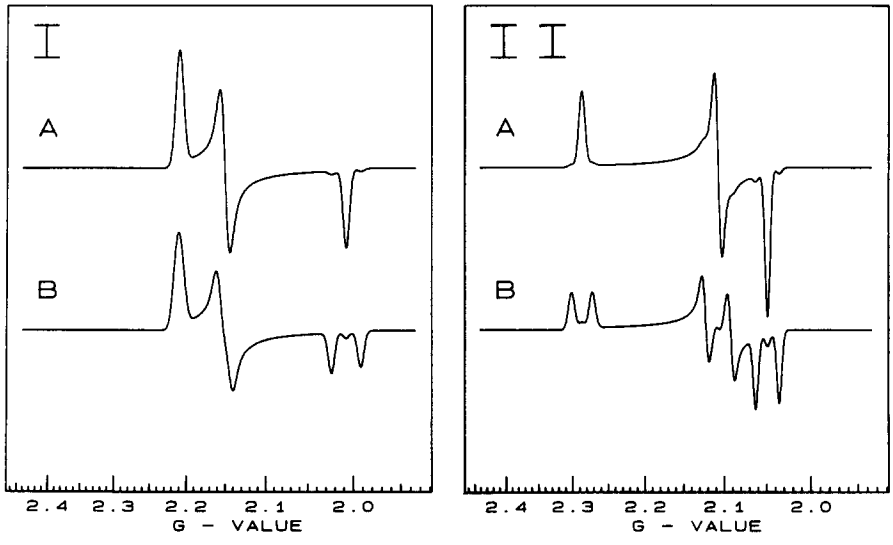

Fig. 20. EPR line shapes used for simulation in Fig. 19. (I-A) Natual Se, dark; (I-B) ^{77}Se, dark; (II-A) Natural Se, light; (II-B) ^{77}Se, light. For parameter see Sorgenfrei et al. [184].

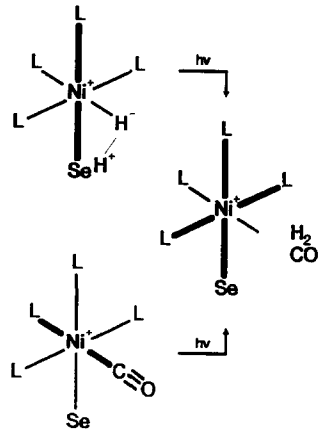

Fig. 21. Model of the coordination of nickel based on EPR experiments with ^{77}Se-enriched hydrogenase and the $Ni_a(I).^{13}CO$ species of the *C. vinosum* enzyme [210]. The thick lines denote either a d_z2 type of orbital or a $d_x2_{-y}2$ orbital holding the unpaired electron. The ligands L are expected to be oxygen and sulphur, rather than nitrogen. (From Sorgenfrei et al. [184].)

illumination, from a direction along the Ni-Se axis to a direction perpendicular to this axis.

The use of D_2O/D_2 had no noticeable effect on the Ni-C signal in the dark of the Se-containing enzyme. Apparently the unpaired spin in the d_z2 orbital did not sense magnetic nuclei. This means that the ligand opposite to Se cannot be a hydride, whereas also dihydrogen is less likely to be there. Hence, it was concluded that the Ni-hydrogen bond was presumably perpendicular to the Ni-Se bond. The ^{13}CO hyperfine splitting found by Van der Zwaan et al. [210] in the dark $Ni_a(I).CO$ species, where the g values indicate a d_z2 type of orbital for the unpaired spin, was explained by assuming that binding of CO, perpendicular to the Ni-Se bond, likewise resulted in a flip of the electronic z-direction into the direction of the Ni-CO bond. This is illustrated in Fig. 21. For convenience the model was drawn with six ligands, but a more realistic structure would be a trigonal bipyramidal one. This model can explain all observations obtained thus far. The model can be verified by studying the $Ni_a(I).^{13}CO$ species in ^{77}Se-enriched enzyme; the dark signal is then expected to show hyperfine interaction with the ^{13}C nucleus, but not with the ^{77}Se nucleus. The anisotropic nature of the hyperfine interaction with ^{77}Se in the dark Ni-C species was assumed to be somehow related to the possible cooperation of Se (as an $R\text{-}Se^-$ base) in the binding and activation of hydrogen. A study of the pH dependence might further elucidate this point.

3.3.5. The $Ni_a(I).H_2$ EPR signal: its intensity and its two-fold splitting

Another intriguing property of the $Ni_a(I).H_2$ signal is that it can show a two-fold splitting at 4.2 K. This phenomenon was first described for the *D. gigas* enzyme by Cammack and coworkers [31,33], who suggested the nickel spin to be interacting with the spin system causing the broad EPR signal (the cubane clusters). Also Teixeira et al. [196] noticed the strange line shape at 4.2 K. Redox titration (with dyes) showed that the 4.2 K signal, designated by these authors as the $g = 2.21$ signal, and the Ni-C signal appeared and disappeared at different potentials [199]. Their interpretation is that the signals represent two different oxidation states of the enzyme: depending on the oxidation state of the cubane clusters (or one of them), there is spin-spin interaction with Ni-C or not.

Also for the *M. thermoautotrophicum* enzyme it was reported [45] that the the two-fold splitting of the Ni-C signal at 4.2 K was dependent on the conditions. In partially purified F_{420}-non-reducing hydrogenase of *M. thermoautotrophicum* reduced with H_2 (no dyes) no splitting was observed at pH 6 over the entire potential range covered [47]. In this case 90% of the nickel observable as Ni(III) in the oxidized enzyme, was detected as $Ni_a(I).H_2$. At pH 8, where only 57% of the nickel was observed in the Ni-C signal, a two-fold splitting was present mainly at lower potentials.

With pure *C. vinosum* enzyme, titrated with H_2 (no dyes) at pH 8, full splitting was observed at 4.2 K over the entire potential range and the signals at 40 K and 4.2 K were always equal in intensity within error [47]. The Ni-C intensity was 55% of the detected Ni(III) concentration. Recently, we have again compared spectra of the pure *C. vinosum* enzyme activated with 1 bar of H_2 and subsequently incubated under 1% H_2 and 99% He, both at pH 6 and 9. The absolute intensity obtained under 1% H_2 differed (60% at pH 9 and 90% at pH 6) and a complete two-fold splitting was only obtained at pH 9. At pH 6 only part (about two-thirds) of the Ni-C signal was split at 4.2 K (Duin, E.C. and Albracht, S.P.J., unpublished observations). The experiments indicate that in this case (no dyes; $n = 2$ reaction) [47] Cammack's explanation (Fig. 15) [33] for the different intensities of the Ni-C signal at pH 8 and pH 6 is not applicable. This leaves the question as to what determines the pH-dependent absolute spin concentration of the Ni-C signal.

Spectra at 9 GHz and 35 GHz reported for the Ni-C signal of the *C. vinosum* enzyme at pH 8 [208] proved that the signal obtained at 4.2 K is a two-fold split version of the Ni-C signal observed at higher temperatures. The 4.2 K splitting has thus far been detected in the enzymes from *D. gigas, D. baculatus, C. vinosum, T. roseopersicina, W. succinogenes* and *M. thermoautotrophicum*. In my opinion it remains to be verified whether the two-fold splitting is indeed caused by a 4Fe cluster from the small subunit. The putative special Fe ion would be another candidate. Also here a study of the soluble *A. eutrophus* enzyme, which lacks

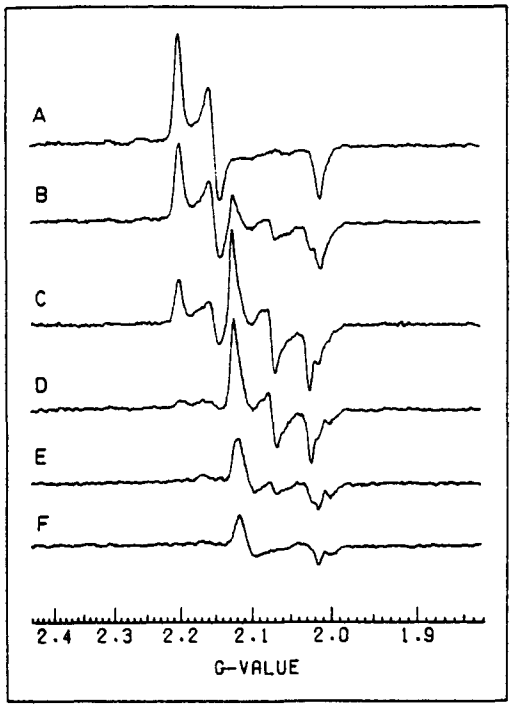

Fig. 22. Effect of CO on the EPR spectrum at 28 K of H_2-reduced enzyme from *C. vinosum*. (A) 1 bar hydrogen. (B) H_2 in the gas phase was replaced by CO by evacuation and flushing once. The sample was frozen after subsequent standing for 1 min at 4°C. (C, D and E) After prolonged standing under CO up to 8 min. (F) After repeated evacuation and flushing with CO and an additional period of 1 h at 20°C. (From Van der Zwaan et al. [207].)

the cubane clusters in the small subunit, might be most instructive.

3.3.6. Binding of carbon monoxide to Ni(II)

Van der Zwaan et al. [207] noticed that when *C. vinosum* enzyme, which was maximally reduced under 1 bar of H_2, was briefly treated with CO without eliminating all the H_2, then the $Ni_a(I).H_2$ signal could be replaced by a $Ni_a(I).CO$ signal (intensity about one quarter of the maximally detectable Ni(III) signal), as already discussed above. These workers also noticed that upon extensive evacuation and flushing with CO, the $Ni_a(I).CO$ signal completely disappeared (Fig. 22).

A minor signal with $g_{xy} = 2.11$ and $g_z = 2.02$, representing only 1% of the maximally detectable Ni(III), persisted (Fig. 22, trace F). This signal showed broadening when evoked with ^{13}CO but was not light sensitive [207,210]. Its line shape shows some resemblance to the CO-induced EPR signal ($g_{xy} = 2.07$, $g_z = 2.02$) in CO dehydrogenase from *Clostridium thermoaceticum* [155,180]. Its origin is not known.

Carbon monoxide can specifically induce the reduction of $Ni_r(III)$ [17,42]. Hydrogenase from *C. vinosum* incubated under Ar with excess ascorbate plus mediating amounts of PMS showed extensive reduction of the 3Fe cluster, but only very little reduction of either $Ni_r(III)$ or $Ni_u(III)$. When CO was introduced a slow

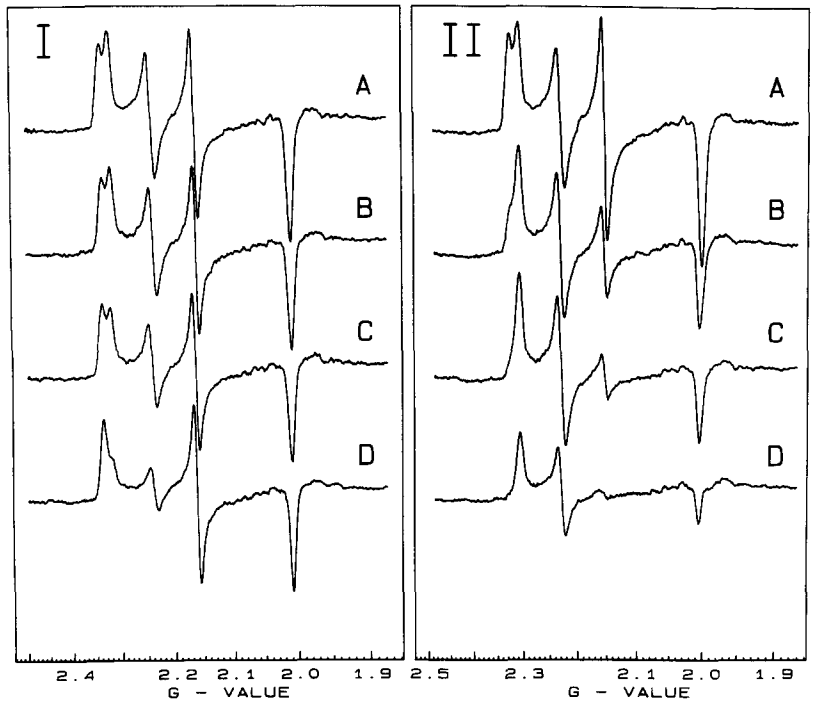

Fig. 23. Specific reduction of $Ni_r(III)$ in *C. vinosum* hydrogenase induced by CO in the presence of ascorbate and phenazinemethosulphate (PMS). Panel I: (A) EPR (9 GHz, 50 K) spectrum after 1 h at 22°C with excess reductant under Ar; (B) after an extra incubation of 3 min at 50°C; (C) after an additional 22 min at 50°C; (D) after 1 h (total time) at 50°C. Panel II: (A) as I-A; (B) after thawing the Ar gas was completely exchanged for CO. The sample was subsequently incubated from 3 min at 50°C; (C) after an additional period of 21 min at 50°C; (D) after 1 h (total time) at 50°C. (From Bagley et al. [17].)

specific disappearance of the Ni_r(III) EPR signal was observed (Fig. 23). One possible way to explain these findings is by assuming a selective binding of CO to Ni_r(II) resulting in an apparent increase of its mid-point potential of at least 150 mV. The binding of CO was further investigated by FTIR studies [17]. In one set of experiments the CO form of the enzyme was prepared as in Fig. 22, trace F. In another set the Ni(II).CO form was prepared as shown in trace II-D of Fig. 23, by incubating oxidized ready enzyme with excess ascorbate, with PMS as mediator, under a CO atmosphere. The FTIR spectra of the enzyme treated with H_2/CO is shown in Fig. 24, left-hand panel. When illuminated at low temperatures, the 2060 cm^{-1} band disappeared and the bands at 1928, 2068 and 2082 cm^{-1} slighlty shifted to higher frequencies. At 200 K in the dark this effect could be reversed. When prepared with ascorbate/PMS/CO at 50°C, the same light minus dark difference spectrum was obtained (Fig. 24, right-hand panel). When prepared with ^{13}CO, the 2060 cm^{-1} band shifted to 2017 cm^{-1}, proving that the band originates from the C-O stretching vibration of metal-bound CO. The origin of the other bands is presently unclear; strong bands in this region are not found in any other proteins. From the EPR and FTIR data together it can be concluded that the most likely explanation for the light-sensitive 2060 cm^{-1} band is that it is due to a Ni(II).CO species. Light induces the photodissociation of the CO, thereby shifting its IR frequency to 2138 cm^{-1}. Warming of the sample to 200 K caused CO to bind to nickel again. The behaviour is completely analogous to the earlier findings with the $S = 1/2$ Ni_a(I).CO species (Fig. 18) [207,210].

The fact that the light minus dark FTIR spectra of the ascorbate-induced Ni(II)-CO species (initially assumed to be a Ni_r(II).CO state) and the H_2/CO-induced Ni(II)-CO species (assumed to be a Ni_a(II).CO state) are the same, implies that the cubane clusters do not contribute to these spectra. Taking the broad EPR signals as due to the reduced cubane clusters, we know for the *C. vinosum* enzyme that these clusters remain oxidized in the ascorbate-induced Ni(II)-CO state, but are reduced in the H_2/CO-induced Ni(II)-CO state. If the unknown bands in the FTIR spectra represent vibrations around the Ni site, then any assumed differences of the ready Ni_r(II).CO state and the active Ni_a(II).CO state might be non-existent in as far as the Ni site is concerned, i.e. the nickel site might have exactly the same structural environment. In this respect it is worthwhile to note that we have indeed observed

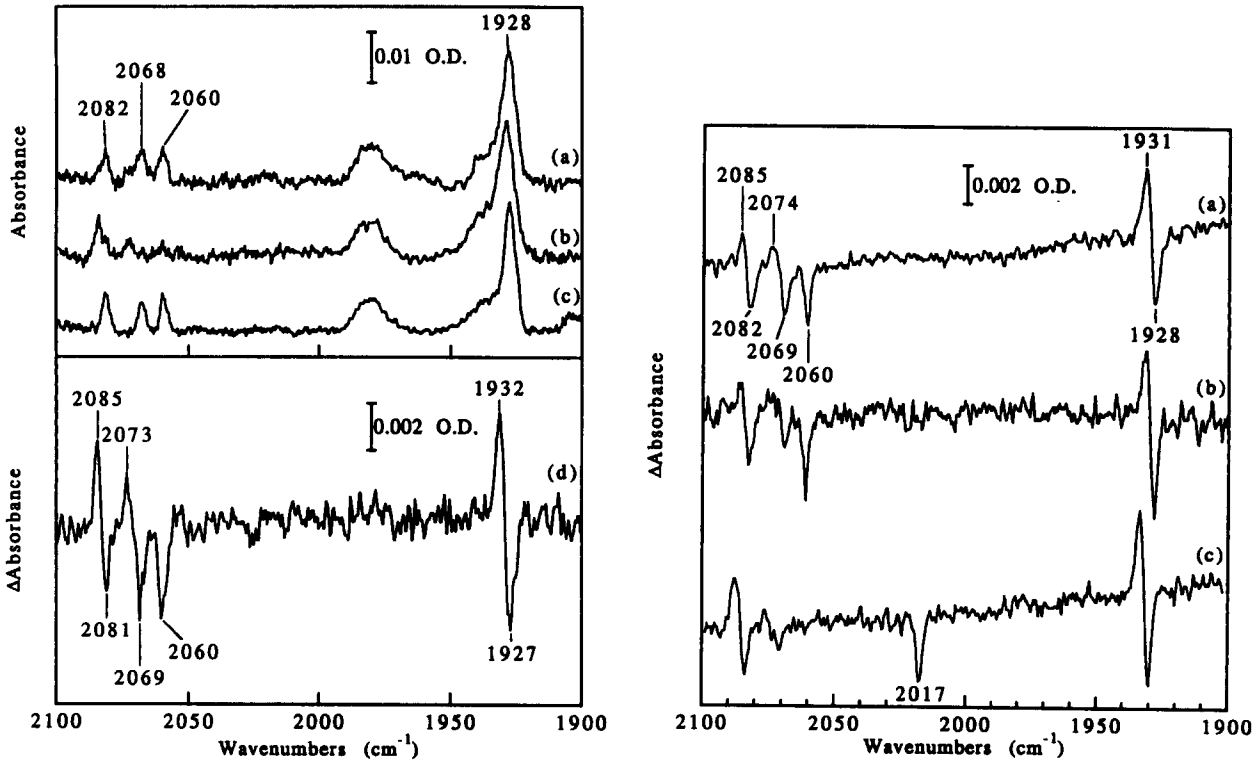

Fig. 24. Binding of CO to divalent nickel in hydrogenase from *C. vinosum* as observed by FTIR spectroscopy at 20 K. Left-hand upper panel: enzyme clamped into the Ni_a(II).CO state by a H_2/CO treatment; (A) dark adapted; (B) illuminated with white light at 20 K; (C) after warming the sample to 200 K and standing in the dark for 10 min; spectrum c was recorded at 78 K. Left-hand lower panel: difference spectrum light minus dark at 20 K. Right-hand panel: light minus dark difference spectra; (A) Ni_a(II).CO state obtained by H_2/CO treatment; (B) Ni_a(II).CO state obtained by treatment with ascorbate plus PMS under CO at 50°C; (C) as B, but now with ^{13}CO (> 90% enriched in ^{13}C). (From Bagley et al. [17].)

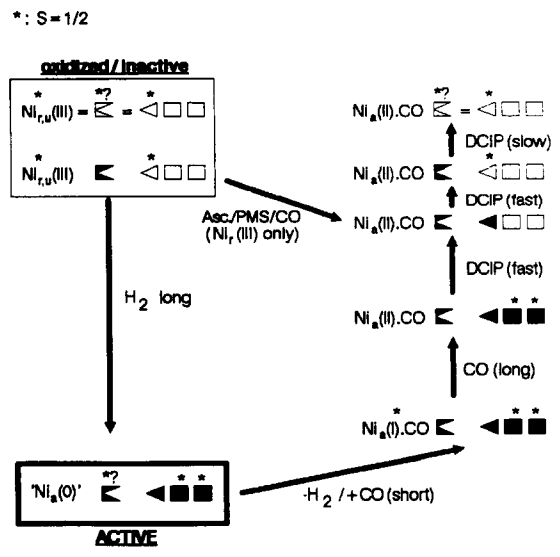

Fig. 25. Schematic representation of the reactions of CO with *C. vinosum* hydrogenase under several conditions, and the redox properties of the resultant CO-enzyme complex.

that the ascorbate/PMS-treated enzyme activates under CO, but not under Ar (Roseboom, W. and Albracht, S.P.J., unpublished observations). Together with the observed slow binding of CO under these conditions (Fig. 23), this indicates that 'reductive activation' might take place before CO can actually bind to nickel. Hence, it is assumed in this review that CO can only bind to Ni_a. The reactions of CO with the *C. vinosum* enzyme are summarized in Fig. 25.

The binding of CO to Ni_a(II) also suggests that H_2 might bind to Ni_a(II). This possibility remains to be verified experimentally. It must be remembered here that in the absence of mediators and at extremely low H_2 concentrations the Ni_a(I).H_2 state is very stable (Fig. 12) and apparently preferred over the putative Ni_a(II).H_2 state. In the presence of mediators, however, Ni_a(I).H_2 is rapidly oxidized to an EPR-silent state under these conditions (Fig. 12).

An interesting case of binding of a gaseous inhibitor involves acetylene. This gas was shown to inhibit nickel hydrogenases from *Azotobacter chroococcum* [181,204], *A. vinelandii* [105] and the enzymes from *D. gigas* and *D. baculatus* [95]. The reaction of acetylene with the enzyme is prevented by H_2 [105,204]. More recently it was shown that acetylene strongly binds to the large subunit of the *A. vinelandii* enzyme [191]. The binding persisted after treatment with various strongly denaturating agents. Acetylene binding also completely protected the otherwise highly oxygen-sensitive enzyme against air. Although binding of acetylene to a metal ion is suspected, it is not yet known whether nickel is involved.

4. The coordination of nickel

4.1. Selenium

In 1982 Yamazaki [228] first reported that Se was a constituent of hydrogenase from *Methanococcus vannielii* in the form of a selenocysteine residue. No mentioning of nickel was made, nor were any EPR spectra reported. Later Se was detected in nickel hydrogenases from *D. baculatum* (formerly *D. desulfuricans*, strain Norway) [160], *D. salexigens* [197], *M. voltae* [145], *D. baculatus* [198] and *Thermodesulfobacterium mobile* [63].

From EXAFS measurements on nickel in the periplasmic selenium-containing enzyme of *D. baculatus*, Eidsness et al. [57] proposed a pseudo-octahedral or possibly a penta-coordinate ligand field around nickel with 1 Se atom at 2.44 Å, 1–2 S atoms (or Cl, which is indistinguishable in size) at 2.17 Å and 3–4 N or O atoms at 2.06 Å. EXAFS on the Se atom indicated 1 C atom at 2.0 Å and a heavy scatterer (Ni or Fe) at about 2.4 Å, in accordance with the assumption of a selenocysteine as ligand to nickel.

EPR measurement with the periplasmic *D. baculatus* hydrogenase, 70% enriched in ^{77}Se (I = 1/2) [96], showed that the $g = 2.23$ and 2.17 lines of the Ni-C EPR spectrum of the partially-reduced enzyme (g_{xyz} = 2.228, 2.174, 2.01) were broadened due to hyperfine splitting of the Se nucleus. (A_{xy} = 1.0 mT, 1.8 mT). There were no data on the g_z. The possible light sensitivity of Ni-C of this particular preparation was not tested. Also no data were shown on the oxidized Ni(III) state. In earlier reports on this enzyme [198], EPR spectra were shown with g values for Ni(III) of g_{123} = 2.20, 2.06, 2.00. This is a most unusual set of g values ($g_z > g_{xy}$; $g_x = g_e$) for a low-spin $3d^7$ system and the g values differ considerably from those of the ordinary Ni hydrogenases (g_{xyz} = 2.3, 2.24 or 2.16, 2.01). The soluble cytoplasmic hydrogenase from *D. baculatus*, which also contains Se, was virtually EPR silent in the oxidized state [198]; in the reduced state it showed the same EPR spectrum as the reduced periplasmic enzyme. Although the membrane-bound enzyme was reported to contain Se as well [198], it showed EPR spectra just like the Ni-S hydrogenases [71,122,198]. The reason for the totally different EPR spectra in the oxidized state of these Se-containing nickel hydrogenases is unknown. The presence of Se seems to have a pronounced effect on the individual reactions involved in the D_2/H_2O exchange reactions of nickel hydrogenases [198], and sometimes also on the activity of the enzyme [183]. The properties of hydrogenase from *M. voltae*, 92% enriched in ^{77}Se, have been discussed already and were summarized in Fig. 21.

4.2. Sulphur, oxygen and nitrogen

The first attempts to characterize the ligands of Ni were reported by Lindahl et al. [129]. From EXAFS measurements on the F_{420}-reducing hydrogenase from *M. thermoautotrophicum* these investigators concluded that 3 S ligands were present in the direct coordination of nickel. Scott and coworkers initially came to higher coordination numbers for S on interpreting EXAFS data from the *D. gigas* enzyme (4–5 S at 2.20 Å [178] and even 6 S [179]). The interpretation of the data was refined as new and well characterized model compounds of nickel became available as references. To date best fits to the data could be obtained by Scott and coworkers [56] by assuming 2 S atoms at 2.24 Å and 2–4 N,O atoms at 2.06 Å as ligand for nickel in the oxidized *D. gigas* enzyme.

Maroney and coworkers [18,136,137,224,225] have carried out extensive X-ray absorption measurements on the enzyme from *T. roseopersicina*. Their most recent interpretation for the Ni-C species is that 2 ± 1 S(Cl) at 2.22–2.25 Å, 2 ± 1 N(O) at 1.92–2.02 Å and 1 distal S(Cl) at 2.70–2.75 Å are present [225] as ligands to nickel. In another publication of the same group [18], where five different states of the enzyme (from completely oxidized to completely reduced) were investigated, it was stated that EXAFS spectra obtained from scattering atoms in the first coordination sphere of Ni in all five states are consistent with a Ni site composed of 3 ± 1 N(O)-donors at 2.00 ± 0.06 Å and 2 ± 1 S-donors at 2.23 ± 0.03 Å. A distal S atom, in addition to the 2 ± 1 S atoms at 2.2 Å, was reported in a 1991 study of this group [224] at 2.5 Å for Ni_r(III) and at 2.4 Å for Ni_u(III). At that time, however, it was concluded that there was no distal S atom present in the Ni-C form. Illumination of the Ni-C form had no detectable effect on the number of S, N or O ligands. Maroney and coworkers also presented evidence that a large scattering atom is present at a distance of about 4.3 Å from the nickel and possibly another one at 6.2 Å. They speculated that these can only be iron atoms and therefore proposed the presence of a novel Ni-Fe-S cluster in this hydrogenase [137].

The pre-edge features, where $1s \rightarrow 3d$ and $1s \rightarrow 4p$ transitions can occur, provides possible information on the type of coordination. Eidsness et al. [56,57] concluded for the *D. gigas* enzyme that the coordination would be tetragonally-distorted octahedral or trigonal-bipyramidal, in line with earlier conclusions based on the EPR spectra of Ni(III) in several hydrogenases [7,29,144]. Maroney and coworkers came to a similar conclusion from X-ray absorption studies on the *T. roseopersicina* enzyme [18,136,137,224,225].

Albracht et al. [12] looked at the effect of ^{33}S ($I = 3/2$) enrichment on the EPR spectrum of Ni(III) and Ni(I) of hydrogenase from *W. succinogenes*. From these studies it was concluded that only 1 S nucleus induced detectable hyperfine splitting in the EPR spectrum of Ni_r(III), whereas the spectra of Ni_a(I) ('dark' and 'light' spectrum) were likewise each perturbed by the nuclear magnetic moment of one ^{33}S atom. As the unpaired electron in the dark and the light-induced states was supposed to probe different directions for possible hyperfine interactions, the possibility of the presence of two S ligands could not be excluded. In view of the interpretation of the EPR spectra to Ni(III) and Ni(I) [12,210], one axial S atom and possibly also one 1 equatorial S were proposed to be present. The recent experiments with ^{77}Se-enriched enzyme from *M. voltae* [184] show that the unpaired electron in both the dark and the light-induced states of the Ni-C species strongly interact with the ^{77}Se nucleus (Fig. 21). This information restricts the number of possible interpretations of the ^{33}S experiment and might be of help in obtaining a more refined analysis. Before doing so, it would be desirable to have one additional piece of information, namely whether the electronic *z*-axes in the Ni(III) and $Ni_a(I).H_2$ species are the same. Also this can be established with a ^{77}Se-enriched hydrogenase.

ESEEM experiments have first been reported for the oxidized enzyme from *M. thermoautotrophicum*. [194]. In the F_{420}-reducing enzyme a weakly interacting N nucleus was detected in this way, ascribed to a possible distal N from histidine or flavin. No such interaction was detected in the F_{420}-non-reducing enzyme, however. A weakly interacting N nucleus has also been detected by spin-echo measurements with the enzymes from *D. gigas* [39] and *T. roseopersicina* [37], which contain no flavin. The problem with weak N-hyperfine interactions is that no conclusion about the precise location of the N-nucleus can be made, i.e. it could be due to a weak interaction from a ligand or from nitrogen in the second coordination sphere [37, 102,194].

On basis of the interpretation of Ni-C as $Ni_a(I).H_2$, Van der Zwaan et al. [210] argued that it is unlikely that N is in the direct coordination of nickel. No evidence for N-superhyperfine splitting is observed in any of the published nickel EPR spectra of hydrogenases. The recent results with the ^{77}Se-enriched enzyme of *M. voltae* [184] suggest that the unpaired spin in the $Ni_a(I).H_2$ (dark and light states) and the $Ni_a(I).CO$ states probe for magnetic nuclei in 5 different directions (Fig. 21). As the EPR line widths of both the Ni(III) and all types of $Ni_a(I)$ species are rather small (0.9–1.5 mT in X-band) this means that the unpaired spin in the d-orbitals does not sense N ligands in those five directions. This observation makes N as a ligand in the Ni-C state less likely. In view of the widely different properties of nickel in the inactive and active state of the enzyme, it cannot be excluded from

EPR measurements, though, that N is an equatorial ligand of Ni(III), where the unpaired spin, being in a d_z2 orbital, probes only two directions. X-ray absorption measurements [18,57,136,137,224,225], however, argue against such a possible change.

From experiments in water 40% enriched in ^{17}O ($I = 5/2$) there is no evidence for any interaction between Ni {$Ni_{r,u}$(III) and Ni_a(I) (dark and light-induced states)} and the oxygen atom of exchangeable water molecules (Van der Zwaan, J.W. and Albracht, S.P.J., unpublished observations). In view of the interpretation of the EPR spectra of the ^{77}Se-enriched hydrogenase [184] (Fig. 21), this would make water binding to at least four of the possible coordination sites of nickel unlikely. Yet, water might be expected to play an essential role in the transfer of protons to and from the active site during turnover.

Studies with O_2 enriched in ^{17}O ($I = 5/2$) [210] revealed that reoxidation of H_2-reduced *C. vinosum* enzyme with $^{17}O_2$ resulted in preparations with Ni_r(III) plus Ni_u(III). The EPR spectra of *both* were broadened by $^{17}O_2$; the *g* values were, however, not changed, nor was there any influence on the power saturation behaviour. Similar results were obtained with the *D. gigas* enzyme [35]. The effect of $^{17}O_2$ on the *C. vinosum* enzyme could not be removed (within 4 h) by flushing with normal O_2 or CO, indicating a tight binding, a very slow equilibration, or the formation of a reduced oxygen adduct. Identical EPR spectra, only without the extra broadening, could be obtained by oxidation of H_2-reduced *C. vinosum* enzyme under strictly anaerobic conditions [210]. Subsequent admission of $^{17}O_2$ then had no effect. These observations make it unlikely that O_2 is a direct ligand to Ni(III). EPR spectra of $S = 1/2$ transition-metal systems are usually highly sensitive to slight changes in the coordination of the metal. Likewise, the $S = 1$ system of oxygen is presumably no longer present when O_2 has reacted with the reduced enzyme.

4.3. The coordination of nickel in active enzyme

In the selenocysteine-containing hydrogenases from *D. baculatus* [57,96] and *M. voltae* [183,184] it is beyond doubt that the selenium is a ligand to nickel. As the selenocysteine in these enzymes replaces the first Cys residue in motif 5L (Fig. 5) in the large subunit (DPCxxCxxH), it is likely that the second Cys is involved in the coordination as well. The amino-acid sequence suggests the Asp and His residues as other possible candidates.

As hydrogen is bound in the $Ni_a(I).H_2$ state and since enzyme in this state can react with yet another hydrogen, it can be argued that if nickel is also directly involved in the second process, then two coordination sites of Ni_a(I) have to be vacant for reactions with hydrogen. Under the reasonable assumption that the maximal coordination number is six, this would leave only four sites available for ligands from the protein (note that in Fig. 21 five protein ligands have been drawn for convenience only). Mutation studies with the enzymes from *E. coli* (hydrogenase-1 [154] and *A. eutrophus* (soluble enzyme) (Massanz, C. and Friedrich, B., personal communications) show that the first Cys residue in motif 5L in the large subunit is most important. If mutated to a Ser residue, there was no synthesis of active hydrogenase anymore. In case of the *Alcaligenes* enzyme, the large subunit was produced, but showed virtually no nickel binding. When the second Cys residue in motif 5L was changed to a Ser residue, then no active enzyme was found in both bacteria as well. In *A. eutrophus* the large subunit accumulated, but now did contain Ni. This strongly suggests (Massanz, C. and Friedrich, B., personal communication) that the first Cys residue in motif 5L is essential for nickel binding in the precursor form, but the second one is not. This result does not exclude the possibility that the second Cys residue is also involved in nickel binding. Przybyla et al. [154] made three more single point mutations in the motif 5L: Asp → Val, Pro → Arg and His → Leu. Only in the last case was a low activity (10–20%) observed. This means that also the conservative Asp and Pro residues are vital for the biosynthesis of active enzyme.

In view of the conservative sequence DPC in motif 5L and the effects of mutation of each of them, it might well be that the two oxygen atoms of the aspartate residue and the S atom of the first Cys residue might form a rigid basis for the coordination of nickel. The proline residue probably puts certain constraints upon the possible relative positions of these 3 atoms. We have used the sequence of the 25-residues long subunit of the *M. voltae* hydrogenase [183] for a modeling study (Moerenhout, J.M. and Albracht, S.P.J., unpublished observations). We replaced the selenocysteine for a normal Cys residue and followed the dynamics of a model minimized in energy by the program SYBYL. It was indeed found that the relative positions of the two oxygen atoms of the Arg residue and the S atom of the Cys residue were rather constant. The position of the S atom from the second Cys residue was, however, rather flexible, as was the position of the terminal His residue. A possible coordination of the Ni_a(I) state might therefore be as depicted in Fig. 26. Ascribing the two conservative thiolates of motif 2L in the large subunit also as ligands to nickel would increase the coordination number to 6 and is considered here as unlikely. It would not be in line with the EPR data on the active ^{33}S-enriched enzyme, nor would it match the EXAFS data on the enzymes from *D. gigas,*

D. baculatus and *T. roseopersicina*. In this respect one also has to remember that the spacing between the block of motifs 1L–3L and the block of motifs 4L–5L is widely different among the hydrogenases. It can differ by up to 210 amino acids (Fig. 5). In the F_{420}-non-reducing enzyme from *M. voltae* there is no covalent attachement at all of motif 5L with the other motifs [183]. The EPR spectra of Ni-C are, however, all virtually identical. This is why this author considers the possibility that the conservative amino-acid sequence motifs 1L and 2L in the large subunit might assist in the creation of a specific environment for a putative Fe atom, which is sometimes observed as a $\{X^{ox} = [3Fe\text{-}4S]^{+}\}$ centre, X possibly being low-spin Fe(III), discussed earlier in this review (Fig. 11).

Three single point mutations have been obtained by Przybyla et al. [154] in motif 2L: Arg → Leu, Cys_1 → Ser and His → Leu. The replacement of the His residue appeared not vital for enzyme production; only its activity was impaired. The presence of the other two conservative residues was essential; no activity could be detected when one of them was mutated.

4.4. The coordination of $Ni_r(III)$ and $Ni_u(III)$

There is also the question as to what causes the difference in coordination between the $Ni_r(III)$ and the $Ni_u(III)$? The difference in g_y and g_x values suggest that the energy differences between the d_{xz}/d_{yz} orbital couple and the d_z2 orbital differ for the ready and the unready Ni(III). Unready nickel cannot be quickly activated by H_2 [70], whereas $Ni_r(III)$ can. Also the presence of reducing equivalents and CO does enable the conversion of $Ni_r(III)$ to the $Ni_a(II)$.CO state, but these conditions have no effect on $Ni_u(III)$. It seems therefore as if in unready enzyme the coordination of nickel leaves no space for the approach of external ligands. EXAFS data [224] suggested a slight change in binding length of a possible distal sulphur as the only difference: 2.5 Å in $Ni_r(III)$ versus 2.4 Å in $Ni_u(III)$. In Ni_a this S atom apparently moves away to 2.7 Å [225]. It is perhaps the position of this distal sulphur atom which determines the properties of unready and ready nickel. It might also cause the strong differences in behaviour of $Ni_{r,u}(III)$ in inactive enzyme and $Ni_a(I)$ in active enzyme. The observation that CO binding to Ni(II) seems only possible after reductive activation is in line with this idea. It remains to be determined whether this distal sulphur is coming from motif 2L, or whether it is from the second Cys residue in motif 5L.

Many enzymes are mainly or completely in the $Ni_u(III)$ state when isolated (*D. gigas, T. roseopersicina, M. thermoautotrophicum*). Hydrogenases from methanogens appear to be exclusively in the unready state whenever they are oxidized. Only under special conditions [46] short-lived $Ni_r(III)$ EPR signals were observed. Bagyinka et al. [18] reported that the ready *T. roseopersicina* enzyme converted to the unready enzyme upon standing, even at 77 K. This all indicates that the unready form of the nickel hydrogenases (and the unready coordination of nickel) is energetically the most stable state one.

5. Formal valence states of nickel

The simplest interpretation of the redox properties of the nickel centre in the enzyme, as monitored with EPR is:

$$Ni(III) \longleftrightarrow Ni(II) \longleftrightarrow Ni(I) \longleftrightarrow Ni(0)$$

As valence-state transitions of more than one can usually only occur at widely different redox potentials in model compounds of nickel, it is unlikely that the actual charge density on the nickel ion in hydrogenase is in agreement with the formal valence states indicated above. Still, for a discussion of the several redox state of the nickel centre it is useful to adhere to this notation.

It must be stressed once more that at temperatures where the reductive activation or the oxidative inactivations can be suppressed, either the Ni(III)/Ni(II) redox equilibrium (with dyes) can be observed, or the $Ni_a(II) \leftrightarrow Ni_a(I) \leftrightarrow Ni_a(0)$ equilibria, but not both types at the same time (Fig. 12). So $Ni_a(II)$ is not in redox equilibrium with any of the $Ni_{r,u}(III)$ or $Ni_{r,u}(II)$ states. Assuming that the rearrangement of the distal S ligand to nickel is a slow process (as is the activation/inactivation), then these observations become somewhat more understandable. The position of this distal S might also contribute to the strong changes in redox behaviour of nickel.

Fig. 26. Computer-generated model based on the 3 kDa subunit of the selenium-containing F_{420}-non-reducing hydrogenase of *M. voltae* [183]. The N-terminal residue is a methionine. The selenocysteine has been replaced by cysteine. The upper image shows a picture of the complete peptide; the lower image concentrates on the conservative motif 5L, which is situated at the upper right in the upper picture. Colours used: C, red; H, white; O, blue; N, green; S, yellow. The blue oxygen atoms of the carboxylic acid group of the Asp residue are nearly in the centre of the lower picture. The yellow thiolate groups of the two Cys residues are protonated in this model and hydrogen bonded to the carboxylic-acid group of the Asp residue. The model was generated by J.M. Moerenhout in the author's laboratory (with thanks to W. Roseboom for photography).

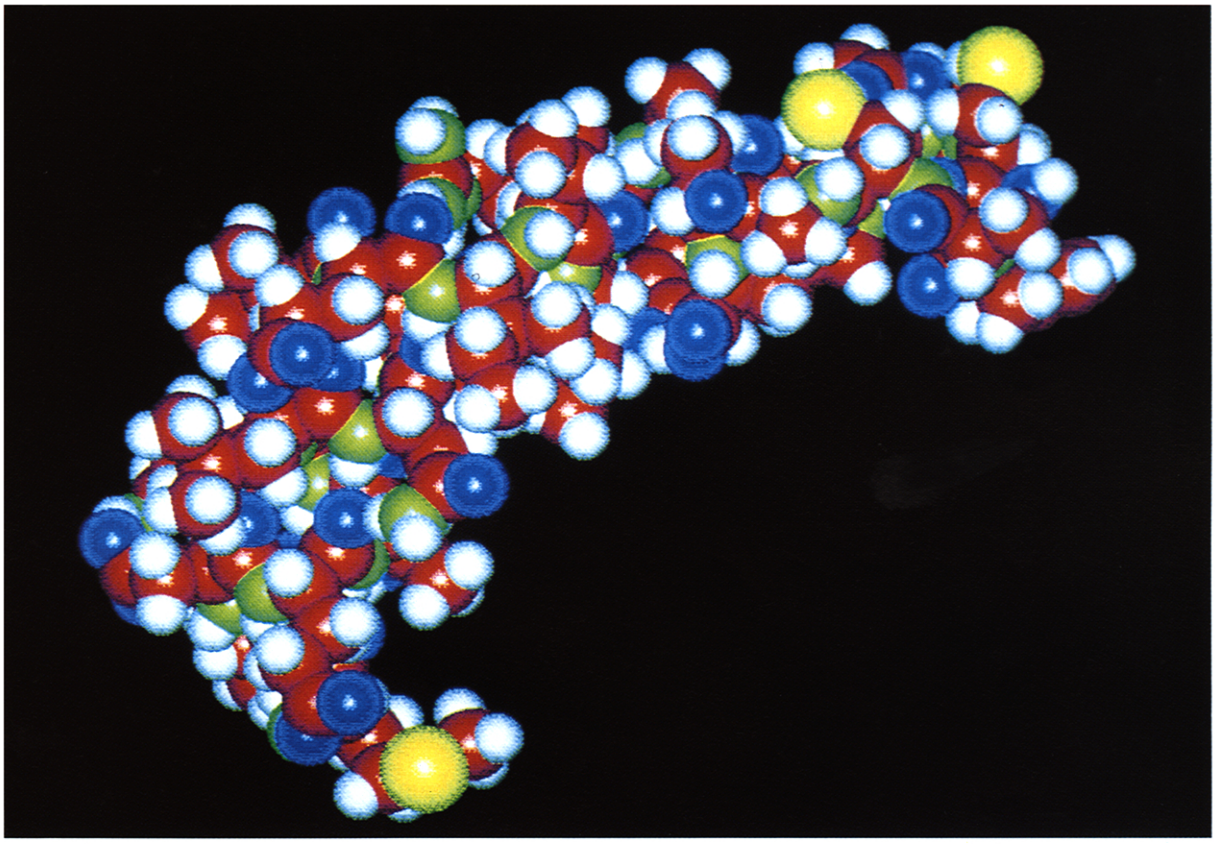

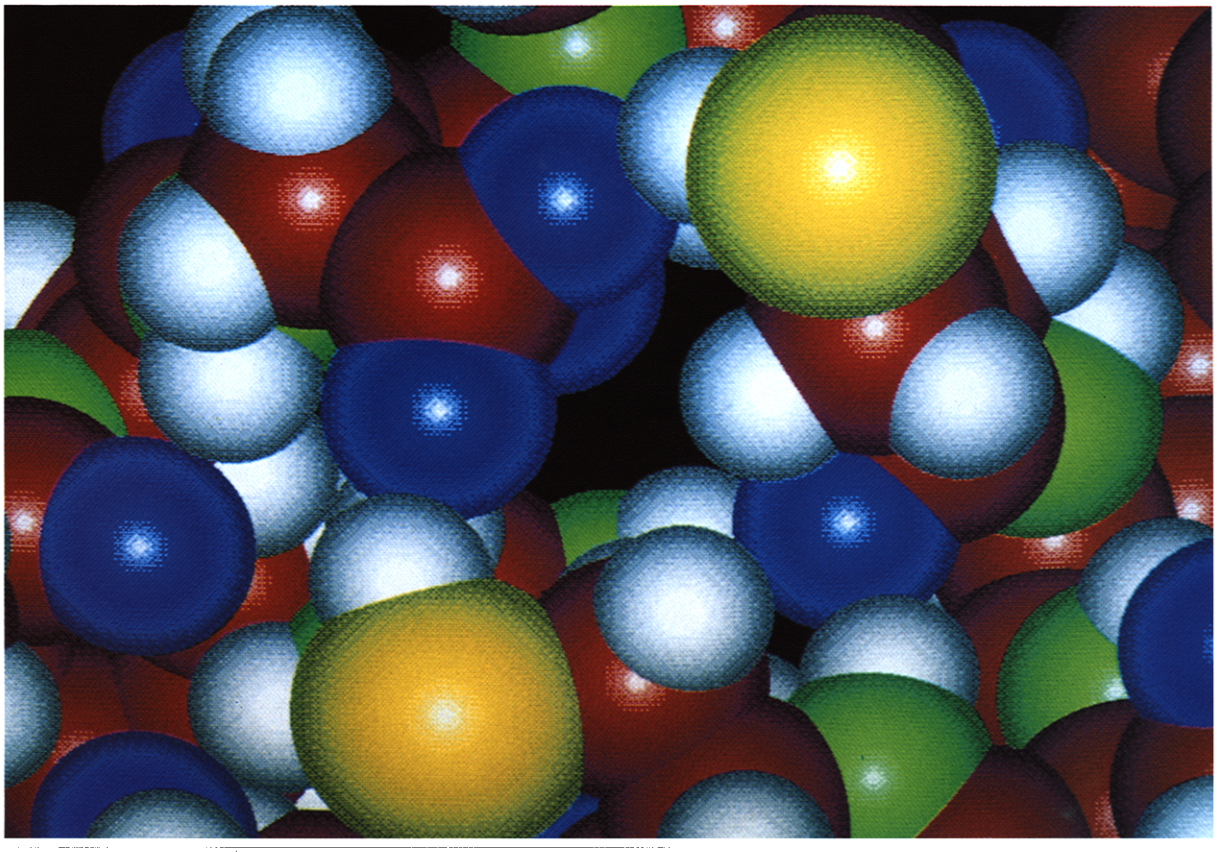

MCD as well as magnetic susceptibility measurements have indicated that nickel in the oxidized enzymes of *M. thermoautotrophicum* [107], *C. vinosum* (Cheesman, M., Van der Zwaan, J.W., Albracht, S.P.J. and Thomson, A.J., unpublished experiments; [40]) and *D. baculatus* [221] is paramagnetic $S = 1/2$, whereas upon reduction to the EPR-silent Ni(II) state no magnetism could be observed. Together with the EPR data this strongly points to a conversion of Ni(III) {$S = 1/2$, $3d^7$} to Ni(II) {$S = 0$, $3d^8$}, being responsible for the observed redox transitions in the inactive enzyme.

The position of the K-edge in X-ray absorption spectroscopy (XAS) of metal compounds reflects the charge density on the metal ion. As outlined by Eidsness et al. [56], also the coordination can be of importance for the precise position of this edge. In model compounds of nickel, this edge usually shifts by 2–3 eV upon a change of the valence state of nickel [56,224]. XAS studies with oxidized and reduced enzyme from *D. gigas* indicated that the variations in energy of the K-edge of Ni were at most 1–2 eV [56]. As the coordination of Ni is also of influence on the position of the K-edge, the assumption had to be made that the coordination in the oxidized and reduced Ni-species was the same. It proved difficult to find model complexes that fulfilled this requirement. Hence, Eidsness et al. [56] concluded in 1988 that XAS measurements are 'currently a rather poor measure of nickel oxidation state'.

More recent data on the K-edge positions of nickel in *T. roseopersicina* hydrogenase in five different oxidation states (Fig. 27) [18] showed no apparent shifts whatsoever. Also the EXAFS spectra were very similar in all cases and illumination of the Ni-C state had no effect [225]. The observed shifts (0.2 eV or less) were within the accuracy of the method. In this study EPR spectra of the complete X-ray absorption cell before and after the X-ray measurements, while kept at temperatures at or below 80 K at all times, were carried out to ensure that the X-ray beam did not permanently change the enzyme in the sample in any way. These results led Maroney and coworkers to state that a redox role for Ni in hydrogenase is not supported by XAS data [18]. Likewise these investigators considered the possibility that the Ni-C state does not involve a Ni-H or Ni-H_2 complex [225].

The X-ray absorption data thus indicate that apart from a possible slight movement of the distal S atom, there are no changes in coordination or bond lengths around the nickel, nor any detectable changes in its apparent charge density. On the other end, the EPR, MCD and magnetic susceptibility measurements show that the nickel centre changes valence state and spin state. The unpaired spin observed in oxidized enzyme and the Ni-C state is very close to nickel, as evidenced by the ^{61}Ni hyperfine coupling, and has a considerable spin-orbit coupling as expected for a 3d electron, leading to g values up to 2.3 [165,223]. In fact, the g values

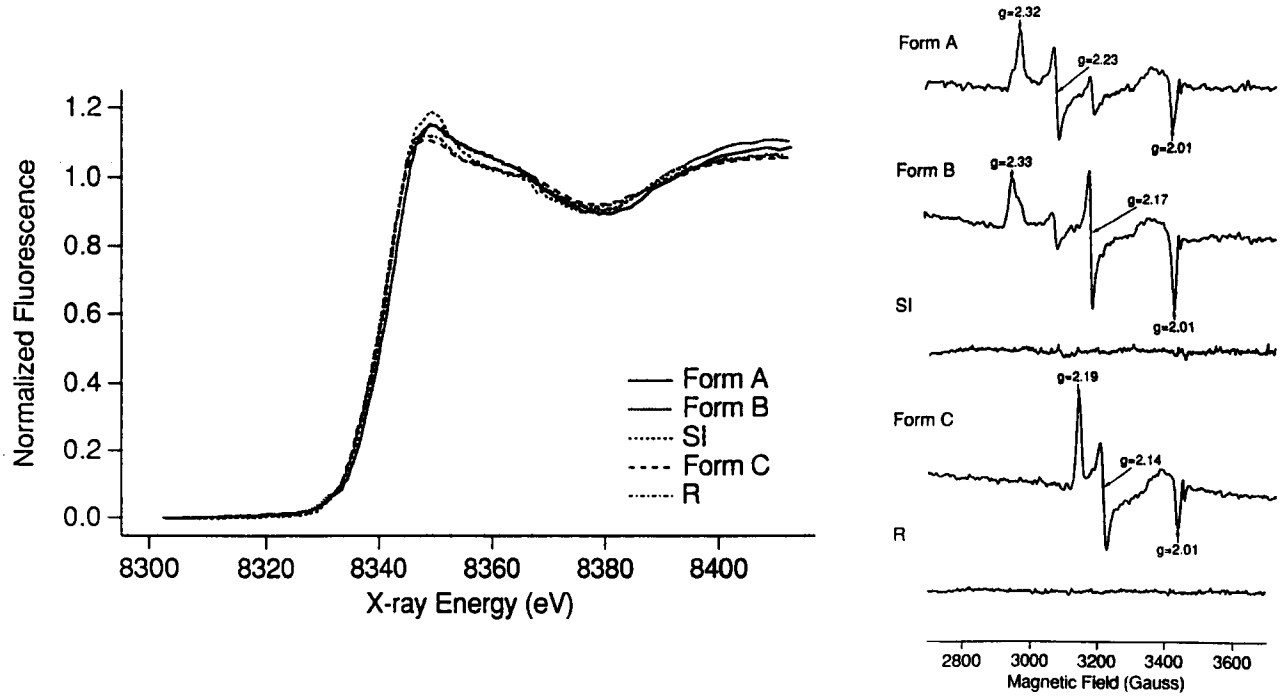

Fig. 27. Nickel K-edge XAS spectra (left-hand panel) and EPR spectra (right-hand panel) at 80 K of *T. roseopersicina* hydrogenase in five different redox states. The same frozen samples were used for both measurements. Form A: mainly Ni_u(III); Form B: mainly Ni_r(III); SI: N_a(II); Form C: Ni_a(I).H_2; R: Ni(0). (From Bagyinka et al. [17] with permission.)

are well within the range observed for either Ni(III) of Ni(I) model compounds [89,146]. It is my opinion, therefore, that the EPR signals ascribed to nickel are indeed due to unpaired spins in orbitals with mainly a 3d character of nickel. The extreme sensitivity of the orbital-magnetic moment of the unpaired spin to subtle changes in the electronic and magnetic environment of the nickel ion enables this 3d electron to report on these changes via EPR. Apparently these changes are too subtle to be of influence on the XAS and EXAFS spectra of nickel. Hence the 3d electron is probably a far better reporter on changes in the nickel centre than is the 1s electron.

The energy required to remove a 1s electron from the nickel ion in any of the redox states of the *T. roseopersicina* enzyme appears the same within the detection limits [18,225]. This points to appreciable charge delocalization (or charge 'buffering') within the nickel site such that the effective charge density on the nickel nucleus is not changed [18,56,224,225]. This in turn suggests quite some covalent character of the bonding between nickel and (some of) its ligands. The thiolates come to mind here. Indeed the superhyperfine splittings observed in the g_{xy} lines of EPR spectra from ^{33}S-enriched *W. succinogenes* enzyme [12] and the ^{77}Se-enriched enzymes from *D. baculatus* [96] and *M. voltae* [184] reflect mixing of the metal d-orbitals with s-character orbitals of the S/Se ligands. Whitehead et al. [225] estimated a spin density of 0.26 on S of two cysteine residues, based on the hyperfine interaction of the non-exchangeable protons in the Ni-C state. This hyperfine interaction was attributed to the β-CH_2 protons of the cysteine residues.

As discussed above, there is quite strong evidence for hydrogen binding to nickel in the Ni-C state. The strong binding of CO to Ni_a(II) also hints to the possible binding of H_2 to N_a(II). Hydrogen, either as H^+, H^- of H_2 could also play an important role in keeping the effective charge density at the nickel ion rather constant. The Ni(III)/Ni(II) states in inactive enzyme and the Ni(II)/Ni(I)/Ni(0) states in active enzyme, obtained in the presence of redox mediators, could then be written like:

$Ni_{r,u}$(III): $(RS^-)_2$.Ni(III)
$(RS^{0.5-})_2$.Ni(II)

$Ni_{r,u}$(II): $(RS^-)_2$.Ni(II)

Ni_a(II): $(RS^-)_2$.Ni(II)

Ni_a(I): $(RS^-)_2$.Ni(I).H_2
$(RS^-)_2$.Ni(III).$(H^-)_2$
$(RS^{0.5-})_2$.Ni(II).$(H^-)_2$

Ni(0): $(RS^-)_2$.Ni(0).H_2
$(RS^-)_2$.Ni(II).$(H^-)_2$

Although a formal valence transition Ni(III)/Ni(II) seems no longer a point of dispute for most workers in the field, a further reduction of the nickel centre to a formal monovalent state is not generally accepted. Yet, a 1-electron reduction (dyes present) of active hydrogenase in the EPR silent Ni_a(II) state leads to the Ni-C signal. Also oxidation of the $S = 1/2$ Ni_a-CO state leads to the EPR-silent Ni_a(II).CO state (Figs. 22 and 24) and this strongly suggests that the former state can indeed be denoted as Ni_a(I).CO. Illumation of this Ni_a(I).CO state leads to an EPR spectrum identical to that obtained after illumination of the Ni-C state (Fig. 18). Hence after illumination of both, the Ni-C state and the Ni_a(I).CO state, one and the same Ni_a(I) state is obtained. It is therefore that the nickel centre in the Ni-C state is considered by this author to be formally monovalent and is denoted as Ni_a(I).H_2.

From MCD measurements (Cheesman, M.R., Van der Zwaan, J.W., Albracht, S.P.J. and Thomson, A., unpublished observations; [40]) no signs for magnetism of nickel could be detected in the fully reduced hydrogenase {Ni(0) state} of *C. vinosum*. Also FTIR spectra showed no light-sensitive bands in this state, in contrast to the Ni-C state (Bagley, K.A., Albracht, S.P.J. and Woodruff, W.H., unpublished experiments). Together with the EPR data, this indicates that upon further reduction of Ni-C there is a conversion of nickel from an $S = 1/2$ state {Ni_a(I).H_2} to an $S = 0$ state {Ni(0)}. As discussed above, the effective charge density on the nickel ion is probably strongly buffered by covalent interactions with its ligands and remains most likely equal to that of a formally divalent nickel ion.

6. Groups tentatively involved in the structure and maintenance of the active site

6.1. The [3Fe-4S] cluster

Already in 1978 [211] it was demonstrated with the oxidized enzyme from *C. vinosum* that the EPR signal, which can now unequivocally be ascribed to a $[3Fe\text{-}4S]^+$ cluster, could be eliminated by reduction with ascorbate in the presence of phenazinemethosulphate (PMS). In view of the midpoint potential of ascorbate (+51 mV at pH 7.2) [19] it was concluded that the species responsible for this signal was unlikely to be a component of the H_2-activating site.

It is now known that certain nickel hydrogenases, e.g. the enzymes from *M. thermoautotrophicum* [7,45, 106,107], and *D. baculatus* [96,199,221] do not show any signs of a 3Fe cluster. In view of the sequence conservatism of the Cys pattern in the small subunits, these findings are highly surprising. Even in the most intact form of the *M. thermoautotrophicum* enzyme, when it is still attached to the heterodisulphide reduc-

tase, no 3Fe cluster could be found after addition of excess DCIP (Hedderich, R. and Albracht, S.P.J., unpublished experiments).

An intriguing possibility, therefore, is that motifs 1L and 2L from the large subunit, together with motifs 1S, 2S and 3S from the small subunit, might form a special environment (including six conservative Cys residues) to accommodate 4 Fe atoms and 4 acid-labile sulphur atoms in a very special 'evolutionary flexible' arrangement. Depending on the presence of non-conservative Cys residues in the several hydrogenases, this very special Fe-S arrangement, might sometimes be a $\{Fe^{ox} = [3Fe\text{-}4S\}^{+}\}$ centre (Fig. 11) with a rather loose electronic interaction between the putative Fe and the 3Fe cluster. In other hydrogenases a $[4Fe\text{-}4S]^{2+(2+:1+)}$ state might be preferred. One could even speculate on the presence of two $[2Fe\text{-}2S]^{2+(2+:1+)}$ clusters, which likewise would be diamagnetic in the oxidized enzyme. At present the cluster clearly is a 'mysterious' cluster ('M-cluster').

Even so, this is in line with the idea that the 3Fe cluster itself is not involved in H_2-activation. It is also unlikely that this cluster on its own plays a role in the transfer of electrons from H_2 to the cubane clusters in hydrogenase or to redox proteins with a low midpoint potential: nickel hydrogenases function in a redox regime where the 3Fe cluster, when detectable, remains reduced continously. It is only at oxidation-reduction potentials where the enzyme becomes inactive that the 3Fe cluster and also nickel become oxidized. In nature such a situation is usually created by oxygen.

In their natural habitat purple sulphur bacteria like *C. vinosum* and *T. roseopersicina*, are daily exposed to changing growth conditions: from photolithotrophic under anaerobic conditions during day time to chemolithotrophic under semi-aerobic conditions at night. It has been shown that these organisms can oxidize sulphur or sulphide either anaerobically in the light or at the expense of O_2 in the dark. They can quickly switch their energy metabolism from one mode to the other [53,110]. Purple sulphur bacteria can also grow on H_2 and CO_2 in the light. The hydrogenases in these bacteria must be able to respond to these daily changes without getting irreversibly inactivated. This also implies that in these bacteria the nickel in hydrogenase possibly indeed exists as Ni(III) during semi-aerobic growth in the dark. The presence of a $[3Fe\text{-}4S]^{0}$ cluster in the vicinity of the nickel centre might help to prevent the formation of the O_2^- radicals, which can be highly devastating when protonated.

$$Ni(II) + O_2 \longrightarrow Ni(III) + O_2^-$$

A reduced 3Fe cluster might safeguard the Ni site by immediately neutralizing any O_2^- radicals when they arise, by supplying an extra electron:

$$O_2^- + [3Fe\text{-}4S]^{0} \longrightarrow O_2^{2-} + [3Fe\text{-}4S]^{+}$$

The resulting H_2O_2 can be eliminated by catalase. This presumed function of the 3Fe cluster is line with its redox potential: this is higher than that of the Ni(III)/Ni(II) couple. Hence nickel will be oxidized before the 3Fe cluster. Also *D. gigas* can survive and grow under semi-aerobic conditions. This bacterium can synthesize a real oxidase [43] and contains the enzymes superoxide dismutase and catalase.

Bastian et al. [21] noted that both hydrogenases from *M. thermoautotrophicum* strain ΔH rapidly and irreversibly inactivated, when H_2-reduced enzyme was exposed to oxygen. We have similar experiences with aerobically-purified F_{420}-non-reducing hydrogenase from *M. thermoaurotrophicum* strain Marburg, which also has no detectable signs of a 3Fe cluster (Fontijn, R.D. and Albracht, S.P.J., unpublished observations). Not only the activity became highly impaired, but also on an SDS-gel many new polypeptide bands appeared. Inactivation was also noted with the fully oxidized *C. vinosum* enzyme with nickel in the Ni_a(II).CO state (Chen, M., Van der Zwaan, J.W. and Albracht, S.P.J., unpublished observations; [42]). When oxygen was admitted to such a preparation, then several new EPR signals from nickel appeared and the activity of the preparation dropped considerably and irreversibly. No such effects were observed with the enzyme after oxidation by O_2 of H_2-reduced enzyme. The effects might be due to formation of O_2^- at the nickel site. The superoxide then probably induces oxidations at multiple sites in the coordination of nickel.

Besides being a reductive safeguard for the nickel site, the 3Fe cluster and the Cys residues from the motifs 1S, 2S and 3S might at the same time be of structural importance to sustain a proper and stable coordination of the putative iron atom (in combination with ligands from motifs 1L and 2L).

It must be recalled here that Sayavedra-Soto and Arp [168] reported Cys → Ser mutations of the individual Cys residues in motif 1S of *A. vinelandii* hydrogenase. This did not lead to a complete loss of activity. A double mutation of the second Cys residue and the preceding (non-conservative) Cys residue did result in the complete absence of activity in cell colonies. As mentioned earlier, a thorough investigation of the properties of the mutant enzymes seems in place.

6.2. Copper

For a number of nickel hydrogenases it has been reported that copper is present in amounts in excess of 10% of the nickel. The F_{420}-non-reducing enzyme from *M. formicium* [4] contained 3.2 Cu per Ni. A Cu(II) EPR spectrum could be obtained only after reduction and re-oxidation of the enzyme. As re-oxidation of active reduced enzyme also lead to extensive irre-

versible inactivation, the presence of this Cu(II) signal was supposed to be correlate to this process. Adams et al. [4] also reported the presence of more than 2 Cu atoms per nickel in hydrogenases from *M. thermoautotrophicum* strain ΔH. In our laboratory we have likewise found up to 2 Cu/Ni in F_{420}-non-reducing hydrogenase from *M. thermoautotrophicum* strain Marburg [46] and variable amounts (0.2–1 Cu/Ni) in enzyme from *C. vinosum* (Coremans, J.C.C., Van der Zwaan, J.W. and Albracht, S.P.J., unpublished observations). The copper did not show up in EPR spectra of oxidized enzyme as isolated, but could only be observed after re-oxidation of reduced, activated enzyme under certain conditions. Copper has also been reported in nickel hydrogenase from *D. gigas* (0.2 Cu/Ni) [73].

In order to verify whether copper was required for activity, both *M. thermoautotrophicum* strain Marburg and *C. vinosum* were grown on Cu-deficient media (Böcher, R., Van Veenhuizen, M., Albracht, S.P.J. and Thauer, R.K., unpublished observations). Growth was not noticeably affected and the specific H_2-uptake activities of cell extracts was the same as usual. The enzyme from the Cu-deficient *C. vinosum* cells was purified and its Cu content was found to be less than 0.05 Cu/Ni. The specific activity was within the range of that of normal preparations. Incidentally, no EPR signals due to Ni(III) could be observed in the aerobic enzyme and in the $g = 2$ region an EPR spectrum was present very similar to that of Fig. 9, I-A. Apparently oxygen could not oxidize Ni(II) in this preparation. These experiments show that Cu is neither required for the biosynthesis of hydrogenase nor for the tested activities (H_2-uptake activity with benzyl viologen or H_2-production activity with reduced methyl viologen).

The Cu content of normal *C. vinosum* hydrogenase preparations also drastically decreases upon extensive purification on a Mono-Q column (Pharmacia) without a drop in specific activity. It was noticed repeatedly with such preparations, however, that reoxidation by air of H_2-reduced enzyme often resulted in a 50% irreversible loss of activity (Bouwens, E.C. and Albracht, S.P.J., unpublished observations). Such a loss of activity was not noticed with routine preparations of the enzyme (without the Mono-Q purification step).

It is curious that when Cu was present in amounts of 1–2 times that of nickel, it was not detectable in EPR spectra of oxidized aerobic enzyme. Extraneous copper bound to proteins is usually detectable as a type-II Cu(II) EPR signal. The behaviour of copper in nickel hydrogenases is reminiscent of type-III copper in copper proteins, a diamagnetic exchange-coupled Cu(II)-Cu(II) pair which also can show up as a Cu(II) EPR signal after oxidation of reduced enzyme [159]. In this respect it might be speculated that the His-rich region present in a number of hydrogenases around motif 3 in the large subunit might play a role in binding of copper. When present, copper might well have a specific helper function, in addition to the 3Fe cluster, in protecting the nickel hydrogenases against oxidative damage by properly modulating the reaction of the reduced enzyme with O_2. Copper is found in many redox enzymes reacting with O_2 [159].

At present I tentatively assume that, although not involved in the H_2-activating reaction or electron transfer, both the [3Fe-4S] cluster and Cu might have a role in the defensive mechanism of the enzyme against oxidative damage by O_2 in nature, in organisms that frequently are exposed to alternating reducing anaerobic conditions and semi-aerobic conditions. In addition, the [3Fe-4S] cluster might be of essential structural assistance for the coordination of the putative Fe ion.

7. Activation

7.1. The first step: removal of oxygen

Most nickel hydrogenases isolated in air are not active. To explain the lag phase very often observed during activity assays of hydrogenase Fisher et al. [75] have proposed already in 1954 a reversible binding of O_2 to the enzyme. Berlier et al. [24] came to a similar conclusion when studying the exchange reaction of the *D. gigas* enzyme. The idea was further worked out by Teixeira et al., [196] who proposed that Ni_u(III) was an oxygenated form of Ni_r(III). Oxygen was assumed to bind quite close to Ni_u(III), may be even as a ligand. Maroney and coworkers [120] have considered the possibility of a nickel-sulfinato complex to explain the deactivation of hydrogenases by oxygen.

As mentioned earlier, studies with O_2 enriched in ^{17}O ($I = 5/2$) [210] made it unlikely that O_2 is a direct ligand to Ni(III). Since the coordination of nickel is not perturbed (no change in EPR signals), also a nickel-sulfinato species is less likely. Also the EPR signals of the $[3Fe\text{-}4S]^+$ cluster and the $\{X^{ox} = [3Fe\text{-}4S]^+\}$ centre were not influenced by the binding. As the broadening of the Ni(III) EPR signal [210] is thus far only observed by oxidation of reduced enzyme by $^{17}O_2$, one cannot tell whether dioxygen or one of its reduction products is bound in the vicinity of Ni(III).

Fernandez et al. [69,72] have studied the reduction and activation of the *D. gigas* enzyme by H_2 in some detail. It was observed that reduction of Ni_u(III) by H_2 in the *D. gigas* enzyme occurred within 5 min, concommitant with the appearance of the broad signal ascribed to the reduced [4Fe-4S] clusters. It is quite likely that under these conditions bound O_2 or any of its partially-reduced reaction adducts will be fully re-

duced. Hence that barrier is eliminated in this way. Activity was, however, not induced yet at this state.

7.2. The second step: transition of unready to ready enzyme

The two forms of trivalent nickel, $Ni_r(III)$ and $Ni_u(III)$, have been described in many hydrogenases. They can be interconverted by redox cycling. It has been shown that full reduction and reoxidation of the *D. gigas* enzyme resulted in considerable changed ratios of $Ni_r(III)/Ni_u(III)$ [31,196]. The $Ni_r(III)$ form was mainly obtained by anaerobic reoxidation of H_2/N_2 treated enzyme with DCIP [31,70,72], although a conversion of $Ni_r(III)$ to $Ni_u(III)$ was observed upon prolonged incubation [34]. Reoxidation with O_2 resulted in enzyme mainly with $Ni_u(III)$.

A similar redox-induced transition has been described, although not recognized at the time, with the *C. vinosum* enzyme [11]. A more recent study with the *C. vinosum* enzyme [210] indicated that reoxidation of H_2/Ar treated enzyme with high partial pressures of O_2 resulted mainly in the appearance of $Ni_r(III)$, whereas low oxygen tensions induced preferentially $Ni_u(III)$. If H_2/Ar-treated *C. vinosum* enzyme was first oxidized with benzyl viologen, whereby the broad signal ascribed to the two $[4Fe\text{-}4S]^+$ clusters was eliminated and the Ni and [3Fe-4S] cluster were EPR silent, then $Ni_u(III)$ or $Ni_r(III)$ could be obtained by oxidation with O_2 or methylene blue, respectively [42]. This indicates that the initial overall redox status of the enzyme as well as the type of oxidant are of importance for the nickel coordination (ready versus unready) obtained. The transition of unready nickel to ready nickel can only be induced under reducing conditions. Berlier et al. [25] have reported that CO could induce the transition 'unready' to 'ready' in the *D. gigas* enzyme without any reduction, although no EPR spectra were shown. With the *C. vinosum* enzyme such an activation could not be observed [210] and in the *T. roseopersicina* enzyme the reverse conversion has been noticed [232].

7.3. The third step: reductive activation

The presence of $Ni_r(II)$ alone is presumably not sufficient to obtain full activity. Apparently there is another redox-linked change which definitely decides whether $Ni_r(II)$ can be converted into $Ni_a(II)$ and so whether it can be further reduced, binds ligands and whether hydrogen can be turned over with high velocity.

Lissolo et al. [130] have proposed that the activation of the *D. gigas* enzyme in the presence of varying concentration of H_2 involved an $n = 1$ redox process ($E'_0 = -310$ mV at pH 7; -60 mV per pH unit). Fernandez et al. [70] found that although reduction of the unready *D. gigas* enzyme was a matter of minutes, activation by H_2 was a much slower process and was enhanced by elevated temperatures (activation energy of 88 kJ/mol). At these temperatures, the presence of redox mediators further accelerates the process. Activation was independent of the enzyme concentration, so there is no involvement of intermolecular electron exchange.

The changes that occur during reductive activation have an important influence on the redox properties of nickel. The redox behaviour at 4°C of $Ni_u(III)$ in the *M. thermoautotrophicum* enzyme and both $Ni_r(III)$ and $Ni_u(III)$ in the *C. vinosum* enzyme, shows that no reduction beyond Ni(II) can occur at any potential before reductive activation has taken place. Once activated, ligand binding to $Ni_a(II)$ is possible and the way for further reduction of $Ni_a(II)$ is likewise open. The nature of the proposed $n = 1$ redox group, involved in the process of reductive activation, is unknown.

8. Reaction with hydrogen without apparent redox changes

Hydrogenases carry out a heterolytic cleavage of H_2 for reasons summarized by Krasna [117]. The reaction of H_2 with the enzyme was studied by monitoring the conversion of *para*-H_2 (anti-parallel nuclear spins) to *ortho*-H_2 (parallel nuclear spins). At room temperature and in the presence of a catalyst, hydrogen is an equilibrium mixture of 25% *para*-H_2 and 75% *ortho*-H_2 [61]. At low temperatures (20 K) this equilibrium shifts completely to the *para* form. The conversion of *para*-H_2 to *ortho*-H_2 catalyzed by hydrogenase can be written as:

$$E + p\text{-}H_2(\uparrow\downarrow) \longleftrightarrow EH^- + H_a^+$$

(H_a^+ coming from H_2) and then in H_2O:

$$EH^- + H_b^+ \longleftrightarrow E + o\text{-}H_2(\uparrow\uparrow)$$

(H_b^+ coming from the bulk water). In D_2O no such conversion was observed, since then the following reactions occur:

$$E + p\text{-}H_2(\uparrow\downarrow) \longleftrightarrow EH^- + H_a^+$$

$$EH^- + D^+ \longleftrightarrow E + HD$$

Eventually also the next two reactions take place:

$$E + HD \longleftrightarrow ED^- + H^+$$

$$ED^- + D^+ \longleftrightarrow E + D_2$$

The assumption was made here that enzyme-bound H^- does not exchange with water.

Krasna and coworkers [68,115,117] reported that the ratio of the rates of HD to DD formation during the H_2/D_2O exchange reaction ranged from 5 for the

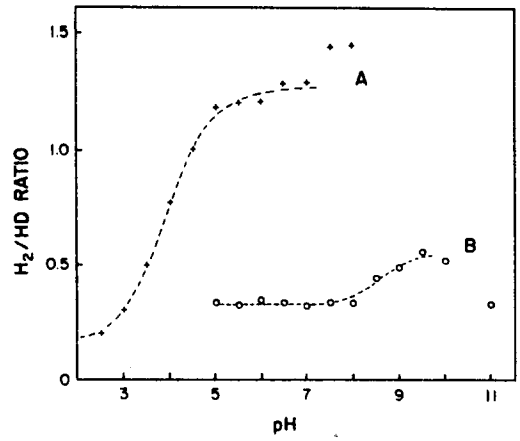

Fig. 28. Variation of the H_2/HD ratios as observed in D_2/H_2O exchange experiments with cytoplasmic hydrogenase from *D. baculatus* (A) and the enzyme for *D. gigas* (B). (From Teixeira et al. [198] with permission.)

enzyme from *Proteus vulgaris* to 0.9 for hydrogenase from *D. desulfuricans*. Krasna pointed out that even for the *P. vulgaris* enzyme the rate of DD formation was greater than would be expected on the assumptions of HD being an obligatory intermediate and an enzyme-bound hydride that did not exchange with water. This indicates either that enzyme-bound H^- might exchange with H_2O as well, or that the observation could be due to a molecular cage effect, by which formed HD reacts again to form DD, before diffusion of HD from the enzyme into the bulk water [117].

A low HD/H_2 ratio, comparable to the value found by Krasna [117] for the *D. desulfuricans* enzyme, was also reported by Lespinat et al. [128] in D_2/H_2O exchange experiments at pH 7 with the selenium-containing enzyme from *D. balculatus*. These investigators found a strong pH dependence for the HD/H_2 ratio in the exchange reaction. Teixeira et al. [198] have recalculated these data and published a plot of the pH dependence (Fig. 28). It is generally assumed that a base nearby the catalytic site might help to bind the proton during the heterolytic cleavage of H_2. The reaction can then be rewritten as:

$$M + D_2 + B^- \longleftrightarrow MD^- + DB$$

In order to explain the effects of Se and pH, it was assumed [128,198] that the hydride and proton acceptor sites can independently exchange with the solvent. In that case, the relative amounts of HD and H_2 produced would depend on the relative rates of exchange of the two sites. At low pH, the base will be always protonated, hence the major product will be HD. At high pH this mechanism is largely suppressed and then the metal-bound D^- might exchange with the solvent before recombination with a proton from the nearby base, resulting in H_2 formation (any protons bound to the base will exchange extremely fast with the solvent). This would also account for the difference in pH dependence of the Se-containing hydrogenase and a normal enzyme like that of *D. gigas* (Fig. 28). The pK_a of free H_2Se (3.77) is more than 3 units lower than that of H_2S (7.06).

9. Crystals: the relative position of the metal centres

It has appeared to be extremely difficult to obtain high-quality crystals of hydrogenases. Recently triclinic crystals of *D. gigas* hydrogenase have been obtained by Volbeda et al. [214]. The crystals diffracted down to 2.5 Å resolution. A first multiple isomorphous replacement map (5 Å resolution) was obtained. There were four features having a particularly high electron density. They presumably represent the four redox centres in the *D. gigas* enzyme. Based on the strength and the shape of the electron densities, Volbeda et al. [214] preliminarily assigned these high densities as a 4Fe cluster, a 3Fe cluster, a 4Fe cluster and Ni. The groups form an almost evenly spaced array (average distance about 12 Å). The angle 4Fe-3Fe-4Fe is 160°; the nickel ion makes an angle of about 120° with this array.

Higuchi and coworkers [214b] have recently located the prosthetic groups of the membrane-bound nickel hydrogenase from *D. vulgaris*, Miyazaki F in electron density maps at 4 Å resolution of crystals of the enzyme. The nickel atom is located near one of the three Fe-S clusters (at 13.8 Å). The second cluster is located at a distance of 13.1 Å from the first cluster (22.4 Å from nickel), whereas the third cluster is yet another 12.2 Å further away (total distance to nickel 32.5 Å).

The findings of these research groups form a breakthrough in the field of nickel hydrogenases. Higher resolution data on these enzymes will no doubt give answers to many questions.

10. Concluding remarks

Three types of unidentified electron acceptors have been described for nickel hydrogenases: (i) An $n = 1$ component involved in the spin-coupling in a number of oxidized enzymes. There is some evidence that this might be a special Fe ion; (ii) An $n = 1$ component involved in the reductive activation process; (iii) A redox component that accepts one of the two electrons of a H_2 molecule when it reacts with active enzyme in the absence of dyes. There is some evidence that this might be a special Fe ion. It is tempting to speculate that all three described redox transitions somehow involve the same centre, possibly the special Fe ion. So this review leads to a tentative working hypothesis that an as yet uncharacterized redox component, possibly a special Fe ion, is an essential part of nickel hydroge-

nases. The possibility is considered that the Ni site and the putative Fe site *together* form the active site in the mature enzyme (Fig. 11). This would allow for an $n = 2$ site for reaction with H_2 in active enzyme. It is speculated that the N-terminal conservative motifs 1L and 2L from the large subunit might possibly provide the major part of the ligands for this putative Fe atom. The [3Fe-4S] cluster in the small subunit might be of essential structural assistance as well. Together, they might form a unique arrangement of 4 Fe atoms and at least 6 Cys residues: the 'M-cluster'. In fully oxidized enzyme the putative Fe atom might be low spin Fe(III). It then might have electronic contact with the 3Fe cluster (the $\{Fe^{ox} = [3Fe\text{-}4S]^+\}$ centre) and weak magnetic interaction with the $S = 1/2$ of the Ni(III) centre. The putative Fe site would be expected to undergo (at least) two redox transitions: from Fe^{ox} {low spin Fe(III)} via Fe^{red1} {low-spin Fe(II); in uncoupled oxidized enzyme} to Fe^{red2}. After reductive activation a reaction like:

$$Ni_a(I).H_2 + Fe^{red1} + H_2 \longleftrightarrow Ni_a(0) + Fe^{red2}$$

might then be the only reversible reaction of the nickel hydrogenases with H_2 (no dyes). In some enzymes this special Fe atom might be a member of a (unusual) $[4Fe\text{-}4S]^{2+(2+:1+)}$ cluster, a variant of the M-cluster with strong cooperation of the putative Fe ion and a [3Fe-4S] cluster. In other enzymes it might be one of the Fe atoms in an arrangement of two [2Fe-2S] clusters, another possible variant of the M-cluster. The ligands and other electronic contacts of the putative iron might participate in charge redistribution during these redox changes. In the presence of redox mediators, hydrogen might be oxidized via a different reaction, not nescessarily involving both nickel and the putative Fe ion. It can be speculated that in the Ni-C state, this putative Fe atom might be possibly also involved in the two-fold splitting of the $Ni_a(I).H_2$ EPR signal at 4.2 K.

If there is truth in this hypothesis, then the name 'Ni-Fe hydrogenases' or [NiFe] hydrogenases, used in publications of other authors to emphasize the role of Fe-S clusters, would gain a new meaning. The availability of crystals and the powerful site-directed mutagenesis tool for hydrogenases, in combination with physicochemical tools to properly characterize mutant enzymes, will certainly greatly contribute to a more detailed understanding of the active site of nickel hydrogenases in the near future. It is hoped that considerations given in this review may be of help in the design of further experiments.

Another interesting experimental tool to probe the possible catalytic properties of nickel in the carboxy-terminal amino-acid sequence of the large subunit would be the direct chemical synthesis of peptides. This approach would circumvent difficulties encountered during cloning and expression of relevant pieces of DNA. It would also allow to quickly replace single or multiple amino acids. A Tyr2His analogue (55 amino acids) of the 2[4Fe-4S] ferredoxin of *C. pasteurianum* has been synthesized in 1991 [182]. Also, a 25 amino-acid residue long analogue of the active site of rubredoxin from *D. gigas* has been succesfully synthesized [44]. Via such an approach it is possible to obtain in about a week sufficient material for most physicochemical studies.

Acknowledgements

I am indebted to many colleagues in the hydrogenase community for the exchange of information and ideas. In particular Mr. E. van Asselt, Dr. K. Bagley, Dr. J.M.C.C. Coremans, Mr. E.C. Duin, Prof. B. Friedrich, Dr. W.R. Hagen, Prof. E. Münck, Prof. D. Sellmann, Mr. O. Sorgenfrei, Prof. R.K. Thauer and Dr. J.W. van der Zwaan are acknowledged for many stimulating discussions. I am very grateful to Drs. Z. Dermoun, M. Frey, M.F. Gorwa and Y. Higuchi for providing experimental results prior to publication. I thank the Netherlands Organization of Pure Research (NWO) and the Netherlands Foundation for Chemical Research (SON) for continued support.

References

[1] Ackrell, B.A.C., Asato, R.N. and Mower, H.F. (1966) J. Bacteriol. 92, 828–838.
[2] Adams, M.W.W., Mortenson, L.E. and Chen, J.-S. (1980) Biochim. Biophys. Acta 594, 105–176.
[3] Adams, M.W.W. and Mortenson, L.E. (1984) J. Biol. Chem. 259, 7045–7055.
[4] Adams, M.W.W., Jin, S.-L.C., Chen, J.-S. and Mortenson, L.E. (1986) Biochim. Biophys. Acta 869, 37–47.
[5] Adams, M.W.W., Eccleston, E. and Howard, J.B. (1989) Proc. Natl. Acad. Sci. USA 86, 4932–4936.
[6] Adams, M.W.W. (1990) Biochim. Biophys. Acta 1020, 115–145.
[7] Albracht, S.P.J., Graf, E.-G. and Thauer, R.K. (1982) FEBS Lett. 140, 311–313.
[8] Albracht, S.P.J., Albrecht-Ellmer, K.J., Schmedding, D.J.M. and Slater, E.C. (1982) Biochim. Biophys. Acta 681, 330–334.
[9] Albracht, S.P.J., Kalkman, M.L. and Slater, E.C. (1983) Biochim. Biophys. Acta 724, 309–316.
[10] Albracht, S.P.J., Van der Zwaan, J.W. and Fontijn, R.D. (1984) Biochim. Biophys Acta 766, 245–258.
[11] Albracht, S.P.J., Fontijn, R.D. and Van der Zwaan, J.W. (1985) Biochim. Biophys. Acta 832, 89–97.
[12] Albracht, S.P.J., Kröger, A., Van der Zwaan, J.W., Unden, G., Böcher, R., Mell, H. and Fontijn, R.D. (1986) Biochim. Biophys. Acta 874, 116–127.
[13] Albracht, S.P.J., Ankel-Fuchs, D., Böcher, R., Ellermann, J., Moll, J., Van der Zwaan, J.W. and Thauer, R.K. (1988) Biochim. Biophys. Acta 955, 86–102.
[14] Albracht, S.P.J. (1993) Biochim. Biophys. 1144, 221–224.
[15] Arizmendi, J.M., Runswick, M.J., Skehel, J.M. and Walker, J.E. (1992) FEBS Lett. 301, 237–242.

[16] Asso, M., Guigliarelli, B., Yagi, T. and Bertrand, P. (1992) Biochim. Biophys. Acta 1122, 50–56.
[17] Bagley, K.A., Van Garderen, C.J., Chen, M., Duin, E.C., Albracht, S.P.J. and Woodruff, W.H. (1994) Biochemistry 33, 9229–9236.
[18] Bagyinka, C., Whitehead, J.P. and Maroney, M.J. (1993) J. Am. Chem. Soc. 115, 3567–3585.
[19] Ball, E.G. (1937) J. Biol. Chem. 118, 219–239.
[20] Bartha, R. and Ordal, E.J. (1965) J. Bacteriol. 89, 1015–1019.
[21] Bastian, N.R., Wink, D.A., Wackett, L.P., Livingston, D.J., Jordan, L.M., Fox, J., Orme-Johnson, W.H. and Walsh, C.T. (1988) in The Bioinorganic Chemistry of Nickel (Lancaster, J.R., Jr., ed.), pp. 227–247, VCH, Weinheim, Germany.
[22] Beinert, H. and Albracht, S.P.J. (1982) Biochim. Biophys. Acta 683, 245–277.
[23] Bell, S.H., Dickson, D.P.E., Rieder, R., Cammack, R., Patil, D.S., Hall, D.O. and Rao, K.K. (1984) Eur. J. Biochem. 145, 645–651.
[24] Berlier, Y.M., Fauque, G., Lespinat, P.A. and LeGall, J. (1982) FEBS Lett. 140, 185–188.
[25] Berlier, Y.M., Fauque, G.D., LeGall, J., Lespinat, P.A. and Peck, H.D., Jr. (1987) FEBS Lett. 221, 241–244.
[26] Böck, A., Forchhammer, K., Heider, J., Leinfelder, W., Sawers, G., Veprek, B. and Zinoni, F. (1991) Mol. Microbiol. 5, 515–520.
[27] Böhm, R., Sauter, M and Böck, A. (1990) Mol. Microbiol. 4, 231–243.
[28] Cammack, R., Lalla-Maharajh, W.V. and Schneider, K. (1982) in Electron Tranport and Oxygen Utilization (Ho, C., ed.), pp. 411–415, Elsevier North Holland.
[29] Cammack, R., Patil, D.S., Aquirre, R. and Hatchikian, E.C. (1982) FEBS Lett. 142, 289–292.
[30] Cammack, R. Hall, D.O. and Rao, K.K. (1985) in Microbial Gas Metabolism: Mechanistic, Metabolic and Biotechnological Aspects (Poole, R.K. and Dow, C.S., eds.), pp. 75–102, Academic Press, London.
[31] Cammack, R., Patil, D.S. and Fernandez, V.M. (1985) Biochem. Soc. Trans. 13, 572–578.
[32] Cammack, R., Rao, K.K., Serra, J. and Llama, M.J. (1986) Biochimie 68, 93–96.
[33] Cammack, R., Patil, D.S., Hatchikian, E.C. and Fernandez, V.M. (1987) Biochim. Biophys. Acta 912, 98–109.
[34] Cammack, R. (1988) Adv. Inorg. Chem. 32, 297–333.
[35] Cammack, R. (1989) J. Inorg. Biochem. 36, 206.
[36] Cammack, R., Bagyinka, C. and Kovacs, K.L. (1989) Eur. J. Biochem. 182, 357–362.
[37] Cammack, R., Kovacs., K.L., McCracken, J. and Peisach, J. (1989) Eur. J. Biochem. 182, 363–366.
[38] Chambers, I., Frampton, J., Goldfarb, P., Affara, N., McBain, W. and Harrison, P.R. (1986) EMBO J. 5, 1221–1227.
[39] Chapman, A., Cammack, R., Hatchikian, E.C., McCracken, J. and Peisach, J. (1988) FEBS Lett. 242, 134–138.
[40] Cheesman, M.R. (1988) Spectroscopic studies of nickel ions in bacterial proteins. PhD Thesis, University of East Anglia, Norwich, UK.
[41] Chen, J.-S. and Mortenson, L.E. (1974) Biochim. Biophys. Acta 371, 283–298.
[42] Chen, M. (1992) Hydrogenase from *Chromatium vinosum*. Function and reactivity of metal centers. PhD Thesis, University of Amsterdam, The Netherlands.
[43] Chen, L., Liu, M.-Y., LeGall, J., Fareleira, P., Santos, H. and Xavier, A.V. (1993) Biochem. Biphys. Res. Commun. 193, 100–105.
[44] Christensen, H.E.M., Hammerstad-Pedersen, J.M., Holm, A., Roepstorff, P., Ulstrup, J., Vorm, O. and Ostergård, S. (1992) FEBS Lett. 312, 219–222.
[45] Coremans, J.M.C.C., Van der Zwaan, J.W. and Albracht, S.P.J. (1989) Biochim. Biophys. Acta 997, 256–267.
[46] Coremans, J.M.C.C. (1991) Redox properties of hydrogenase. PhD Thesis, University of Amsterdam, Amsterdam, The Netherlands.
[47] Coremans, J.M.C.C., Van Garderen, C.J. and Albracht, S.P.J. (1992) Biochim. Biophys. Acta 1119, 148–156.
[48] Coremans, J.M.C.C., Van der Zwaan, J.W. and Albracht, S.P.J. (1992) Biochim. Biophys. Acta 1119, 157–168.
[49] Coyle, C.L. and Stiefel, E.I. (1988) in The Bioinorganic Chemistry of Nickel (Lancaster, J.R., Jr., ed.), pp. 1–28, VCH, Weinheim, FRG.
[50] Crabtree, R.H. (1986) Inorg. Chim. Acta 125, L7–L8.
[51] Daniels, L., Fox, J., Jacobson, F., Orme-Johnson, W.H. and Walsh, C. (1981) 7th Int. Symp. on Flavins and Flavoproteins, Ann Arbor, USA.
[52] DerVartanian, D.V., Kruger, H.J., Peck., H.D., Jr. and LeGall, J. (1985) Rev. Port. Quim. 27, 70–73.
[53] De Wit, R. and Van Gemerden, H. (1987) FEMS Microbiol. Ecol. 45, 117–126.
[54] Doddema, H.J. (1980) The proton-motive force in *Methanobacterium thermoautotrophicum*. Ph.D. Thesis, University of Nijmegen, Sneldruk Boulevard Enschede, Enschede, The Netherlands.
[55] Dross, F., Geisler, V., Lenger, R., Theis, F., Krafft, T., Fahrenholz, F., Kojro, E., Duchêne, Tripier, D., Juvenal, K. and Kröger, A. (1992) Eur. J. Biochem. 206, 93–102.
[56] Eidsness, M.K., Sullivan, R.J. and Scott, R.A. (1988) in The Bioinorganic Chemistry of Nickel (Lancaster, J.R., Jr., ed.), pp. 73–91, VCH, Weinheim, FRG.
[57] Eidsness, M.K., Scott, R.A., Prickril, B.C., DerVartanian, D.V., LeGall, J., Moura, I., Moura, J.J.G. and Peck, H.D., Jr. (1989) Proc. Natl. Acad. Sci. USA 86, 147–151.
[58] Ellermann, J., Hedderich, R., Böcher, R. and Thauer, R.K. (1988) Eur. J. Biochem. 172, 669–677.
[59] Emptage, M.H., Kent, T.A., Huynh, B.H., Rawlings, J., Orme-Johnson, W.H. and Münck, E. (1980) J. Biol. Chem. 255, 1793–1796.
[60] Fan. C., Teixeira, M., Moura, J., Moura, I., Huynh, B.-H., LeGall, J., Peck, H.D., Jr. and Hoffman, B.M. (1991) J. Am. Chem. Soc. 113, 20–24.
[61] Farkas, A. (1935) Orthohydrogen, Parahydrogen and Heavy Hydrogen. Cambridge University Press, London.
[62] Fauque, G., Teixeira, M., Moura, I., Lespinat, P.A., Xavier, A.V., DerVartainian, D.V., Peck, H.D., Jr., LeGall, J. and Moura, J.J.G. (1984) Eur. J. Biochem. 142, 21–28.
[63] Fauque, G., Berlier, Y., Czechowski, M., Lespinat, P.A., Moura, J.J.G. and LeGall, J. (1988) Abstract, Int. Symp. on the Mol. Biol. of Hydrogenases, Helen, Georgia, USA.
[64] Fauque, G., Peck, H.D., Jr., Moura, J.J.G., Huynh, B.H., Berlier, Y., DerVartanian, D.V., Teixeira, M., Przybyla. A.E., Lespinat, P.A., Moura, I. and LeGall, J. (1988) FEMS Microbiol. Rev. 54, 299–344.
[65] Fearnley, I.M., Runswick, M.J. and Walker, J.E. (1989) EMBO J. 8, 665–672.
[66] Fearnley, I.M. and Walker, J.E. (1992) Biochim. Biophys. Acta, 1140, 105–134.
[67] Fee. J.A., Findling, K.L., Yoshida, T., Hille, R., Tarr, G.E., Hearshen, D.O., Dunham, W.R., Day, E.P., Kent, T.A. and Münck, E. (1984) J. Biol. Chem. 259, 124–133.
[68] Feigenblum, E. and Krasna, A.I. (1970) Biochim. Biophys. Acta 198, 157–164.
[69] Fernandez, V.M., Aguirre, R and Hatchikian, E.C. (1984) Biochim. Biophys. Acta 790, 1–7.
[70] Fernandez, V.M., Hatchikian, E.C. and Cammack, R. (1985) Biochim. Biophys. Acta 832, 69–79.

[71] Fernandez, V.M., Rao, K.K., Fernandez, M.A. and Cammack, R. (1986) Biochimie 68, 43–48.
[72] Fernandez, V.M., Hatchikian, E.C., Patil, D.S. and Cammack, R. (1986) Biochim. Biophys. Acta 883, 145–154.
[73] Fernandez, V.M., Rua, M.L., Reyes, P., Cammack, R. and Hatchikian, E.C. (1989) Eur. J. Biochem, 185, 449–454.
[74] Filipiak, M., Hagen, W.R. and Veeger, C. (1989) Eur. J. Biochem. 185, 547–553.
[75] Fisher, H.F., Krasna, A.I. and Rittenberg, D. (1954) J. Biol. Chem. 209, 569–578.
[76] Fox, J.A., Livingston, D.J., Orme-Johnson, W.H. and Walsh, C.T. (1987) Biochemistry 26, 4219–4227.
[77] Friedrich, B., Heine, E., Finck, A. and Friedrich, C.G. (1981) J. Bacteriol. 145, 1144–1149.
[78] Friedrich, B. and Schwartz, E. (1993) Annu. Rev. Microbiol. 47, 351–383.
[79] Fu, C. and Maier, R.J. (1993) J. Bacteriol. 175, 295–298.
[80] Fu, W., Drozdzewski, P.M., Morgan, T.V., Mortenson, L.E., Juszczak, A., Adams, M.W.W., He, S.-H., Peck, H.D., Jr., DerVartanian, D.V., LeGall, J. and Johnson, M.K. (1993) Biochemistry, 32, 4813–4819.
[81] Gaffron, H. and Rubin, J. (1942) J. Gen. Physiol. 26, 219–240.
[82] Gollin, D.J., Mortenson, L.E. and Robson, R.L. (1992) FEBS Lett. 309, 371–375.
[83] Graf, E.-G. and Thauer, R.K. (1981) FEBS Lett. 136, 165–169.
[84] Grove, D.M., Van Koten, G., Zoet, R., Murrall, N.W. and Welch, A.J. (1983) J. Am. Chem. Soc. 105, 1379–1380.
[85] Gubriel, R.J., Ohnishi, T., Robertson, D.E., Daldal, F. and Hoffman, B.M. (1991) Biochemistry 30, 11579–11584.
[86] Gunsalus, R.P., Romesser, J.A. and Wolfe, R.S. (1978) Biochemistry 17, 2374–2377.
[87] Hagen, W.R., Van Berkel-Arts, A., Krüse-Wolters, K.M., Dunham, W.R. and Veeger, C. (1986) FEBS Lett. 201, 158–162.
[88] Hagen, W.R., Van Berkel-Arts, A., Krüse-Wolters, K.M., Voordouw, G. and Veeger, C. (1986) FEBS Lett. 203, 59–63.
[89] Haines, R.I. and McAuley, A. (1981) Coord. Chem. Rev. 39, 77–119.
[90] Halboth, S. and Klein, A. (1992) Mol. Gen. Genet. 233, 217–224.
[91] Harden, A. (1901) J. Chem. Soc. (London) 79, 601–628.
[92] Haschke, R.H. and Campbell, L.L. (1971) J. Bacteriol. 105, 249–258
[93] Hatchikian, E.C., Forget, N., Fernandez, V.M., Williams, R. and Cammack, R. (1992) Eur. J. Biochem. 209, 357–365.
[94] Hausinger, R.P. (1987) Microbiol. Rev. 51, 22–42.
[95] He, S.-H., Woo, S.B., DerVartanian, D.V., LeGall, J. and Peck, H.D., Jr. (1989) Biochem. Biophys. Res. Commun. 161, 127–133.
[96] He, S.H., Teixeira, M., LeGall, J., Patil, D.S., Moura, I., Moura, J.J.G., DerVartanian, D.V., Huynh, B.H. and Peck, H.D., Jr. (1989) J. Biol. Chem. 264, 2678–2682.
[97] Heiden, S., Hedderich, R., Setzke, E. and Thauer, R.K. (1993) Eur. J. Biochem. 213, 529–535.
[98] Heinekey, D.M. and Oldham, J. (1993) Chem. Rev., 93, 913–926.
[99] Hoppe-Seyler, F. (1887) Z. Physiol. Chem. 11, 561–568.
[100] Hornhardt, S., Schneider, K. and Schlegel, H.G. (1986) Biochimie 68, 15–24.
[101] Hornhardt, S., Schneider, K., Friedrich, B., Vogt, B. and Schlegel, H.G. (1990) Eur. J. Biochem. 189, 529–537.
[102] Houseman, A.L.P., Oh, B.-H., Kennedy, M.C., Fan, C., Werst, M.H., Beinert, H., Markley, J.L. and Hoffman, B.H. (1992) Biochemistry 31, 2073–2080.
[103] Huynh, B.H., Czechowski, M.H., Krüger, H.-J., DerVartanian, D.V., Peck, H.D., Jr. and LeGall, J. (1984) Proc. Natl. Acad. Sci. USA 81, 3728–2732.
[104] Huynh, B.H., Patil, D.S., Moura, I., Teixeira, M., Moura, J.J.G., DerVartanian, D.V., Czechowski, M.H., Prickril, B.C., Peck, H.D., Jr. and LeGall, J. (1987) J. Biol. Chem. 262, 795–800.
[105] Hyman, M.R. and Arp, D.J. (1987) Biochemistry 26, 6447–6454.
[106] Jacobson, F.S., Daniels, L., Fox, J.A., Walsh, C.T. and Orme-Johnson, W.H. (1982) J. Biol. Chem. 257, 3385–3388.
[107] Johnson, M.K., Zambrano, I.C., Czechowski, M.H., Peck, H.D.,Jr., DerVartanian, D.V. and LeGall, J. (1986) in The Bioinorganic Chemistry of Nickel (Lancaster, J.R., Jr., ed.), pp. 36–44, VCH, Weinheim, FRG.
[108] Juszczak, A., Aono, S. and Adams, M.W.W. (1991) J. Biol. Chem. 266, 13834–13841.
[109] Kaserer, H. (1906) Zent. Bakt. Par. II 16, 681.
[110] Kämpf, C. and Pfennig, N. (1986) J. Basic Microbiol. 26, 517–531.
[111] Kent, T.A., Dreijer, J.-L., Kennedy, M.C., Huynh, B.H., Emptage, M.H., Beinert, H. and Münck, E. (1982) Proc. Natl. Acad. Sci. USA 79, 1096–1100.
[112] Kojima, N., Fox, J.A., Hausinger, R.P., Daniels, L., Orme-Johnson, W.H. and Walsh, C. (1983) Proc. Natl. Acad. Sci. USA 80, 378–382.
[113] Kortlüke, C. and Friedrich, B. (1992) J. Bacteriol. 174, 6290–6293.
[114] Köster, M.W.F. (1993) EPR und Mößbaueruntersuchungen an zwei Hydrogenasen von *Nocardia opaca* und *Alcaligenes eutrophus* und deren Untereinheiten. Ph.D. Thesis, Medizinische Universität Lübeck.
[115] Krasna, A.I., Riklis, E. and Rittenberg, D. (1960) J. Biol. Chem. 235, 2717–2720.
[116] Krasna, A.I. (1978) Methods Enzymol. 53, 296–314.
[117] Krasna, A.I. (1979) Enzyme Microb. Technol. 1, 165–172.
[118] Kubas, G.J., Ryan, R.R., Swanson, B.I., Vergamini, P.J. and Wasserman, H.J. (1984) J. Am. Chem. Soc. 106, 451–452.
[119] Kubas, G.J. (1988) Acc. Chem. Res. 21, 120–128.
[120] Kumar, M., Colpas, G.J., Day, R.O. and Maroney, M.J. (1989) J. Am. Chem. Soc. 111, 8323–8325.
[121] Kumar, M. and Ragsdale, S.W. (1992) J. Am. Chem. Soc. 114, 8713–8715.
[122] Lalla-Maharajh, W.V., Hall, D.O., Cammack, R., Rao, K.K. and LeGall, J. (1983) Biochem. J. 209, 445–454.
[123] Lancaster, J.R., Jr. (1980) FEBS Lett. 115, 285–288.
[124] Lancaster, J.R., Jr. (1982) Science 216, 1324–1325.
[125] Lancaster, J.R., Jr. (1988) The Bioinorganic Chemistry of Nickel, VCH, Weinheim, FRG.
[126] Leclerc, M., Colbeau, A., Cauvin, B. and Vignais, P.M. (1988) Mol. Gen. Genet. 214, 97–107.
[127] LeGall, J., DerVartanian, D.V., Spilker, E., Lee, J.-P. and Peck, H.D.,Jr. (1971) Biochim. Biophys. Acta 234, 525–530.
[128] Lespinat, P.A., Berlier, Y., Fauque, G., Czechowski, M., Dimon, B. and LeGall, J. (1986) Biochimie 68, 55–61.
[129] Lindahl, P.A., Kojima, N., Hausinger, R.P., Fox, J.A., Teo, B.K., Walsh, C.T. and Orme-Johnson, W.H. (1984) J. Am. Chem. Soc. 106, 3062–3064.
[130] Lissolo, T., Pulvin, S. and Thomas, D. (1984) J. Biol. Chem. 259, 11725–11729.
[131] Lissolo, T., Choi, E.S., LeGall, J. and Peck, H.D., Jr. (1986) Biochem. Biophys. Res. Commun. 139, 701–708.
[132] Livingston, D.J., Fox, J.A., Orme-Johnson, W.H. and Walsh, C.T. (1987) Biochemistry 26, 4228–4237.
[133] Lorentz, B., Schneider, K., Kratzin, H. and Schlegel, H.G. (1989) Biochim. Biophys. Acta 995, 1–9.
[134] Lutz, S., Jacobi, A., Schlensog, V., Böhm, R., Sawers, G. and Böck, A. (1991) Mol. Microbiol. 5, 123–135.
[135] Margerum, D.W. and Anliker, S.L. (1988) in The Bioinorganic Chemistry of Nickel (Lancaster, J.R., Jr., ed.), pp. 29–51, VCH, Weinheim, Germany.

[136] Maroney, M.J., Colpas, G.J. and Bagyinka, C. (1990) J. Am. Chem. Soc. 112, 7076–7078.
[137] Maroney, M.J., Colpas, G.J., Bagyinka, C., Baidya, N. and Mascharak, P.K. (1991) J. Am. Chem. Soc. 113, 3962–3972.
[138] Matsubara, H. and Saeki, K. (1992) Adv. Inorg. Chem. 38, 223–280.
[139] Menon, N.K., Peck, H.D., Jr., LeGall, J. and Przybyla, A.E. (1987) J. Bacteriol. 169, 5401–5407.
[140] Menon, A.L., Stults, L.W., Robson, R.L. and Mortenson, L.E. (1990) Gene 96, 67–74.
[141] Menon, N.K., Robbins, J., Wendt, J.C., Shanmugam, K.T. and Przybylz, A.E. (1991) J. Bacteriol. 173, 4851–4861.
[142] Meyer, J. and Gagnon, J. (1991) Biochemistry 30, 9697–9704.
[143] Morton, J.R. and Preston, K.F. (1984) J. Chem. Phys. 81, 5775–5778.
[144] Moura, J.J.G., Moura, I., Huynh, B.H., Krüger, H.-J., Teixeira, M., DuVarney, R.G., DerVartanian, D.V., Ljungdahl, P., Xavier, A.V., Peck, H.D., Jr. and LeGall, J. (1982) Biochem. Biophys. Res. Commun. 108, 1388–1393.
[145] Muth, E., Mörschel, E. and Klein, A. (1987) Eur. J. Biochem. 169, 571–577.
[146] Nag, K. and Chakravorty, A. (1980) Coord. Chem. Rev. 33, 87–147.
[147] Nakos, G. and Mortenson, L.E. (1971) Biochim. Biophys. Acta 227, 576–583.
[148] Nakos, G. and Mortenson, L.E. (1971) Biochemistry 10, 2442–2449.
[149] Odom, J.M. and Peck, H.D., Jr. (1981) FEMS Microbiol. Lett. 12, 47–50.
[150] Odom, J.M. and Peck, H.D., Jr. (1984) Annu. Rev. Microbiol. 38, 551–592.
[151] Pakes, W.C.C. and Jollyman, W.H. (1901) J. Chem. Soc. (London) 79, 386–391.
[152] Payne, M.J., Chapman, A. and Cammack, R. (1993) FEBS Lett. 317, 101–104.
[153] Pilkington, S.J., Skehel, J.M., Gennis, R.B. and Walker, J.E. (1991) Biochemistry 30, 2166–2175.
[154] Przybyla, A.E., Robbins, J., Menon, N. and Peck, H.D., Jr. (1992) FEMS Microbiol. Rev. 88, 109–136.
[155] Ragsdale, S.W., Ljungdahl, L.G. and DerVartanian, D.V. (1982) Biochem. Biophys. Res. Commun. 108, 658–663.
[156] Ragsdale, S.W. and Ljungdahl, L.G. (1984) Arch. Microbiol. 139, 361–365.
[157] Reeve, J.N., Beckler, G.S., Cram, D.S., Hamilton, P.T., Brown, J.W., Krzycki, J.A., Kolodziej, A.F., Alex, L., Orme-Johnson, W.H. and Walsh, C.T. (1989) Proc. Natl. Acad. Sci. USA 86, 3031–3035.
[158] Reeve, J.N. and Beckler, G.S. (1990) FEMS Microbiol. Rev. 87, 419–424.
[159] Reinhammer, B. (1983) in The Coordination Chemistry of Metalloenzymes (Bertini, I., Drago, R.S. and Luchinat, C., eds.), pp. 177–200, D. Riedel.
[160] Rieder, R., Cammack, R. and Hall, D.O. (1984) Eur. J. Biochem. 145, 637–643.
[161] Roberts, L.M., Barondeau, D. and Lindahl, P.A. (1993) J. Inorg. Biochem. 51, 53.
[162] Rospert S., Voges, M., Berkessel, A., Albracht, S.P.J. and Thauer, R.K. (1992) Eur. J. Biochem. 210, 101–107.
[163] Runswick, H.J., Gennis, R.B., Fearnley, I.M. and Walker, J.E. (1989) Biochemistry, 28, 9452–9459.
[164] Saillard, J.-Y. and Hoffmann, R. (1984) J. Am. Chem. Soc. 106, 2006–2026.
[165] Salerno, J.C. (1988) in The Bioinorganic Chemistry of Nickel (Lancaster, J.R., Jr., ed.), pp. 53–71, VCH, Weinheim, FRG.
[166] Sauter, M. (1992) Der Formiat-Hydrogenlyase-Komplex von *Escherichia coli*: Untersuchungen zu Struktur und Funktion. PhD Thesis, Ludwig-Maximilians-Universität München.
[167] Sauter, M., Böhm, R. and Böck, A. (1992) Mol. Microbiol. 6, 1523–1532.
[168] Sayavedra-Soto, L.A. and Arp, D.J. (1993) J. Bacteriol. 175, 3414–3421.
[169] Schindler, F. and Winter, J. (1987) Biochim. Biophys. Acta 913, 81–88.
[170] Schink, B. and Schlegel, H.G. (1979) Biochim. Biophys. Acta 567, 315–324.
[171] Schlegel, H.G. and Schneider, K. (1978) in Hydrogenases: Their Catalytic Activity, Structure and Function (Schlegel, H.G. and Schneider, K., eds.), pp. 15–44, Erich Goltze KG, Göttingen.
[172] Schlegel, H.G. and Schneider, K. (1978) Hydrogenases: Their Catalytic Activity, Structure and Function (Schlegel, H.G. and Schneider, K., eds.), Erich Goltze KG, Göttingen.
[173] Schlesier, M. and Friedrich, B. (1981) Arch. Microbiol. 129, 150–153.
[174] Schneider, K., Cammack, R., Schlegel, H.G. and Hall, D.O. (1979) Biochim. Biophys. Acta 578, 445–461.
[175] Schneider, K. and Schlegel, H.G. (1981) Biochem. J. 193, 99–107.
[176] Schneider, K., Patil, D.S., Cammack, R. (1983) Biochim. Biophys. Acta 748, 353–361.
[177] Schneider, K., Schlegel, H.G. and Jochim, K. (1984) Eur. J. Biochem. 183, 533–541.
[178] Scott, R.A., Wallin, S.A., Czechowski, M., DerVartanian, D.V., LeGall, J., Peck, H.D., Jr. and Moura, I. (1984) J. Am. Chem. Soc. 106, 6864–6865.
[179] Scott, R.A., Czechowski, M., DerVartanian, D.V., LeGall, J., Peck, H.D., Jr. and Moura, I. (1985) Rev. Port. Quim. 27, 67–70.
[180] Shin, W. and Lindahl, P.A. (1993) Biochim. Biophys. Acta 1161, 317–322.
[181] Smith, L.A., Hills, S. and Yates, M.G. (1976) Nature 262, 209–210.
[182] Smith, E.T., Tomich, J.M., Iwamoto, T., Richards, J.H., Mao, Y and Feinberg, B.A. (1991) Biochemistry 30, 11669–11676.
[183] Sorgenfrei, O., Linder, D., Karas, M. and Klein, A. (1993) Eur. J. Biochem. 213, 1355–1358.
[184] Sorgenfrei, O., Klein, A. and Albracht, S.P.J. (1993) FEBS Lett. 332, 291–297.
[185] Stephenson, M. and Stickland. L.H. (1931) Biochem. J. 25, 205–214.
[186] Stephenson, M. and Stickland, L.H. (1931) Biochem. J. 125, 215–220.
[187] Stokkermans, J., Van Dongen, W., Kaan, A., Van den Berg, W. and Veeger, C. (1989) FEMS Microbiol. Lett. 58, 217–222.
[188] Stokkermans, J. (1993) Molecular studies on iron-sulfur proteins in *Desulfovibrio*. PhD Thesis, Agricultural University of Wageningen, The Netherlands.
[189] Strekas, Y., Antanaitis, B.C. and Krasna, A.I. (1980) Biochim. Biophys. Acta 616, 1–9.
[190] Sugiura, Y., Kuwahara, J. and Suzuki, T. (1983) Biochem. Biophys. Res. Commun. 115, 878–881.
[191] Sun, J.-H., Hyman, M.R. and Arp, D.J. (1992) Biochemistry 31, 3158–3165.
[192] Surerus, K.K., Chen, M., Van der Zwaan, J.W., Rusnak, F.M., Kolk, M., Duin, E.C., Albracht, S.P.J. and Münck, E. (1994) Biochemistry 33, 4980–4993.
[193] Tabillon, R., Weber, F. and Kaltwasser, H. (1980) Arch. Microbiol. 124, 131–136.
[194] Tan, S.-L., Fox, J.A., Kojima, N., Walsh, C.T. and Orme-Johnson, W.H. (1984) J. Am. Chem. Soc. 106, 3064–3066.
[195] Teixeira, M., Moura, I., Xavier, A.V., DerVartanian, D.V., LeGall, J., Peck, H.D., Jr., Huynh, B.H. and Moura, J.J.G. (1983) Eur. J. Biochem. 130, 481–484.
[196] Teixeira, M., Moura, I., Xavier, A.V., Huynh, B.H., DerVarta-

nian, D.V., Peck, H.D., Jr., LeGall, J. and Moura J.J.G. (1985) J. Biol. Chem. 260, 8942–8950.
[197] Teixeira, M., Moura, I., Fauque, G., Czechowski, M., Berlier, Y., Lespinat, P.A., LeGall, J., Xavier, A.V. and Moura, J.J.G. (1986) Biochimie 68, 75–84.
[198] Teixeira, M., Fauque, G., Moura, I., Lespinat, P.A., Berlier, Y., Prickril, B., Peck, H.D., Jr., Xavier, A.V., LeGall, J. and Moura, J.J.G. (1987) Eur. J. Biochem. 167, 47–58.
[199] Teixeira, M., Moura, I., Xavier, A.V., Moura, J.J.G., LeGall, J., DerVartanian, D.V., Peck, H.D., Jr. and Huynh, B.-H. (1989) J. Biol. Chem. 264, 16435–16450.
[200] Teixeira, M., Moura, I., Fauque, G., DerVartanian, D.V., LeGall, J., Peck, H.D., Jr., Moura, J.J.G. and Huynh, B.-H. (1990) Eur. J. Biochem. 189, 381–386.
[201] Telser, J., Hoffman, B.M., Brutto, R.L., Ohnishi, T., Tsai, A.-L., Simpkin, D. and Palmer, G. (1987) FEBS Lett. 214, 117–121.
[202] Thauer, R.K., Diekert, G. and Schönheit, P. (1980) Trends Biochem. Sci. 5, 304–306.
[203] Tran-Betcke, A., Warnecke, U., Böcker, C., Zaborosch, C. and Friedrich, B. (1990) J. Bacteriol. 172, 2920–2929.
[204] Van der Werf, A.N. and Yates, M.G. (1978) in Hydrogenases, Their Catalytic Activity, Structure and Function (Schlegel, H.G. and Schneider, K., eds.), pp. 307–326, Erich Goltze KG, Göttingen.
[205] Van der Westen, H.M., Mayhew, S.G. and Veeger, C. (1978) FEBS Lett. 86, 122–126.
[206] Van der Zwaan, J.W., Albracht, S.P.J., Fontijn, R.D. and Slater, E.C. (1985) FEBS Lett. 179, 271–277.
[207] Van der Zwaan, J.W., Albracht, S.P.J., Fontijn, R.D. and Roelofs, Y.B.M. (1986) Biochim. Biophys. Acta 872, 208–215.
[208] Van der Zwaan, J.W., Albracht, S.P.J., Fontijn, R.D. and Mul, P. (1987) Eur. J. Biochem. 169, 377–384.
[209] Van der Zwaan, J.W. (1987) On the active site of nickel hydrogenases. Ph.D. Thesis, University of Amsterdam, Amsterdam, The Netherlands.
[210] Van der Zwaan, J.W., Coremans, J.M.C.C., Bouwens, E.C.M. and Albracht, S.P.J. (1990) Biochim. Biophys. Acta, 1041, 101–110.
[211] Van Heerikhuizen, H., Albracht, S.P.J., Ten Brink, B., Evers-Van Twist, L. and Slater, E.C. (1978) in Hydrogenases, Their Catalytic Activity, Structure and Function (Schlegel, H.G. and Schneider, K., eds.), pp. 151–158, Erich Goltze KG, Göttingen.
[212] Van Heerikhuizen, H., Albracht, S.P.J., Slater, E.C. and Van Rheenen, P.S. (1981) Biochim. Biophys. Acta 657, 26–39.
[213] Vignais, P.M. and Toussaint, B. (1994) Arch. Microbiol. 161, 1–10.
[214] Volbeda, A., Piras, C., Charon, M.H., Hatchikian, E.C., Frey, M. and Fontecilla-Camps, J.C. (1993) Joint CCP4 ESF-EACBM Newsletter on Prot. Cryst., 28, 30–33.
[214b]Higuchi, Y., Okamoto, T., Fujimoto, K., Misaki, S., Morimoto, Y and Yasuoka, N. (1994) Acta Crystallogr. sect. D, D50, in press.
[215] Voordouw, G. and Brenner, S. (1985) Eur. J. Biochem. 148, 515–520.
[216] Voordouw, G., Hagen, W.R., Krüse-Wolters, K.M., Van Berkel-Arts, A. and Veeger, C. (1987) Eur. J. Biochem. 162, 31–36.
[217] Voordouw, G., Menon, N.K., LeGall, J., Choi, E.-S., Peck, H.D., Jr. and Przybyla, A.E. (1989) J. Bacteriol. 171, 2894–2899.
[218] Voordouw, G. (1992) Adv. Inorg. Chem., 38, 397–422.
[219] Walsh, C.T. and Orme-Johnson, W.H. (1987) Biochemistry 26, 4901–4906.
[220] Wang, G., Benecky, M.J., Huyhn, B.H., Cline, J.F., Adams, M.W.W., Mortenson, L.E., Hoffman, B.M. and Münck, E. (1984) J. Biol. Chem. 259, 14328–14331.
[221] Wang, C.-P., Franco, R., Moura, J.J.G., Moura, I. and Day, E.P. (1992) J. Biol. Chem. 267, 7378–7380.
[222] Weaver, P.F., Lien, S. and Seibert, M. (1980) Solar Energy 24, 3–45.
[223] Wertz, J.E. and Bolton, J.R. (1972) Electron Spin Resonance. Elementary theory and practical applications, McGraw-Hill Book Company, New York.
[224] Whitehead, J.P., Colpas, G.J., Bagyinka, C. and Maroney, M.J. (1991) J. Am. Chem. Soc. 113, 6288–6289.
[225] Whitehead, J.P., Gurbiel, R.J., Bagyinka, C., Hoffman, B.M. and Maroney, M.J. (1993) J. Am. Chem. Soc. 115, 5629–5635.
[226] Wood, H.G. (1985) Annu. Rev. Bioch. 54, 1–41.
[227] Wu, L.-F. and Mandrand, M.A. (1993) FEMS. Microbiol. Rev. 104, 243–270.
[228] Yamazaki, S. (1982) J. Biol. Chem. 257, 7926–7929.
[229] Zaborasch, C., Schneider, K., Schlegel, H.G. and Kratzin, H. (1989) Eur. J. Biochem. 181, 175–180.
[230] Zinoni, F., Birkman, A., Stadtman, T.C. and Böck, A. (1986) Proc. Natl. Acad. Sci. USA 83, 4650–4654.
[231] Zirngibl, C., Van Dongen, W., Schwörer, B., Von Bünau, R., Richter, M., Klein, A. and Thauer, R.K. (1992) Eur. J. Biochem. 208, 511–520.
[232] Zorin, N.A. (1986) Biochimie 68, 97–101.